수의학 박사학위논문

Detection of potential zoonotic viruses in animals and evaluation of antiviral activities of chitosan and nano-graphene oxide against coronaviruses

동물에서 잠재적 인수공통 바이러스 검출 및
코로나바이러스에 대한 키토산과 나노그래핀
옥사이드의 항바이러스 효능 연구

2022 년 2 월

서울대학교 대학원
수의학과 수의병인생물학 및 예방수의학 전공
김 청 웅

Detection of potential zoonotic viruses in animals and evaluation of antiviral activities of chitosan and nano-graphene oxide against coronaviruses

By
Kim, Cheong Ung

Supervisor: Prof. Yang, Soo-Jin, D.V.M., Ph.D.

February 2022

Department of Veterinary Medicine
The Graduate School of
Seoul National University

Detection of potential zoonotic viruses in animals and evaluation of antiviral activities of chitosan and nano-graphene oxide against coronaviruses

지도교수 양 수 진

이 논문을 수의학 박사학위논문으로 제출함

2022 년 2 월

서울대학교 대학원

수의학과 수의병인생물학 및 예방수의학 전공

김 청 웅

김청웅의 박사 학위논문을 인준함

2022 년 2 월

위 원 장 유 한 상

위 원 조 성 범

위 원 최 강 석

위 원 양 수 진

위 원 박 건 택

Detection of potential zoonotic viruses in animals and evaluation of antiviral activities of chitosan and nano-graphene oxide against coronaviruses

Kim, Cheong Ung

(Supervised by Prof. Yang, Soo-Jin)

Veterinary Pathobiology and Preventive Medicine, Department of Veterinary Medicine, The Graduate School of Seoul National University

Abstract

Emerging zoonotic diseases have the potential to cause serious human health problems and economic losses. While some zoonotic diseases, such as avian influenza and rabies, have been well investigated, the occurrence and prevalence of newly emerged viral pathogens in livestock and wildlife reservoir species is not well known. Thus, in this study, potential zoonotic viruses in bats and pigs were isolated and genetically analyzed to evaluate the risk of cross-

species transmission to humans.

The viral isolate from *Eptesicus serotinus*, HCQD-2020 strain, was subjected to next-generation sequencing and bioinformatic analyses. Sequence annotation results indicated that this strain contains seven common open reading frames (ORFs) in the typical order 5'- UTR-ORF1ab-S-ORF3-E-M-N-ORF7-3'-UTR. The comparison of the whole-genome sequence and the conserved amino acid sequence of replicated proteins also revealed that the new strain was distantly related with other known species in the alphacoronavirus genus. Additionally, phylogenetic and *in silico* prediction analyses suggested that this novel species of alphacoronavirus strain is capable of cross-species infection, especially in the order Artiodactyla.

To investigate the prevalence of Torque teno sus virus (TTSuV) in livestock animals, TTSuVs were isolated from pigs with respiratory problems (n = 470). Phylogenetic analyses of these viruses were conducted to evaluate the cross-species transmission of the viruses. In total, positive rates of 16% (75/470) and 36% (168/470) were detected for TTSuV1 and TTSuV2, respectively. Thirty-eight (8%) of the 470 pigs were detected as co-infections of TTSuV1 and TTSuV2. Whole genome sequencing analyses revealed that two strains, M117 and N86, belong to subtype 1b and 1c of TTSuV1 and the N116 strain was located in subtype 2b. Furthermore, two field strains, M256 and N119 were determined to be within genogroup 3 of subgroup 3c, which contains highly

conserved ORFs of *Anelloviruses*.

Development of effective disinfectants against zoonotic pathogens is one of the most urgent prerequisites for prevention of transmission and outbreak of zoonoses. Therefore, the antiviral effects of two natural substances, chitosan and nano-graphene oxide (nanoGO), against coronaviruses were evaluated. When 1% chitosan solution was used at a 100-800-fold dilution concentration, the porcine epidemic diarrhea virus (PEDV) titer decreased over 4 $\log_{10}$ $TCID_{50/}$/mL compared to the control virus. Similarly, 1% nanoGO solution with 500-800 fold dilution concentration effectively reduced PEDV and BCoV infection titers over 4 $\log_{10}$ $TCID_{50/}$/mL compared to the control groups. Cytotoxicity of chitosan and nanoGO was not observed in Vero cell lines at all concentrations tested, suggesting that chitosan and nanoGO have strong antiviral activities against coronaviruses without cytotoxic effect. Although future studies of cytotoxicity in other cell lines are required, chitosan and nanoGO are safe ingredients for use as non-toxic disinfectants against zoonotic viral diseases such as coronaviruses. Furthermore, continuous surveillance of novel zoonotic viral pathogens in wildlife and livestock animals along with the development of an effective decontamination strategy should be maintained to respond to crises caused by zoonotic pathogens.

Keywords: Phylogenetic analysis; Alphacoronavirus; Torque Teno virus (TTV); Chitosan; Nano-graphene Oxide (nanoGO); Disinfectant

Student number: 2016-21763

Contents

List of Figures

List of Tables

Abbreviations

BCoV	**Bovine coronavirus**
CDC	**Centers for Disease Control and Prevention**
COVID-19	**Disease caused by severe acute respiratory syndrome coronavirus 2**
CoVs	**Coronaviruses**
CPE	**Cytopathic effect**
DMV	**Double-membrane vesicles**
FeCoV	**Feline coronavirus**
HEV	**Hendra virus**
HCoV	**Human coronavirus**
IBV	**Infectious bronchitis virus**
ICTV	**International Committee for Taxonomy of Viruses**
IFA	**Indirect immunofluorescence assay**
MERS	**Middle east respiratory syndrome**
MHV	**Murine hepatitis virus**
nanoGO	**Nano-graphene oxide**
Nsp	**Nonstructural proteins**
ORF	**Open reading frame**
PEAV	**Porcine enteric alphacoronavirus**
PEDV	**Porcine epidemic diarrhea virus**
RdRp	**RNA dependent RNA polymerase**
RTC	**Replication-transcription complex**
SARS	**Severe acute respiratory syndrome**
SARS-CoV-2	**Severe acute respiratory syndrome coronavirus 2**
TGEV	**Transmissible gastroenteritis virus**
TRS	**Transcriptional regulatory sequence**
TTSuV	**Torque teno sus virus**
TTV	**Torque teno virus**
UTR	**Untranslated region**

General introduction

Zoonotic diseases are infectious diseases that can be transmitted naturally from vertebrate animals to humans or from humans to vertebrate animals. They are caused by pathogenic viruses, bacteria, parasites, and fungi. They have been reported for many centuries and threatened the public health. The emergence of new zoonotic diseases increased the public health impact over the past few decades. Emerging zoonotic diseases have potentially serious impacts on public health and the economy. The past 30 years has seen a rise in emerging infectious diseases in humans, and over 70% have been zoonotic (K. E. Jones et al., 2008). Zoonotic diseases have always been one of the most prevalent diseases in human (e.g., anthrax, plague, and tuberculosis), which have come from domestic animals, poultry, and livestock. However, with changes in the environment, human behavior, and habitat, these infections are increasingly emerging from wildlife species. There have been increased reports of zoonotic diseases. This increase is the result of an improved ability to detect and identify agents. Advanced technology has increased the sensitivity and range of detection and diagnostic capability. However, if the pathogen does not cause serious disease outbreaks, it may still go undetected. Bats in the order *Chiroptera* are the second most species-rich mammalian order, with over 1,200 species spread across almost every part of the world (Peixoto, Braga, & Mendes,

2018). After the discovery of bats as natural reservoirs of Hendra virus (HeV) in Australia, studies on bats as reservoirs of important zoonotic viruses increased. Research on bats and viruses has more than doubled in the last decade with at least one new publication per week in the literature on bat viruses. In many respects, bats represent an ideal reservoir for pathogens. Their flight ability allows them to disseminate and acquire pathogens over a wide geographical range; they live in large colonies or roosts (sometimes in the millions); and they enjoy remarkable longevity for their body size (L. F. Wang, Walker, & Poon, 2011). The number and diversity of viruses identified in bats are extraordinary and are the subject of many recent reviews (Calisher, Childs, Field, Holmes, & Schountz, 2006).

Zoonotic diseases have been receiving increased attention as a research topic, with an overall rate of publications increasing from 1 to 3 per annum in 2006, 18 per annum in 2012, and more than 33 per annum in 2017 (White & Razgour, 2020), contributing to a better understanding of pathogens, their hosts and factors affecting disease.

Recent molecular studies show that some isolates from animals have genetic similarities with those from humans. Several strains of alphacoronavirus and betacoronavirus detected in bats have been known to induce diseases such as COVID-19, responsible for the current pandemic, as well as many serious infectious diseases in livestock (Maciej F Boni et al., 2020). More than one-

third of the viruses detected in bats belong to the *Coronaviridae* family (Letko, Seifert, Olival, Plowright, & Munster, 2020).

It is reported that Torque teno virus (TTV, genus *Alphatorquevirus*) isolates were founde in humans and other animals. Their modes of transmission between humans and other putative host animals have been reported in terms of zoonotic potential. Several studies have reported evidence of zoonotic TTV transmission between humans and other primates.

The COVID-19 pandemic caused by the SARS-CoV-2 outbreak has resulted in approximately 20 million infections and more than 739,000 deaths as of the end of August 11, 2020 (Zhang & Holmes, 2020). The pandemic has caused a severe threat to public health and safety, which urgently requires effective therapeutic and control strategies (Tang et al., 2020). To date, no drug or vaccine for SARS-CoV-2 has been officially approved (L. q. Li et al., 2020). The development of effective strategies to prevent the transmission and infection of SARS-CoV-2 can alleviate the current situation to a certain extent.

Many disinfectants are effective against covert viruses such as the SARS-CoV-2. The most commonly recommended disinfectants are 70% ethanol and chlorinated disinfectants such as sodium hypochlorite and calcium hypochlorite. However, an increased number of poisoning cases and health problems associated with these disinfectants has been reported.

The results of the adverse effects of disinfectants observed between the

participants are reported in the previous study. The most important skin effects on the hands and feet were found to be itching, redness, dryness, and sores. Eye effects included eye irritation and itching, tearing, and decreased vision. Lung irritation, shortness of breath, cough, and sneezing are some of the frequent effects observed in the respiratory system. Abdominal pain, diarrhea, and vomiting have been common gastrointestinal symptoms. Other adverse effects of disinfectants include throat irritation, obsessive-compulsive disorder, lack of concentration, headaches, dizziness, and fatigue.

Chitosan which is extracted from shellfish such as crabs and shrimp is a non-toxic and hydrophilic polysaccharide (Tomihata & Ikada, 1997). It has been widely used in the medical and bioengineering fields for wound healing, drug delivery, and cell culture, and has a variety of advantageous features, including low toxicity, low cost, antimicrobial activity, biodegradability, and biocompatibility (Khor & Lim, 2003). Among these advantages, its non-toxic nature and antimicrobial activity make it a promising substance for use as a less harmful disinfectant.

Graphene oxide (GO), an ultrathin carbon material, is one of these agents that has been demonstrated with the function of broad-spectrum antiviral activity (Z. Song et al., 2015; Ye et al., 2015). GO has also been regarded as an excellent candidate for virus-prevention (Lu Chen & Jiangong Liang, 2020). Nano-graphene oxide (nanoGO), a graphene oxide with nanoscale lateral

dimension (Sanchez, Jachak, Hurt, & Kane, 2012), displays antiviral activity which was demonstrated in previous studies. Faced with the serious pandemic of COVID-19, nanoGO was considered a great virucidal material to be applied in antiviral surfaces and coatings (Palmieri & Papi, 2020).

Considering the devastating consequences of global pandemics caused by the novel coronavirus (SARS-CoV-2), it is important to investigate the prevalence of potential zoonotic viruses in wildlife and livestock animals. In addition, the development of effective decontamination strategies to reduce the transmission of such zoonotic diseases should be accompanied by the surveillance program. In this study, viruses with zoonotic potential were isolated from Korean bats and domestic pigs that showed clinical symptoms such as respiratory problems. Genetic features of the viruses were examined using whole-genome sequence analyses and phylogenetic relationship analyses. Evaluation of antiviral activities of nontoxic chitosan and nano-graphene against coronaviruses was also carried out in this study.

Literature review

1. Coronavirus

1.1. Structure of coronavirus

Coronaviruses (CoVs) belong to the subfamily *Coronavirinae* in the family of *Coronaviridae* of the order *Nidovirales*, and this subfamily includes four genera: alphacoronavirus, betacoronavirus, gammacoronavirus, and deltacoronavirus (Figure 1). The genome of CoVs is a single-stranded positive-sense RNA (+ssRNA) (~30 kb) with a 5′-cap structure and 3′-poly-A tail. The genomic RNA is used as a template to directly translate polyprotein 1a/1ab (pp1a/pp1ab), which encodes nonstructural proteins (Nsps) to form the replication-transcription complex (RTC) in double-membrane vesicles (DMVs) (Snijder et al., 2006). Subsequently, a nested set of subgenomic RNAs (sgRNAs) are synthesized by RTC in a manner of discontinuous transcription (Hussain et al., 2005). These subgenomic messenger RNAs (mRNAs) possess common 5′-leader and 3′-terminal sequences. Transcription termination and subsequent acquisition of a leader RNA occurs at transcription regulatory sequences, located between open reading frames (ORFs). These minus-strand sgRNAs serve as the templates for the production of subgenomic mRNAs (Sawicki, Sawicki, & Siddell, 2007). The genome and subgenomes of a typical CoV contain at least six ORFs. The first ORFs (ORF1a/b), about two-thirds of the whole genome length, encode 16 Nsps (Nsp1-16), except gammacoronavirus that lacks Nsp1.

There is a −1 frameshift between ORF1a and ORF1b, leading to the production of two polypeptides: pp1a and pp1ab. These polypeptides are processed by virally encoded chymotrypsin-like protease ($3CL^{pro}$) or main protease (M^{pro}) and one or two papain-like protease into 16 Nsps (Ziebuhr, Snijder, & Gorbalenya, 2000). Other ORFs in the one-third of the genome near the 3′- end encodes at least four major structural proteins: envelope (E), membrane (M), nucleocapsid (N), and spike (S) proteins. Besides these four main structural proteins, different CoVs encode special structural and accessory proteins, such as HE protein, 3a/b protein, and 4a/b protein (Figure 2). All the structural and accessory proteins are translated from the sgRNAs of CoVs (Hussain et al., 2005). The CoV genome is much larger, with roughly 30kb in length, the largest known RNA viruses. The 3′-5′ exoribonuclease is unique to CoVs among all RNA viruses, probably providing a proofreading function of the RTC (Ogando et al., 2019). Sequence analysis shows that the 2019-nCoV carries a typical genome structure of coronavirus and belongs to the cluster of beta coronaviruses that includes SARS-CoV, and MERS-CoV (Figure 1).

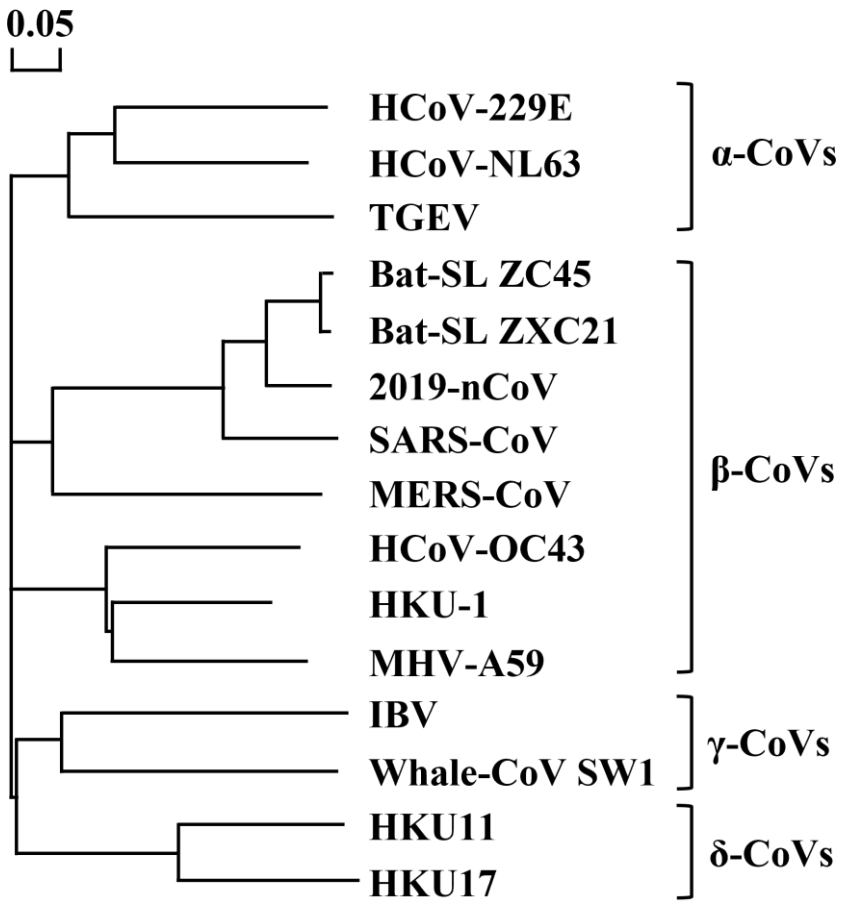

Figure 1. The phylogenetic tree of coronaviruses (CoVs).

Viral names: HCoV, human coronavirus; TGEV, transmissible gastroenteritis virus; SARS-CoV, severe acute respiratory syndrome coronavirus; MERS-CoV, middle east respiratory syndrome coronavirus; HKU, coronaviruses identified by Hong Kong University; MHV, murine hepatitis virus; IBV, infectious bronchitis virus; Whale- CoV SW1, Beluga Whale coronavirus SW1.

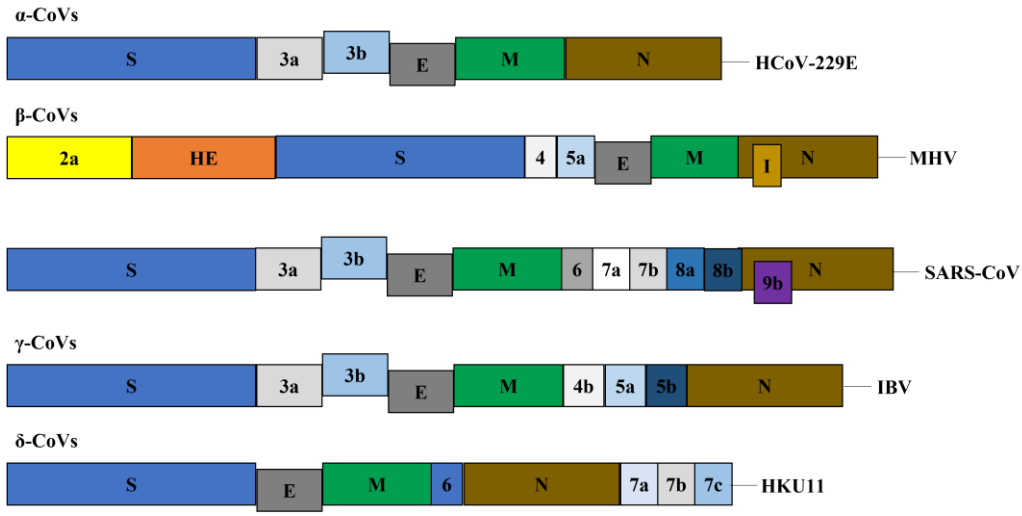

Figure 2. The genome structure of four genera of coronaviruses.

S, spike protein; E, envelope protein; M, membrane protein; N, nucleocapsid protein; HE, hemagglutinin-esterase. Viral names: HCoV, human coronavirus; MHV, murine hepatitis virus; SARS-CoV, severe acute respiratory syndrome coronavirus; IBV, infectious bronchitis virus; HKU, coronaviruses identified by Hong Kong University.

1.2. Diversity of coronavirus pathogenesis

Different CoVs display diverse host ranges and tissue tropism. Usually, alphacoronaviruses and beta coronaviruses infect mammals. In contrast, gammacoronaviruses and deltacoronaviruses infect birds and fish, but some of them can also infect mammals (P. C. Woo et al., 2012). Before 2019, there were only six CoVs that were known to infect humans and cause respiratory diseases. HCoV-229E, HCoV-NL63, and HCoV-OC43 cause mild upper respiratory disease, and rarely, some can cause severe infection in infants, and the elderly. SARS-CoV and MERS-CoV can infect the lower respiratory tract and cause severe respiratory syndrome in humans (Shuo Su et al., 2016). Some CoVs can infect livestock, birds, bats, mice, whales, and many other wild animals, and they can cause great economic loss. For example, in 2016, and HKU2-related bat CoV, swine acute diarrhea syndrome CoV, caused a large-scale outbreak of the fatal disease in pigs in Southern China, and more than 24 000 piglets were dead.62 This is the first documented spillover of a bat CoV that caused severe disease in livestock (Simas et al., 2015). The new CoV, 2019-nCoV, which belongs to betacoronaviruses based on sequence analysis (Figure 1), can also infect the lower respiratory tract and cause pneumonia in humans, but it seems that the symptoms are milder than SARS and MERS. Up to 20 January 2020, 291 cases in total have been confirmed in China by sequence analysis, clinical diagnosis, and epidemiological examination, including 270 cases in Wuhan and

21 cases in Beijing, Shanghai, and Guangdong. Many of the patients have direct or indirect contact with the Wuhan Huanan Wholesale Market that is believed to be the original place of the outbreak of the 2019-nCoV. As the Wuhan market also sells animals, the natural host of 2019-nCoV awaits to be identified. Due to the possibility of transmission from animal to human, CoVs in livestock and other animals including bats and wild animals sold in the market should be constantly monitored. In addition, more and more evidence indicates the new virus 2019-nCoV is spread via the route of human-to-human transmission because there are infections of people who did not visit Wuhan but had close contact with family members who had visited Wuhan and got infected. The major pathogenic CoVs are listed in Table 1 for a better understanding of the pathogenesis of CoVs.

Table 1. List of important pathogenic coronaviruses in human and animal hosts.

Genus	Host	Virus	Symptom
Alpha	Human	Human CoV-229E	Mild respiratory tract infectious
Alpha	Human	Human CoV-NL63	Mild respiratory tract infectious
Alpha	Pig	PRCV/ISU-1	Mild respiratory tract infectious
Alpha	Pig	TGEV/PUR46-MAD	Diarrhea, with 100% mortality in piglets less than 2-wk-old
Alpha	Pig	PEDV/ZJU-G1-2013	Severe watery diarrhea
Alpha	Pig	SeACoV-CH/GD-01	Severe and acute diarrhea and acute vomiting
Alpha	Dog	Canine CoV/TU336/F/2008	Mild clinical signs, diarrhea
Alpha	Camel	Camel alphacoronavirus isolate camel/Riyadh	Asymptomatic
Alpha	Cat	Feline infectious peritonitis virus	Fever, vasculitis, and serositis, with or without effusions
Beta	Human	Human CoV-HKU1	Pneumonia
Beta	Human	Human CoV-OC43	Mild respiratory tract infections
Beta	Human	SARS-CoV	Severe acute respiratory syndrome, 10% mortality rate
Beta	Human	MERS-CoV	Severe acute respiratory syndrome, 37% mortality rate
Beta	CoW	Bovine CoV/ENT	Diarrhea
Beta	Horse	Equine CoV/Obihiro12-1	Fever, anorexia, leucopenia
Beta	Mouse	MHV-A59	Central nervous system disease and hepatitis
Gamma	Whale	Beluga Whale CoV/SW1	Pulmonary disease, terminal acute liver failure
Gamma	Chicken	IBV	Severe respiratory disease
Delta	Bulbul	Bulbul coronavirus HKU11	Respiratory disease (collected from the respiratory tract of dead wild birds)
Delta	Sparrow	Sparrow coronavirus HKU17	Respiratory disease (collected from the respiratory tract of dead wild birds)

1.3. Coronavirus in bat

The longer range of migration compared to land mammals. Bats are also the largest second-largest order of mammals, accounting for about a fifth of all mammalian species, and are distributed worldwide (Fan et al., 2019). Phylogenetic analysis classified bats into two large suborders—the *Yinpterochiroptera*, consisting of one *Pteropodidae* (megabat) and five *Rhinolophoidea* (microbat) families, and the *Yangochiroptera* comprising a total of thirteen microbat families (Teeling et al., 2005). It is hypothesized that flight provided the selection pressure for coexistence with viruses, while the migratory ability of bats has particular relevance in the context of disease transmission (L.f. Wang & Cowled, 2015). Indeed, bats were linked to a few highly pathogenic human diseases, supporting this hypothesis. Some of these characterized well-characterized bat viruses, including bat lyssaviruses (Rabies virus), henipaviruses (Nipah virus and Hendra virus), Coronaviruses (CoVs; SARS-CoV, MERS-CoV, and SADS-CoV), and filoviruses (Marburg virus, Ebola virus, and Mengla virus), pose a great threat to human health (X. L. Yang et al., 2019). A comprehensive analysis of mammalian virus-host-virus relationships demonstrated that bats harbor a significantly higher proportion of zoonotic viruses than other mammalian orders (Olival et al., 2017). Viruses from most of the viral families can be found in bats (L. f. Wang & Cowled, 2015). Bats are now recognized as important reservoir hosts of CoVs. Although

civet cats were initially identified as the animal origin of SARS-CoV, bats were soon found to be the most likely reservoir hosts of this virus (Guan et al., 2003). Long-term surveillance revealed an average of 10% SARS-related CoV nucleotide positivity in bats, including some viruses that can use the same human entry receptor ACE2 as SARS-CoV (Ge et al., 2013). Similarly, bats have been proposed to harbor the progenitor viruses of MERS-CoV, although dromedary camels can transmit this virus to humans directly (Fan et al., 2019). The most recent SADS-CoV spillover was traced back to bats (Peng Zhou et al., 2018). In addition, bats also carry alph-CoVs that are related to pathogenic human 229E- and NL63-CoVs, as well as pandemic swine coronavirus PEDV (Lacroix et al., 2017). In collectively, bats carry major alpha-(10 out of 17) and beta-(7 out of 12) CoV species that may spill over to humans and cause disease. Attributed to the wide distribution of bats, CoVs can be found worldwide (Leopardi et al., 2018).

2. Torque Teno virus (TTV)

2.1. Structure of Torque teno virus (TTV)

In 1997, by means of representational difference analysis (RDA) (Lisitsyn, Lisitsyn, & Wigler, 1993), the first “TT” virus (TTV) isolate was identified from a Japanese patient (with initials T.T.) with posttransfusion hepatitis of

unknown etiology (Nishizawa et al., 1997). Subsequent studies revealed that TTV and TTV-like viruses with marked genetic variability are nonenveloped, single-stranded (negative sense), circular DNA viruses with a genomic length of 3.6–3.9 kb (Miyata et al., 1999; Mushahwar et al., 1999; Nishizawa et al., 1997; Peng et al., 2002). The International Committee on Taxonomy of Viruses (ICTV) proposed that the abbreviation "TT" of "TTV" stands for "Torque teno," deriving from the Latin terms "torque" meaning "necklace" and "tenuis" meaning "thin." These terms reflect the arrangement of the genomic organization of TTV (De Villiers & Zur Hausen, 2009). TTV has a common presumed genomic organization with four open reading frames (ORFs, ORF1–ORF4) (Figure 3). Three distinct messenger RNAs (mRNAs)—of 2.9–3.0 kb, 1.2 kb, and 1.0 kb with common 5′ and 3′ termini that are transcribed from the genomic, minus-strand of TTV DNA—have been observed in culture cells transfected with recombinant TTV DNA as well as in bone marrow cells obtained from an infected human (Kamahora, Hino, & Miyata, 2000). These three mRNAs have in common short splicing of approximately 100 nt. The 1.2-kb and 1.0-kb mRNAs possess additional splicing of approximately 1,700 nt and 1,900 nt, respectively, leading to the creation of two novel ORFs (ORF3 and ORF4) (De Villiers & Zur Hausen, 2009).

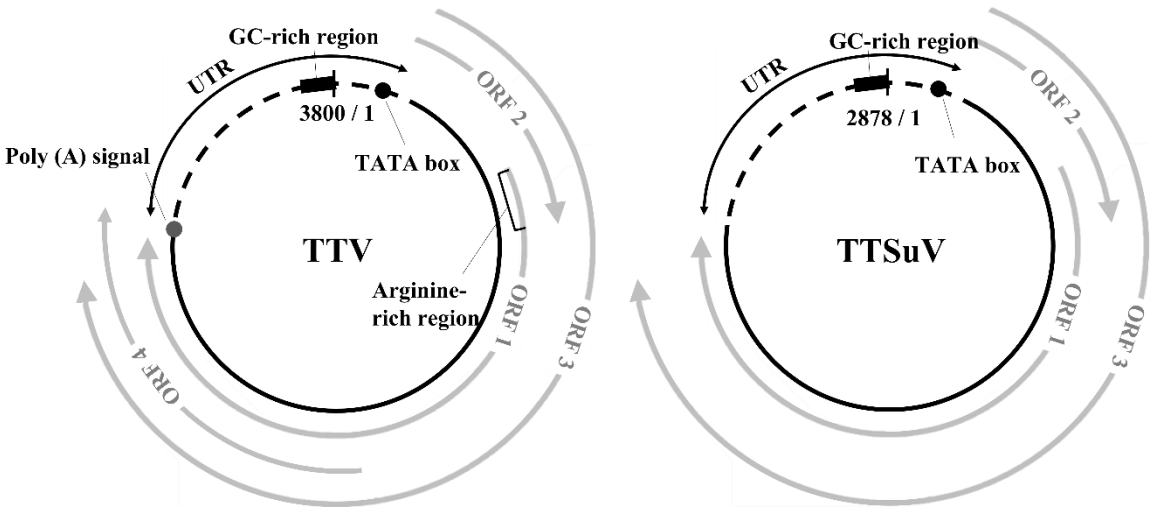

Figure 3. Genomic organization Torque teno virus (TTV) and Torque teno sus virus (TTSuV). *Arrows* represent overlapping open reading frames (ORFs)

2.2. Diversity of Torque teno virus-host

TTV has an extremely wide range of sequence divergence, and the TTV genomes are tentatively classified into at least 39 genotypes with a sequence divergence of more than 30% from one another, or into five major phylogenetic groups (groups 1–5) with sequence divergence of more than 50% from one another (Hallett, Clewley, Bobet, McKiernan, & Teo, 2000; Hijikata, Takahashi, & Mishiro, 1999; Ukita et al., 2000). Infection of TTVs is not restricted to human hosts. Although many aspects of TTV infection including the precise host range and cross-species infection remain to be elucidated, increasing lines of evidence indicate that nonhuman primates, *Tupaia* (tree shrews: *Tupaia belangeri chinensis*), and livestock and some companion animals are infected with TTVs (Abe, Inami, Ishikawa, Nakamura, & Goto, 2000; Brassard et al., 2008; Romeo et al., 2000). The entire nucleotide sequences of species-specific TTVs that infect nonhuman primates as well as domestic animals including pig (*Sus domesticus*), cat (*Felis catus*), and dog (*Canis familiaris*), have been determined (Inami, Obara, Moriyama, Arakawa, & Abe, 2000; Niel, Diniz-Mendes, & Devalle, 2005) (Table 2). Furthermore, TTV DNA has been detected in serum samples obtained from domesticated farm animals such as chickens, cows, and sheep (Brassard et al., 2008; Leary, Erker, Chalmers, Desai, & Mushahwar, 1999). However, the TTVs in these farm animals have not been fully characterized yet.

Table 2. Classification of Torque teno virus (TTV).

Family	Genus	Host	Virus	Symptom
Anelloviridae	*Alfatorquevirus*	Human	Torque teno virus	Unknown but incriminated Hepatitis A-C, Chronic Hepatitis B-C, Thalassemia, Fever, Pulmonary fibrosis
Anelloviridae	*Iotatorquevirus*	Pig	Torque teno sus virus 1	Unknown but incriminated in PDNS and PMWS
Anelloviridae	*Kappatorquevirus*	Pig	Torque teno sus virus 2	Unknown but incriminated in PDNS and PMWS
Anelloviridae	*Thetatorquevirus*	Dog	Torque teno canis virus	Unknown
Anelloviridae	*Etatorquevirus*	Cat	Feline torque teno virus	Unknown

* PDNS, Porcine dermatitis and nephropathy syndrome; PMWS, Post-weaning multisystemic wasting syndrome.

2.3. Torque teno virus in pigs (Torque teno sus virus)

Porcine Torque teno virus (TTV), now known as torque teno sus virus (TTSuV), was first identified in Japan in 2002 from domestic pigs (Okamoto et al., 2002), even though evidence of TTSuV infection in pigs was retrospectively traced back to as early as 1985 in Spain (Segalés et al., 2009). Torque teno sus virus is a small, single-stranded, circular DNA virus in the family *Anelloviridae*, which also comprises its homologous counterpart of human TTV (Meng, 2012). At least two species of TTSuV, TTSuV1 (genus *Iotatorquevirus*) and TTSuV2 (genus *Kappatorquevirus*) have been identified from pigs worldwide (Huang & Meng, 2010). Both TTSuV1 and TTSuV2 genomes contain a single-stranded, circular, negative-sense DNA molecule of approximately 2.8 kb consisting of four ORFs (ORF1, ORF2, ORF1/1, and ORF2/2 previously known as ORF3), as well as a short stretch of sequence with high GC content in the untranslated region (Cortey, Olvera, Grau-Roma, & Segalés, 2011) (Figure 3). The ORF1 of TTSuV is predicted to encode a capsid and replication-associated protein (Maggi & Bendinelli, 2009). TTSuV appears to be ubiquitous in both healthy and diseased pigs worldwide. TTSuV has been detected in serum, feces, saliva, semen, and tissue samples of infected pigs, indicating its potential diverse transmission routes including both horizontal and vertical transmissions (Aramouni, Segalés, Cortey, & Kekarainen, 2010; Huang et al., 2010; Pozzuto et al., 2009). Co-infections with TTSuV1 and TTSuV2 at a high prevalence rate

have been documented in pigs worldwide using PCR and real-time PCR assays (Bigarré et al., 2005). Multiple infections of TTSuV with distinct genotypes or subtypes of the same species in the same pig have been reported (Huang & Meng, 2010). TTSuV has been detected in pig populations from Japan, the United States, Canada, Brazil, Spain, Germany, China, Thailand, and Korea (Aramouni et al., 2010; Gallei, Pesch, Esking, Keller, & Ohlinger, 2010; S.-S. Lee, Sunyoung, Jung, Shin, & Lyoo, 2010; Niel et al., 2005).

The pathogenicity of TTSuV in pigs remains largely unknown. In swine, experimental infection of gnotobiotic pigs with swine Torque Teno virus 1 or 2 (TTSuV1 or 2) causes mild to moderate respiratory, hepatic, and nephritic lesions, indicating that TTSuVs can act as a primary pathogen in swine (Ssemadaali, Effertz, Singh, Kolyvushko, & Ramamoorthy, 2016).. In experimental coinfections, TTSuV's potentiated other swine viral diseases (Krakowka & Ellis, 2008). Therefore, the question of whether TTVs can establish cross-species infections is of considerable importance. Contamination of swine-derived laboratory enzymes such as trypsin and some veterinary vaccines with TTSuVs is also reported (Kekarainen & Segalés, 2009). Current screening protocols for blood donors do not include the detection of TTVs. However, given their ubiquitous nature, TTVs are also potential contaminants of the blood supply (Bernardin, Operskalski, Busch, & Delwart, 2010). Humans are likely to frequently ingest TTSuVs in food and water. Both pork products

and human feces contain TTSuV DNA (Jiménez-Melsió, Parés, Segalés, & Kekarainen, 2013). Moreover, with the availability of improved technology, there is an increased interest and potential for the use of swine-based xenotransplantation products (Scobie & Takeuchi, 2009). In terms of public health, it is important to determine whether TTSuVs can cause infection in humans.

3. Chitosan

3.1. Structure of chitosan

Chitosan is a linear polysaccharide composed of randomly distributed β- (1 → 4)- linked D- glucosamine and N- acetyl- D- glucosamine (Figure 4). The chain length of chitosan is variable, but most chitosan products exhibit a molecular weight range of 3,800– 200,000 Daltons.

Most chitosan of commercial use is synthesized via the alkaline treatment (e.g., NaOH) and deacetylation of chitin extracted from shrimp shells. Chitosan can also be synthesized from fungal chitin grown in industrial quantities.

Chitosan is a non-toxic and hydrophilic polysaccharide (Tomihata & Ikada, 1997). It has been widely used in the medical and bioengineering fields for wound healing, drug delivery and cell culture, and has a variety of advantageous features, including low toxicity, low cost, antimicrobial activity,

biodegradability, and biocompatibility (Khor & Lim, 2003).

Chitosan has several uses, among which are biocontrol in bioprinting (Costantini et al., 2021), weight loss (Qinna et al., 2013) and as an edible antimicrobial film in food production (Amor et al., 2021).

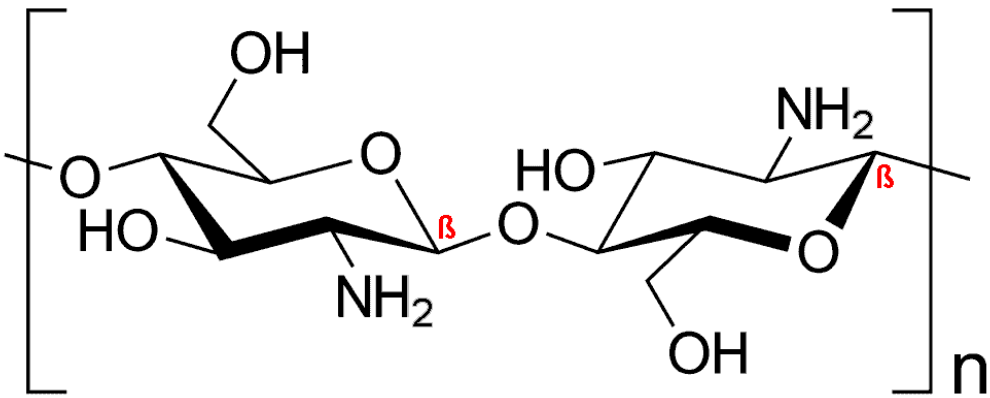

Figure 4. Schematic diagram of the basic molecular structure of deacetylated chitosan. where n indicates the repeat of the formula, resulting in the molecular weight range of 3800–20,000 Daltons.

3.2. Antiviral activity of chitosan

The chitosan has antiviral activity in various biological systems. Properties of chitosan polymers determine its efficacy in viral suppression. Chitosan concentration, molecular weight, degree of acetylation and amination, as well as chemical modification play an important role in its antiviral properties (Chirkov, 2002). It reported that antiviral activity is weakly affected by its degree of acetylation (Davydova et al., 2011). It has been suggested that the antimicrobial properties of chitosan are greatly affected by the repeated amino groups on the backbone of the polymer structure (Divya, Vijayan, George, & Jisha, 2017).

To understand the mechanisms of the antiviral activity of chitosan and its derivatives, figuring out the stages of viral infection to a host cell is crucial. Traditionally, the viral life cycle is of four major steps: attachment and entry into a target cell, replication of the viral genome, maturation of viral proteins and genome packaging into the infectious progeny, and dissemination to the next target cell (Figure 5) (J. E. Jones, Le Sage, & Lakdawala, 2021).

There are three types of mechanisms of antiviral activity of chitosan: (i) the direct killing of the virus, (ii) inhibiting viral adsorption and subsequent host cell invasion, and (iii) improvement of immunity.

First, the electrostatic interaction between the polycationic positive charge of chitosan and the negatively charged surface of the virus can inhibit the infectious ability of the virus and/or directly kill the virus by disrupting its

protective membrane (Mansouri et al., 2004; Raafat & Sahl, 2009).

Second, the chitosan inhibits viral adsorption and subsequent host cell invasion. The initial step in the viral infectious life cycle is adsorption to the host cell through binding to the cell surface by electrostatic interaction, which is followed by a subsequent viral invasion of the host cell. The viral invasion process is often associated with the endocytosis of the virus, the fusion of the viral particle with the host cell membrane, and the subsequent translocation of the virus into the host cell. It was reported that 3,6-sulphated chitosan directly inhibits human papillomavirus (HPV) by binding to the viral capsid proteins and thus, blocking virus-host cell adsorption (Gao, Liu, Wang, Zhang, & Zhao, 2018). Other sulfated chitosan-oligosaccharide derivatives have been reported to block the interaction between HIV-1gp120 and CD4+ cell surface receptors, which inhibits virus-host cell fusion and subsequent viral entry into the host cell. Moreover, sulfated polysaccharides can interact with the positively charged regions of cell surface glycoproteins, leading to a shielding effect on these regions, and thus preventing the binding of viruses to the cell surface (Artan, Karadeniz, Karagozlu, Kim, & Kim, 2010; Gao et al., 2018). It was reported that the N-carboxymethyl chitosan N, O-sulphate, a polymer derived by the sulfation of N-carboxymethyl chitosan, inhibits HIV-1 adsorption to the cell surface receptor CD4+ and reverse transcription of the viral genome (Sosa, Fazely, Koch, Vercellotti, & Ruprecht, 1991).

Third, the chitosan improved host immunity by activation of NK cells or induction of other immune responses. chitosan alone or its derivatives demonstrates a universal value as a prophylactic antiviral agent. To explore the universality of chitosan-induced protective effects, the chitosan intranasal vaccine was tested against two strains of influenza virus, influenza A virus (H1N1) and avian influenza virus (H9N2). The data obtained provide strong evidence that intranasal administration of chitosan can induce an effective immune protection against diverse strains of influenza viruses (Sui et al., 2010; Zheng et al., 2016).

Antiviral activity of chitosan

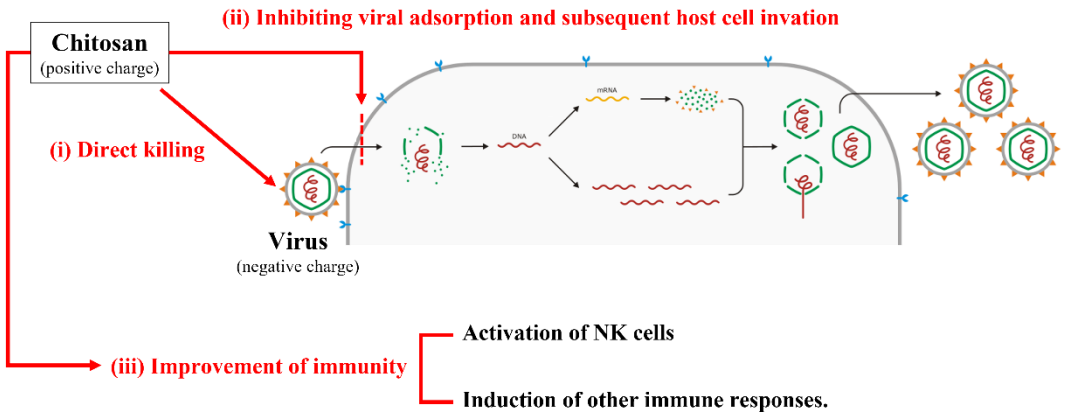

Figure 5. Schematic diagram of the proposed mechanisms of antiviral activity of chitosan. The viral life cycle is of four major steps: attachment and entry into a host cell, replication of the viral genome, maturation of viral proteins and genome packaging into the infectious progeny, and dissemination to the next target cell.

4. Nano-graphene oxide (nanoGO)

4.1. Structure of nanoGO

Graphene is a two-dimensional, crystalline allotrope with a hexagonal lattice structure made from pure carbon atoms. They are best known for its unique properties containing high optical transparency, the best heat conductivity at room temperature, and the ability to be flexible all within a strong, nano-sized material. Graphene was first discovered by the mechanical exfoliation of 3D graphite crystals and peeling away a single layer of graphene with Scotch tape. Since then, graphene has gained recognition for its attributes and different methods have been tested to find the best way to produce large-scale amounts with low costs, but it is still challenging to manufacture with these specifications. Graphene oxide (GO) happens to be a great precursor to obtaining graphene with higher yields and lower costs. To obtain GO, graphite oxide is first produced by utilizing graphite crystals that have been oxidized with strong oxidizing agents, such as sulfuric acid. Through sonication, graphite adopts oxygen-containing functional groups that allow the material to be dispersed in the water while increasing interlayer distance (J. Song, Wang, & Chang, 2014). Then, graphite oxide can be exfoliated into either single or multilayers of oxygen-functionalized graphene oxide (GO). The difference between graphite oxide and GO is based on their different structures but

chemical composition remains alike. GO is a single-layered material made of carbon, hydrogen, and oxygen molecules, which ultimately becomes inexpensive yet abundant (Ray, 2015). Nano-graphene oxide (nanoGO), a graphene oxide with nanoscale lateral dimension (Sanchez et al., 2012), displays antiviral activity which was demonstrated in previous studies.

4.2. Antiviral activity of nanoGO

NanoGO displays antiviral activity which was demonstrated in previous studies. Graphene oxide (GO) is the oxidized form of graphene with hydroxyl, epoxide, ketone, and carboxyl functional groups located on its surface. The presence of oxygen on the edges and basal planes of GO increases its hydrophilicity, water dispersibility, and bonding capacity compared to graphene (Aliyev et al., 2019; Ege, Kamali, & Boccaccini, 2017). Due to its physicochemical properties, high surface-to-volume ratio, and extremely high mechanical strength, GO is widely used in the medical field as an antibacterial and anti-cancer agent (Rhazouani et al., 2021). Additionally, studies have shown that due to its two-dimensional structure, sharp edges, and negatively charged surface, this nanomaterial can interact with viruses and disrupt their plasma membrane or generate reactive oxygen species.

There are four types of mechanisms of antiviral activity of GO: (i) virus inactivation, (ii) host cell receptor inactivation, (iii) photothermal destruction,

and (iv) electrostatic trapping (Figure 6).

First, GO prevents viruses from infecting host cells by directly inactivating the virus. The antiviral activity of GO was evaluated against the Porcine epidemic diarrhea virus (PEDV). This study found that GO significantly inhibits infection of PEDV for a 2-log reduction in virus titers at non-cytotoxic concentrations (Ye et al., 2015). GO inhibited the entry of viruses into host cells by causing structural destruction (Ye et al., 2015). Another study showed that GO could effectively capture environmental viruses such as foot and mouth disease and endemic gastrointestinal avian influenza A virus. It may break down their surface proteins and extract viral RNA in an aqueous environment through GO surface bio-reduction. The GO has been proven to be an excellent nanomaterial for high throughput virus detection and disinfection, demonstrating its great potential to prevent environmental infections (Z. Song et al., 2015).

Second, GO inhibits the entry of viruses into host cells by binding with receptors. In vivo and in vitro studies have suggested that the hypericin-GO complex (GO/HY) has antiviral activity against New Duck Virus Disease (NDRV), a serious infectious disease of poultry. Hypericin has broad-spectrum antiviral activity against various viruses such as chronic hepatitis C virus and Sendai virus. The antiviral activity of the GO/HY complex was evaluated in DF-1 cells and ducklings contaminated with NDRV. The GO/HY complex

showed dose-dependent inhibition of NDRV replication, which can be attributed to virus inactivation or inhibition of virus binding (Figure 6). Indirect immunofluorescence assay showed significantly suppressed protein expression in NDRV-infected DF-1 cells treated with GO/HY.

Third, GO has photocatalytic characteristics. It has been proven that GO has an excellent photocatalytic activity which could also be exploited to inhibit virus activity (Krishnamoorthy, Mohan, & Kim, 2011). For constant photodegradation, the virus must remain close to the surface of the GO under UV irradiation (Figure 6). The aptamer-enhanced GO caused the inactivation of viruses and damaged the viral capsid proteins and nucleic acids during irradiation (Hu, Mu, Wen, & Zhou, 2012).

Fourth, GO has a higher negative charge which allows its interaction with positively charged viruses. GO has more chances to interact with viruses through electrostatic interactions prior to viral entry, resulting in virus damage due to its single-layer structure and sharp edge (Ye et al., 2015). This characteristic explains the fact that it has an important antiviral activity against certain viruses.

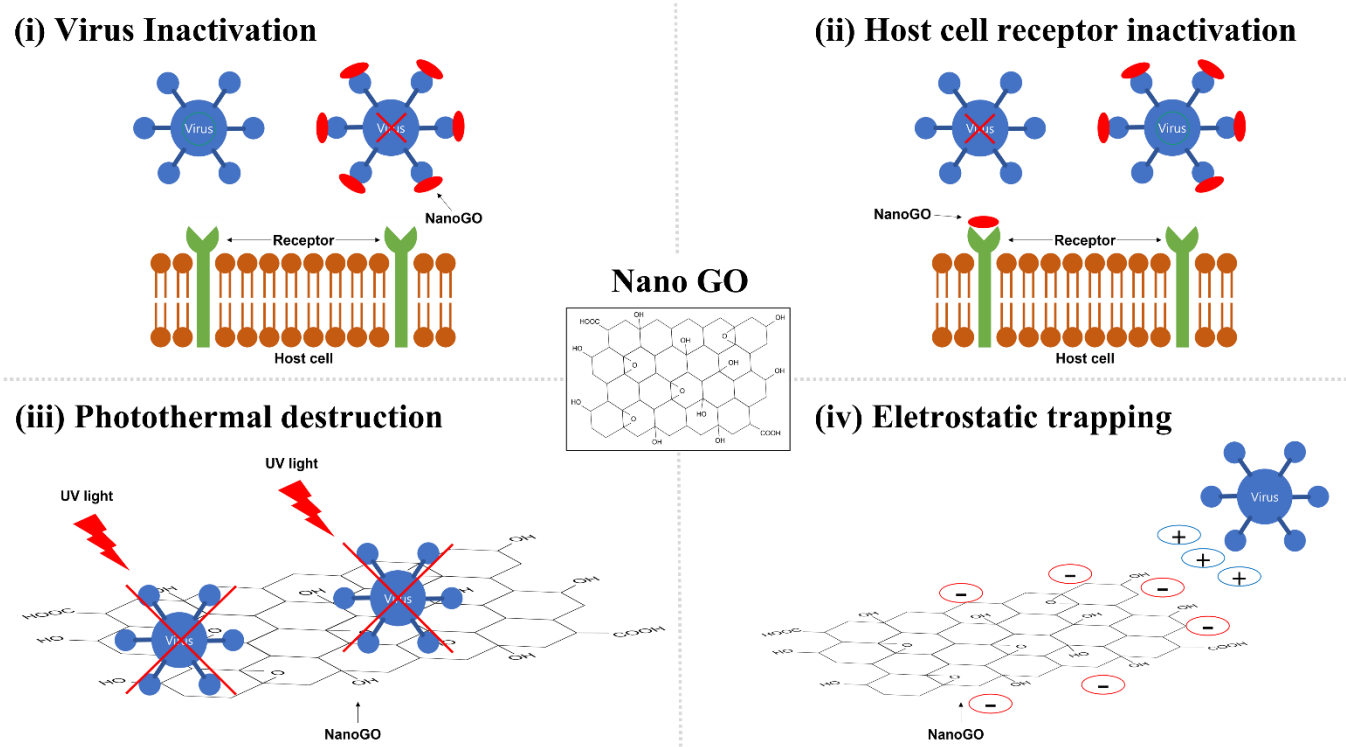

Figure 6. Description of the proposed mechanisms of GO's antiviral activity.

(i) virus inactivation, (ii) host cell receptor inactivation, (iii) photothermal destruction, and (iv) electrostatic trapping.

Chapter I. Detection of potential zoonotic viruses: alphacoronavirus in bat and torque teno virus in pig

Abstract

The animal can serve as reservoirs for diseases that can be a source of new diseases through cross-species transmission. The recent emergence of zoonotic viruses emphasizes the importance of virus surveillance in animals. Coronavirus and Torque teno virus (TTVs) has recently been found in humans and animals with high genetic variation. However, it has been unclear whether the isolates from animals have zoonotic potential or not. Up to date, few phylogenetic studies focused on the coronavirus in bats, and TTVs in pigs from South Korea. This study aimed to determine the phylogenetic characterization of these viruses in Korea.

In the present study, the genome of HCQD-2020, a novel alphacoronavirus detected in a bat (*Eptesicus serotinus*), was assembled, and described using next general sequencing and bioinformatics analysis. The comparison of the whole genome sequence and the conserved amino acid sequence of replicated proteins revealed that the new strain was distantly related with other known species in the alphacoronavirus genus. this study provided genetic characteristics of a possible new species belonging to alphacoronavirus.

A survey was carried out for 2 years to investigate the appearance of TTSuVs and TTVs in sick pigs. It is revealed that the swine torque teno virus 2 (TTSuV2, genus *Kappatorquevirus*) is around 2 times more prevalent than

swine torque teno virus 1 (TTSuV1. genus *Iotatorquevirus*). Furthermore, the Torque teno virus of genogroup 3 (TTV3) in swine pooled organ samples were identified. The complete genome sequences of each strain are 98.4 % homology. In the phylogenetic analysis of the ORF1, the two strains are located close to the TUPB (GeneBank accession no. AF247137) strain subgroup c of genogroup 3. Our study provided information on TTSuV's prevalence in swine farms in Korea and highlighted the presence of TTV genogroup 3 strains in pigs.

These results suggest that isolates harboring in animals might have zoonotic potential or have cross-transmissibility among heterogeneous hosts.

Keywords : Potential zoonotic analysis; Bat alphacoronavirus; Torque teno virus; Phylogenetic analysis

1.1. Introduction

Zoonotic diseases are those diseases or infections that can be transmitted between humans and wild and domestic animals (Slingenbergh, Gilbert, Balogh, & Wint, 2004). For years, scientists and policy actors have been warning about the risk of emerging infectious diseases (EIDs) and recommending how to avoid outbreaks (Dobson & Carper, 1996; Morse et al., 2012). There is evidence of an increasing rate of emergence of novel EIDs. During the last century, on average two new viruses per year spilled from their animal hosts into human populations (Woolhouse, Scott, Hudson, Howey, & Chase-Topping, 2012). Zoonotic pathogens exist in many different animal hosts and there are many ways, both direct to indirect, in which transmission to humans occurs (Webster, Borlase, & Rudge, 2017). Although the likelihood of transmission occurring through vector-borne and aerosol droplets is broadly similar (Loh et al., 2015). Surveillance and genetic analysis of viruses in animals are essential to investigate pathogens with potential zoonotic diseases.

Studies have been reported on viruses that are infected with various species or have various genetic diversity such as coronavirus in bats, and torque teno viruses in pigs. However, little research has been conducted on these viruses in animals in Korea. The following research has been performed to determine the genetic characteristic and phylogenetic relationships of these viruses in South

Korea. Coronavirus is considered one of the most diverse viruses because of its large genome size, high mutation rate, and recombination between homologous RNA regions (P. C. Woo, Lau, Huang, & Yuen, 2009). The studies focusing on the highly conserved region of RNA-dependent RNA polymerase (RdRp) encoding genes reported that many potentially new coronavirus species were detected in wild animals around the world (Lin et al., 2017; C. S. Smith et al., 2016; Wen Wang et al., 2015). The diversity of coronavirus and high recombinant rates increased the risk of host switch and ecological niche adaptations (P. C. Woo, Lau, & Yuen, 2006).

Bats are natural reservoirs for a large variety of viruses, including many important zoonotic viruses that cause severe diseases in humans and livestock (Wu et al., 2016). Several strains of alphacoronavirus and betacoronavirus detected in bats have been known to induce diseases like the current coronavirus disease 2019 (COVID-19) pandemic and many serious infectious diseases in livestock (M. F. Boni et al., 2020; P. C. Y. Woo et al., 2012). Serological evidence revealed the multi-infection of SARS-related coronavirus from bats to humans (H. Li et al., 2019). It is important to continue active surveillance and genetic analysis of newly detected coronaviruses in bats. A genomic-based approach provides a more in-depth analysis of the diversity of bat coronaviruses in terms of genetic variation. As a result, the complete genomic was described characteristics of HCQD-2020, a novel

alphacoronavirus isolated from a Korean bat species, *Eptesicus serotinus*.

Torque teno virus (TTV) is the virus that was first isolated from a human with a circular single-stranded DNA genome (Hsiao, Wang, Lin, & Liu, 2016). Of the TTVs, *Alphatorquevirus* is a genus mainly found in humans and primates and can be divided into at least 7 different genogroups with great genetic diversity (Hsiao et al., 2016; Mi et al., 2014; Ninomiya, Takahashi, Nishizawa, Shimosegawa, & Okamoto, 2008). Among of them, genogroup 3 is the most prevalent (AbuOdeh et al., 2015; Pinho-Nascimento, Leite, Niel, & Diniz-Mendes, 2011).

Besides humans, TTVs were found in a wide range of other hosts such as primates, pigs, cats, and dogs. The TTVs of pig origin can be classified into two major groups: Torque teno sus virus 1 (TTSuV1, genus *Iotatorquevirus*) and Torque teno sus virus 2 (TTSuV2, genus *Kappatorquevirus*), consisted of 3 subtypes (1a to 1c) and 7 subtypes (2a to 2g) (K. Li et al., 2013), respectively. TTSuV1 was known to cause clinical symptoms in gnotobiotic pigs (Ellis, Allan, & Krakowka, 2008; Krakowka et al., 2008). In addition, TTSuV1 and TTSuV2 were reported to have correlations to post-weaning multisystemic wasting syndrome (Kekarainen, Sibila, & Segalés, 2006; Nieto, Aramouni, Grau-Roma, Segales, & Kekarainen, 2011).

It is reported that TTV’s common human infecting agent can be found in the pig’s serum (Ssemadaali, Effertz, Singh, Kolyvushko, & Ramamoorthy, 2016).

Evidence about the possible infection of TTSuV1 to human cells was reported, which raised the question of the possibility of transmission of TTVs between humans and animals. Recently, a study based on molecular analysis supported the hypothesis of possible transmission of TTVs from humans to animals (Sarairah, Bdour, & Gharaibeh, 2020).

Therefore, this study aims to investigate: i) the occurrence and genetic characteristics of coronaviruses in bats in Korea; and ii) the appearance of TTSuVs (TTSuV1, TTSuV2) and TTV genogroup 3 (TTV 3) in sick pigs from domestic swine farms in South Korea during the 2017 – 2018 period.

1.2. Materials and methods

1.2.1. Genomic characterization of alphacoronavirus isolated from bats

1.2.1.1. Sampling, RNA-extraction, and RT-PCR

From July to September 2020, six carcasses of different microbat species (*Eptesicus serotinus*, *Myotis petax*, *M. ikonnibovi*, and *Pipistrellus abramus*) were collected from Kangwon and Gyeongbuk provinces (Table 3). Samples were kept in ice packages then transferred to the College of Veterinary Medicine, Seoul National University. Organs of the bat carcasses (lung, intestine, and liver) were homogenized in 1mL of Dulbecco's Modified Eagle Medium (DMEM) followed by three cycles of the freeze-thaw procedure. 150 µl of this homogenized solution was used for RNA extraction using a DNA/RNA extraction kit (iNTRON Biotech, Korea) according to the manufacture's protocol. Previously published pancoronavirus primers (Poon et al., 2005) were applied for screening the presence of coronavirus in the bat samples (Table 4). RT-PCR reactions using the TOPScript One-step RT-PCR kit (Enzynomics, Korea) were performed under the condition of initial heating of 50ºC for 30 min, 95ºC for 10 min; followed by 40 cycles of 95ºC for 30 sec, 55ºC for 30 sec and 72ºC for 30 sec; and a final elongation step at 72ºC for 7 min. Corrected bands were purified by gel extraction followed by directed DNA sequencing.

1.2.1.2. Whole-genome sequencing, genome assembly, and annotation

To prepare RNA samples for next-generation sequencing (NGS), 0.5 mL of the homogenized solution was treated with 10 µL of RNase (4 mg/mL) (Biosesang, Korea) and 10 µL of DNase (10 U/µL) (Promega, USA) for 30 min. The nuclease-treated solution was filtered through a 0.2 µm filter (Sartorius, Germany). Finally, particle-associated RNA was extracted as described above. The RNA sample was sent to Macrogen for NGS using a library of 346 bp in size.

Raw data of 101 bp pair-end sequencing was filtered to remove the low-quality base calling by FastQC using the recommended parameters. Filtered reads were assembled *de novo* using SPAdes software (Bankevich et al., 2012). A scaffold related to coronavirus was detected by Blastn by comparing it with the coronavirus database. Next, the 3'-end sequencing was performed as described elsewhere (Scotto–Lavino, Du, & Frohman, 2006).

The whole-genome sequence of the novel coronavirus was annotated by the Z-curve tools (L. L. Chen, Ou, Zhang, & Zhang, 2003). Putative structural and non-structural proteins were validated by the Blastp method. Functional domains of the proteins were analyzed by Interpro (https://www.ebi.ac.uk/interpro/search/sequence-search) (Mitchell et al., 2019) using the following databases: CATH-gene3D, CDD, MobiDB, HAMAP, PANTHER, Pfam, PIRSF, PRINTS, ProDom, PROSITE, SFLD, SMART, SUPERFAMILY,

and TIGRFAMs. RNA structural elements were scanned with the Rfam database (https://rfam.xfam.org/) (Kalvari et al., 2021).

1.2.1.3. Sequence alignment and phylogenetic construction

Recombinant events were commonly detected and continuously played roles in the evolution of coronaviruses (Graham & Baric, 2010; S. Su et al., 2016). For classification with previously known, well-defined viruses of the alphacoronavirus genus, this study did not perform recombination analysis prior to phylogenetic reconstructions. All phylogenetic trees were inferred based on the whole genome, structural- and nonstructural- protein-encoding genes rather than the genomic fragment in between the predicted breakpoints.

The obtained genome, structural- and nonstructural- protein-encoding genes were aligned with those of the representative species belonging to the alphacoronavirus genus by the MAFFT algorithm (Katoh & Standley, 2013). Phylogeny trees were constructed using Iqtree2 (Minh et al., 2020) using the best-fit substitution model, automatically selected by option "-m MFP" (Kalyaanamoorthy, Minh, Wong, Von Haeseler, & Jermiin, 2017). Statistical support was obtained by performing ultrafast bootstrap approximation (Hoang, Chernomor, Von Haeseler, Minh, & Vinh, 2018). The constructed trees have been displayed by Figure Tree v1.4.4 (https://github.com/rambaut/Figuretree/).

1.2.1.4. Potential host prediction

To investigate the cross-infection of this strain, an online web tool (available at http://host-predict.cvr.gla.ac.uk/) was used to predict the potential reservoir host (Babayan, Orton, & Streicker, 2018). A model combining genomic biases and the phylogenetic neighborhood was applied in this study for greater accuracy. In detail, the coding sequence of all putative genes and the whole genome of the HCQD-2020 strain were used for prediction. The results were represented as a box-plot graph displaying the min, 25^{th} percentile, median, 75^{th} percentile, and max probability scores of each group of reservoir hosts. The higher the score, the more significant was the probability that a group of hosts acted as a reservoir.

1.2.1.5. Virus isolation

The virus was isolated using the spinoculation method described in a previous study with some modifications (Guo, Wang, Yu, & Wu, 2011). In brief, Vero cells in Dulbecco's Modified Eagle Medium (DMEM) plus 5% FBS were mixed with the virus and centrifuged at 500g for 30 min. Next, the cells were remixed and centrifuged twice. Finally, the cells were seeded in a T25 flask and incubated at 37 °C, 5% CO_2 for 12 h. The cells were then washed thrice to remove any unbound cells. The infected cells were inoculated with the DMEM containing 0.3% tryptose phosphate broth and 0.05% yeast extract and trypsin (10 μg/mL). The cells were observed daily and the virus was passaged by the same method. The present virus was confirmed by RT-PCR using specific

primers. Viral particles were analyzed by JEM-2100 transmission electron microscopy (TEM) (JEOL, Japan) utilizing the negative staining method.

1.2.2. Genomic characterization of torque teno virus isolated from swine farm

1.2.2.1. Sampling and DNA-extraction

January 2017 to December 2018, 470 clinical samples (sera, tissues in the lung, kidney, liver, and lymph node, samples are pooled in each group) from 9 provinces of South Korea were sent to the lab for diagnosis of respiratory viral diseases. The total DNA was extracted using a Viral DNA/RNA Extraction Kit (iNTRON Biotech, Korea) and was immediately used for amplification or stored at -20 °C.

1.2.2.2. Detection of TTSuV1, TTSuV2, and TTV3

Methods for detection of TTSuV1 and TTSuV2 were following the previous studies (K. Li et al., 2013). it was further investigated the most widely spread TTV3 to confirm cross-species infection. Detection of TTV3 using AI-1F and AI-1R as mentioned below (Dencs, Hettmann, Szomor, Kis, & Takács, 2009). The PCR reaction was performed using an i-StarMaster Mix PCR Kit (iNTRON Biotech, Korea). For genetic characterization, TTSuVs of the 3 strains (M117, N86, and N116) were completely sequenced by a primer walking method (K. Li et al., 2013). The specific PCR products were purified

by the gel extraction method and further processed for TA cloning and transformation (Kim et al., 2014). Putative ORFs of the obtained sequences were predicted using the ORF finder tool (https://www.ncbi.nlm.nih.gov/orffinder/) with the minimum length of 50 amino acids and the start codon was selected as ATG and alternative initiation codons as suggested by Tanaka et al. (2001). Functional analyses of the putative protein were detected by BLAST (Johnson et al., 2008). Sequence alignment was applied by MAFFT using the default option (Katoh & Standley, 2013).

1.2.2.2. Phylogenetic analysis of TTSuV1, TTSuV2, and TTV3

To the phylogenetic study, the best nucleotide substitution model, the complete genome sequence model was selected automatically by specifying the '-m TEST' option in IQ-TREE version 1.3.8 (L. T. Nguyen, Schmidt, von Haeseler, & Minh, 2014). In this study, the best plot model (GTR+G4) was used for phylogenetic analysis. For genotyping, it was collected from the TTSuVs reference sequences (K. Li et al., 2013) and the TTVs reference sequences (Hsiao et al., 2016).

1.3. Results

1.3.1. Genetic characterization of coronaviruses

1.3.1.1. Coronavirus detection in bat samples

To examine the presence of coronavirus in the bat samples collected in this study, organ samples of each bat including the lungs, intestine, and liver were applied for RNA extraction followed by RT-PCR using the pan-CoV primers. Of which, only the intestinal sample from *E. serotinus* collected from Gyeongbuk exhibited a single band of 440 bp as expected. All other samples were negative with coronavirus. Therefore, this band was extracted for Sanger sequencing. Phylogenetic analysis indicated that this isolate belonged to the alphacoronavirus genus (Figure 7).

1.3.1.2. Whole-genome assembly and annotation

Whole-genome sequencing using the Illumina platform was carried out to further analyze the genomic characteristics of the isolate detected in this study. A total of 7.2 Gbps with the percentage of high-quality base calling of 98.74% and 96.46% for Q20 and Q30 was obtained. A near complete genome (28,752 nucleotides excluding the poly-A tail with the average depth of 30X) of the alphacoronavirus strain HCQD-2020 (GenBank accession number: MW924112) was obtained and annotated. Sequence annotation showed that this strain contains

seven common open reading frames (ORFs) in the typical order 5′-UTR-ORF1ab-S-ORF3-E-M-N-ORF7-3′-UTR (Figure 8). Hexanucleotide transcriptional regulatory sequences (TRSs) required for the transcription of complete and subgenomic RNA were also identified (Table 5). Additionally, the putative signal sequences including a partial 5′-UTR, a 3′-UTR, and a coronavirus frameshifting stimulation element conserved the slippery sequence (Table 6). Characteristics of putative nonstructural proteins (NSP) 1-16 are described in Table 7. The appearance of a small ORF (or ORFs), with unknown function, (normally named as ORF7) downstream of the nucleocapsid encoding gene has been reported in some other species belonging to this genus. Nevertheless, in this study, neither Blastn nor Blastp revealed homology sequences for putative ORF7 of the HCQD-2020 strain.

1.3.1.3. Phylogenetic analysis suggested that HCQD-2020 strain might be a novel species belonging to the alphacoronavirus genus.

A whole-genome comparison indicated that our strain was mostly related to BatCoV Anlong57 (KY770851) and SAX2011 (NC_028811) with the percentage identity of 56.1% and 55.7%, respectively (Figure 9). Additionally, amino acid comparison of seven highly conserved regions in replicate proteins of HCQD-2020 with other members of alphacoronavirus indicated that the highest similar regions of HCQD-2020 with other known species was

approximately 80% in Nsp12, Nsp13, and Nsp14 (Figure 10b) which were far below the cutoff value of a new species at 90% amino acid identity according to the International Committee on Taxonomy of Viruses (ICTV). In other regions, the amino acid sequence's similarity was under 75% (Figure 10a, 10b). More specifically, Nsp3 was the most distantly related between HCQD-2020 and other strains, with amino acid identity ranging from 27 – 52%; followed by Nsp5, with the rank of 40 - 67% (Figure 10a). On the other hand, conserved regions located in ORF1b were more conserved between the present strain and others, with the difference being about 19 - 45% (Figure 10b). Phylogeny based on the whole genome sequence also indicated that our strain is distantly related to other known species belonging to alphacoronavirus (Figures 11, 12). This result suggests that HCQD-2020 might be a new species belonging to alphacoronavirus.

Further classifications were conducted based on the topology of phylogeny constructed based on two main nonstructural protein-encoding genes, ORF1a and ORF1b, and four main structural protein-encoding genes. Except for the highly similar topological trees based on the ORF1a and ORF1b (Figures 13a, 13b), the remaining phylogenetic trees revealed the change in the position of the HCQD-2020 strain within the alphacoronavirus genus (Figures 13c to 13f). Even so, this strain was placed on a separate branch from the other known species of alphacoronavirus, further supporting that HCQD-2020 is likely a

novel species.

1.3.1.4. Virus isolation and in silico cross-species infectious ability examination

Bat coronaviruses are mostly significant due to their risk of zoonotic diseases. In this study, an *in silico* analysis is applied to predict the potential infection of this virus in another host. The results indicated that, besides its natural reservoir of microbats (*Vespertilioniformes*), this strain can also infect other hosts belonging to the order Artiodactyla (Figure 14) with equal probability. In detail, the q1, median, and q3 of the probability scores of the Artiodactyla host group were 0.03, 0.13, and 0.43, respectively, while the corresponding values for the vespbat host group were 0.02, 0.1, and 0.44. These results indicated the risk of cross-species infection of the HCQD-2020 strain.

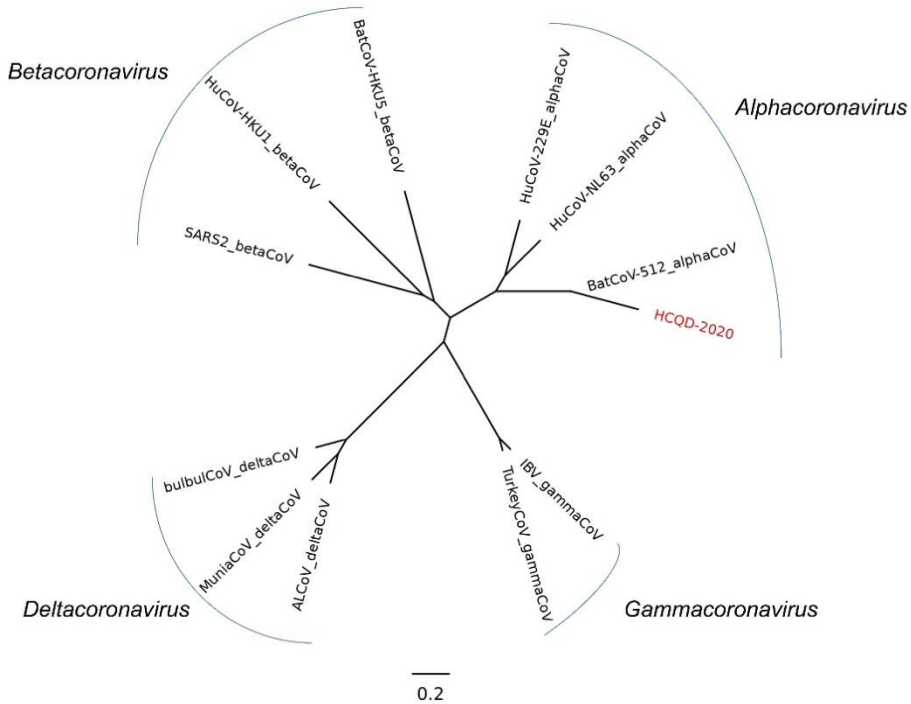

Figure 7. Initial classification of HCQD-2020 strain within subfamily *Coronavirinae* using the conserved region of RdRp encoding fragment. HCQD-2020 belongs to the genus alphacoronavirus, highly supported by the bootstrap value. Our strain was highlighted as red.

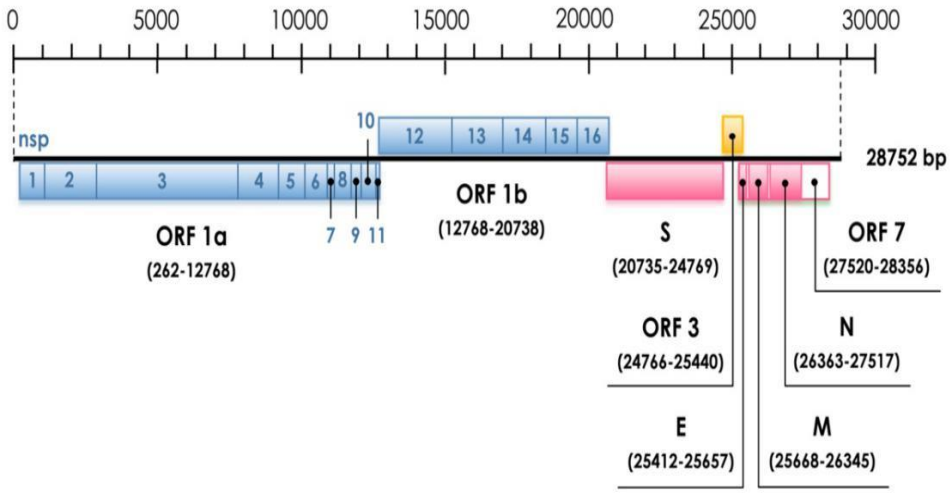

Figure 8. Genome organization and whole-genome phylogenetic analysis of novel alphacoronavirus strain HCQD-2020. This strain contained seven open reading frames (ORFs): ORF1a, ORF1b (light blue box as non-structural proteins); S, E, M, N (pink box as structural proteins); ORF3 (orange box as accessory protein) and unknown function ORF7 (white box).

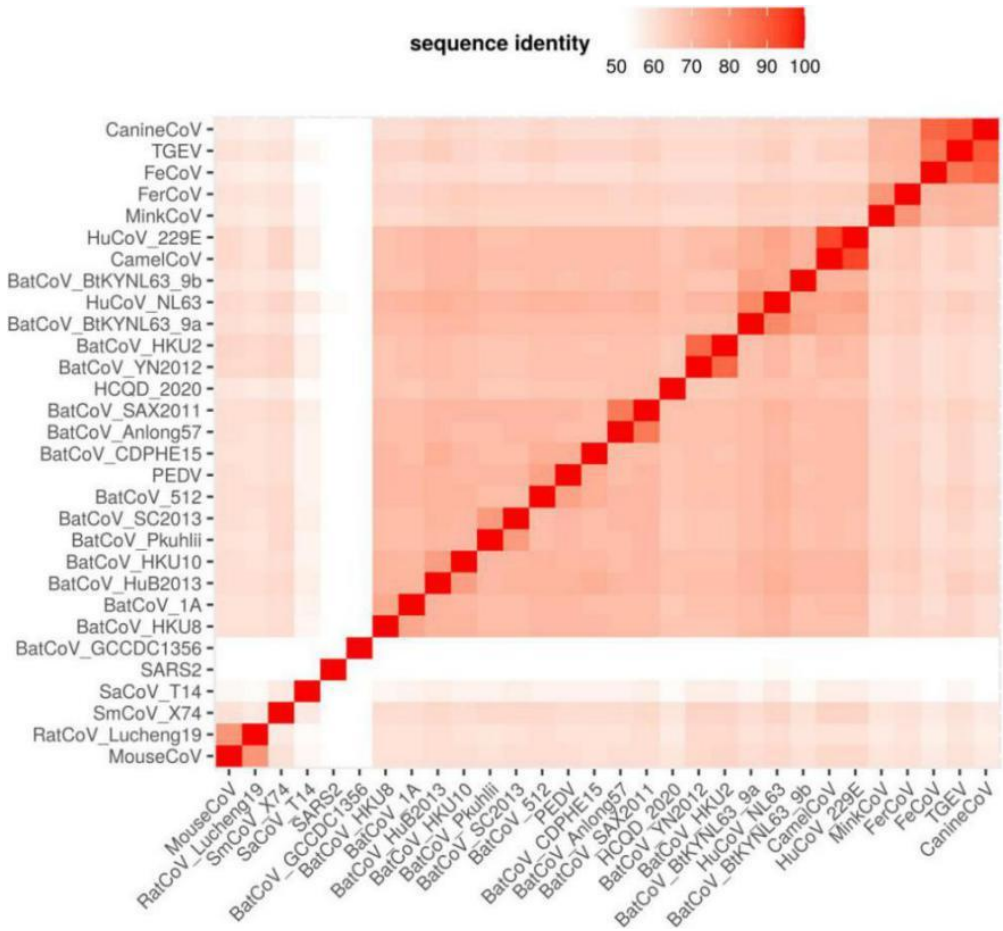

Figure 9. Heatmaps represented whole genome comparisons between HCQD-2020 and other known species of alphacoronavirus and betacoronavirus. The color scale represented the sequence identity in the percentage of each sequence pair. The similarities between the HCQD-2020 strain and other strains were very low.

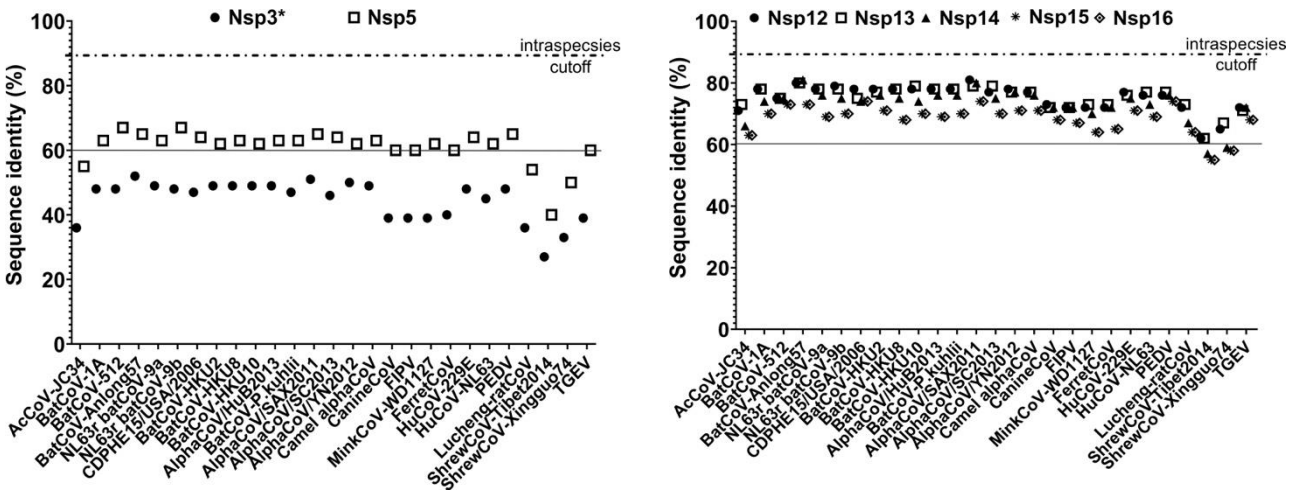

(a) **(b)**

Figure 10. Amino acid sequence comparisons of conserved domains in replicated polyproteins between the HCQD-2020 strain and other alphacoronaviruses. The conserved regions of Nsp3 and Nsp5 in ORF1A (**a**) and Nsp12 - Nsp16 in ORF1b (**b**) were compared between HCQD-2020 strains and other reference strains * For Nsp3: Only papain-like protease and ADP-ribose binding domains were applied for comparison. The solid lines were used to highlight the low similarity of Nsp3 and Nsp5 compared with the remaining Nsps

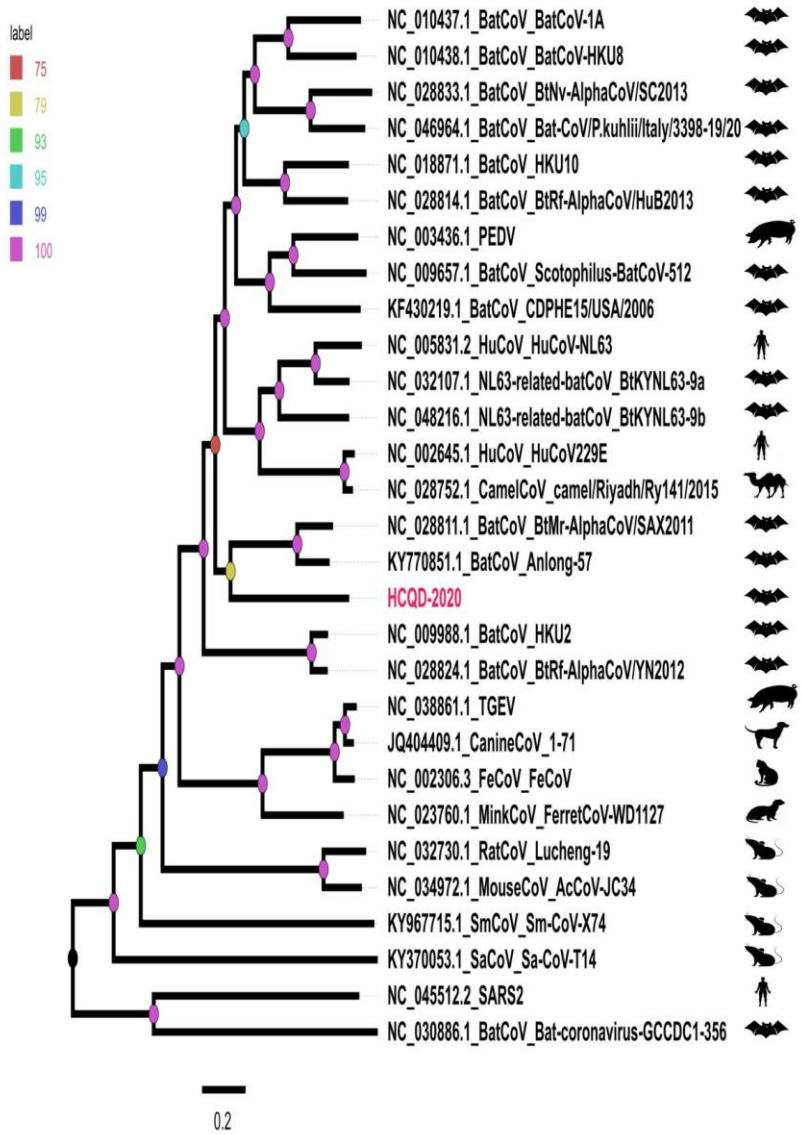

Figure 11. Phylogenetic tree represents the relationship among species and their hosts in the *alphacorona* genus constructed from the whole-genome sequence. SARS-CoV-2 and GCCDC1-356 belonging to betacoronavirus were used as out group. The present strain was highlighted in red.

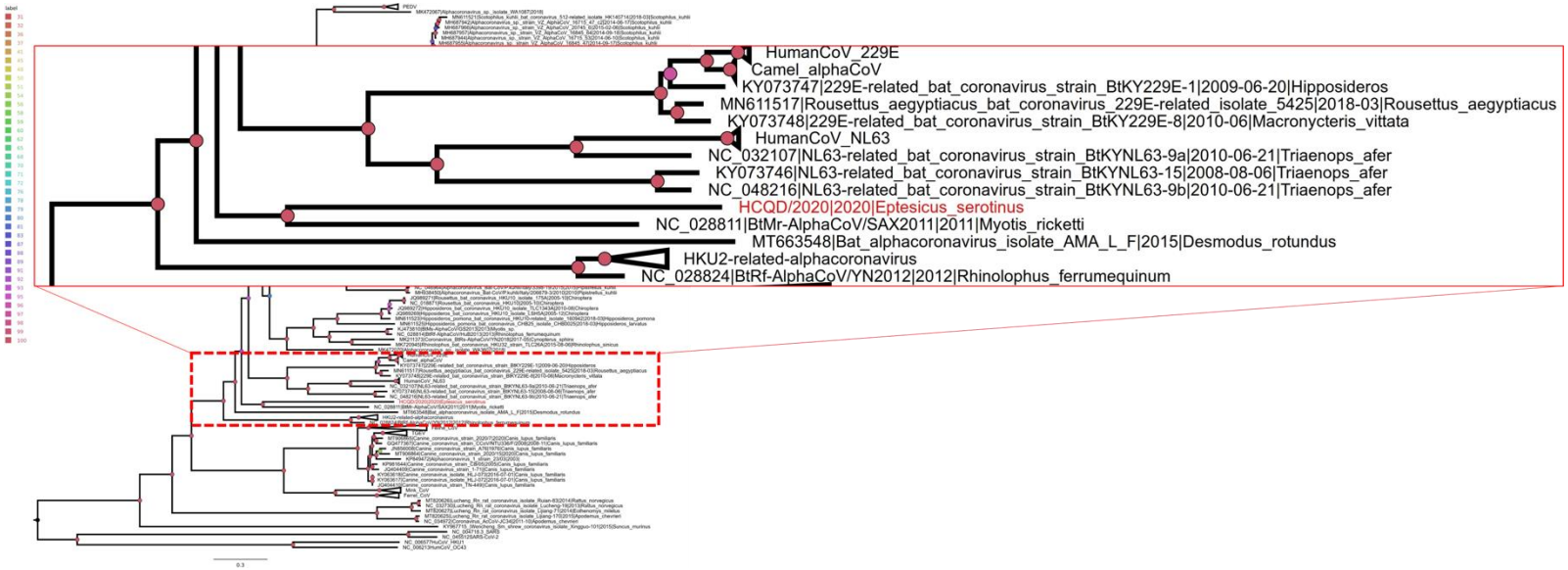

Figure 12. Phylogenetic tree construction based on whole-genome sequence analysis results indicated that the HCQD-2020 strain was distantly related with other published strains belonging to alphacoronavirus. The present strain was highlighted as red.

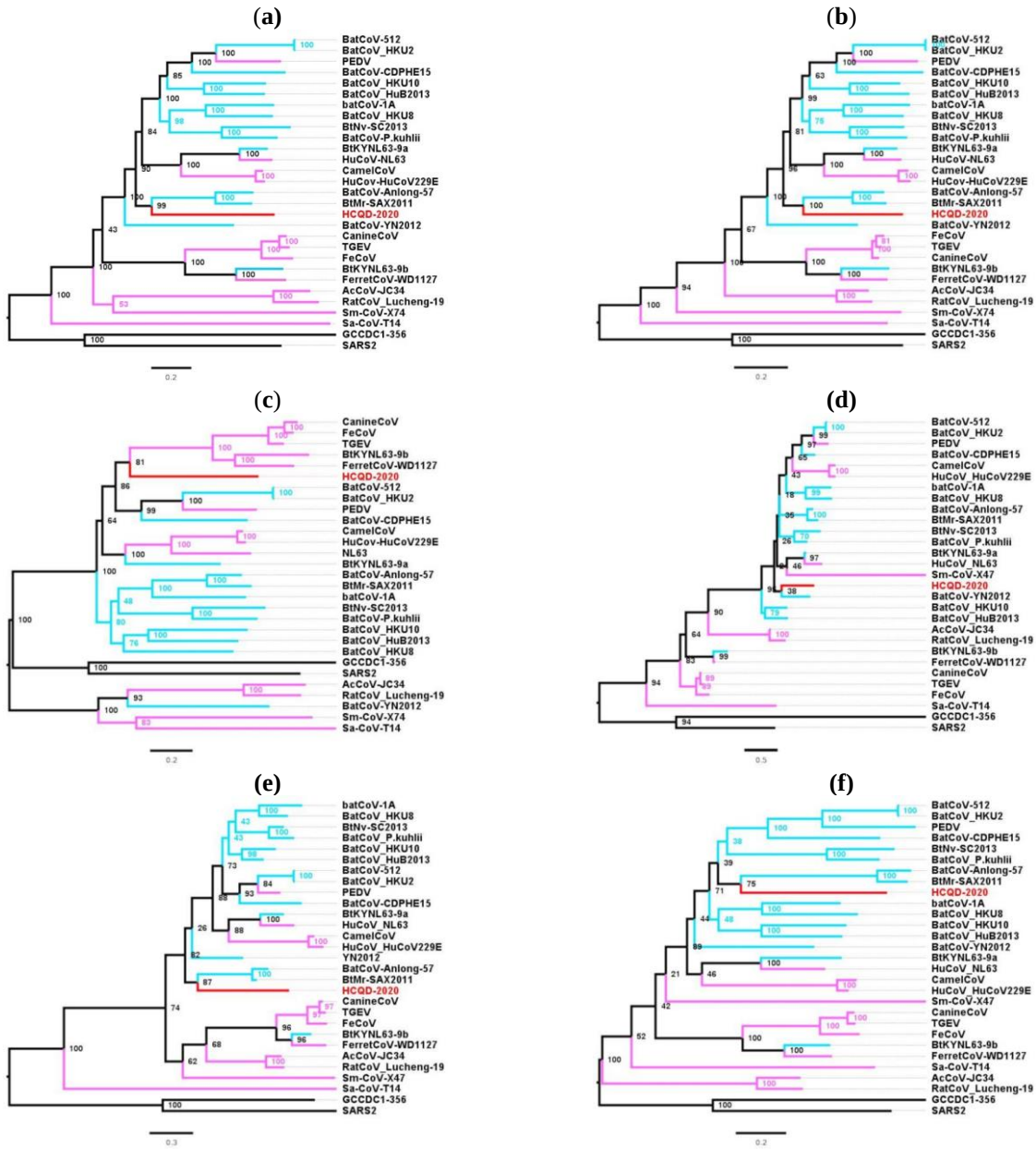

Figure 13. Phylogenetic analysis of the novel coronavirus based on the main nonstructural and structural protein-encoding genes. Phylogenetic tree construction is based on the ORF1a (**a**), ORF1b (b), S (c), E (d), M (e), and N (f) genes, respectively. The present strain is highlighted in red. The coronavirus species originating from bats are presented in light blue while the non-bat mammalian host coronaviruses are labeled in pink. The scale bar indicates the number of substitutions per site.

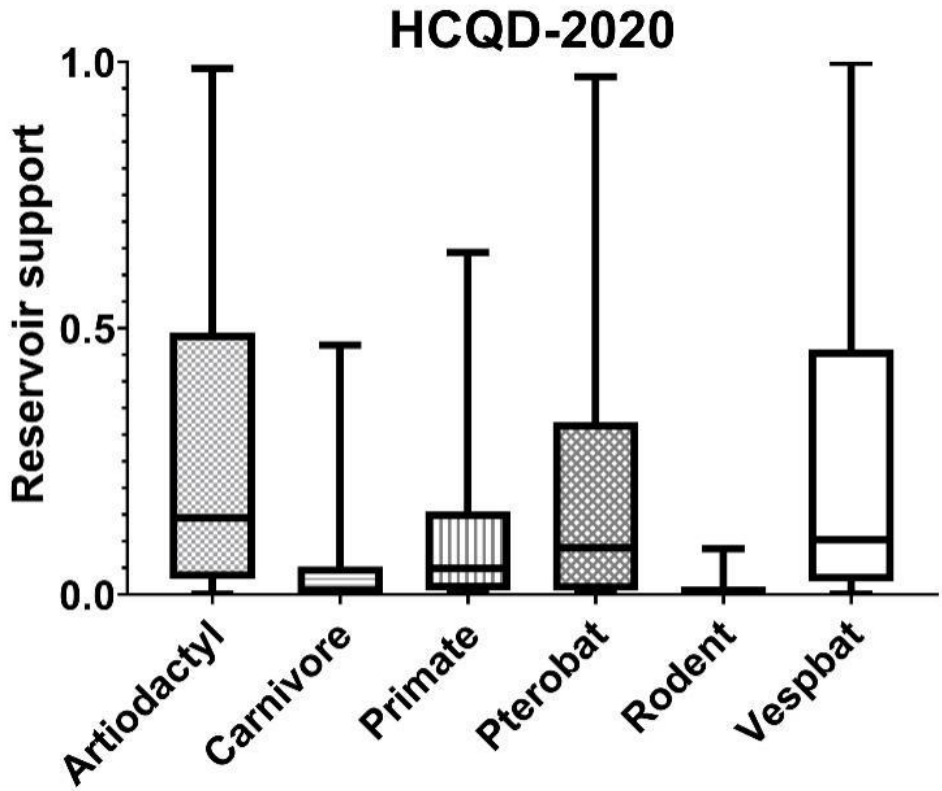

Figure 14. Potential host prediction of HCQD-2020 strain cross-infection in other orders of mammalians using viral host predictor tools. The boxes represented values between 25th and 75th percentile of the probability scores while the whiskers showed the min and max probability scores.

Table 3. Information of bat samples collected in this study.

Bat species	No of samples	Collection date	Collection location
Eptescus serotinus	1	20/07/2020	Gyeongbuk
Myotis aurascens	2	03/08/2020	Gyeongbuk
Myotis petax	1	05/09/2020	Kangwon
Myotis ikonnikovi	1	05/09/2020	Kangwon
Pipstellus abranus	1	13/09/2020	Gyeongbuk

Table 4. Oligonucleotide sequences of primers used for screening pancoronavirus.

Primer name	Sequence	Reference
Pan-CoF	GGTTGGGACTATCCTAAGTGTGA	Poon et al., (2005)
Pan-CoR	CCATCATCAGATAGAATCATCATA	
alpha-F	GCACAAGTGCTTACAGAGGTTG	This study
alpha-R	CAACACCGTCATCAGACAGG	

Table 5. ORFs and TRS location of novel coronavirus strain HCQD-2020.

ORFs	Length (nt/aa)	TRS location	TRS sequence(s) (distance to ATG)[1]
ORF1ab	20477/6824	36	CCCCTC**AACTAAAC**GAA(215)ATG
S	4035/1344	20731	GTTTC**AACCAAAT**GAAAAA
ORF3	675/224	24723	AGTCG**AACTAAAC**TCA(34)ATG
E	246/81	25342	TATTG**AACTAAGT**GAC(61)ATG
M	678/225	25658	TGTCT**AACTAAAT**CAA(1)ATG
N	1155/384	26530	TAATC**AATTAAAC**AAA(4)ATG
ORF7	837/278	27514	ACTC**AACTAAAC**ATG

[1] The TRS sequences were highlighted as bold. The number indicated the distance in nucleotide from TRS to start codon. Initial codons were underlined.

Table 6. Secondary structural genomic elements of novel alphacoronavirus strain HCQD-2020.

RNA structural elements	Position	Rfam	Note
5’ UTR	1 - 289	RF03116	
-1 frameshift element	12762 - 12768		Conservative heptamer TTTAAAC
Frameshifting stimulation	12770 - 12848	RF00507	
3’ UTR	28408 - 28753	RF03121	

Table 7. Putative nonstructural proteins and the cleavage sites of polyprotein 1a and 1 ab of the HCQD-2020 strain.

Nsp	First - last amino acid residues [1]	Protein size	Cleavage sequence	Putative functional domains
Nsp1	M1 - G282	282	GNVEAG|DVVFTS	Unknown function, PFAM: PF19211
Nsp2	D283 - G890	608	FKRGGG|VTFGGD	Unknown function, PFAM: PF19212
Nsp3	V891 – G2580	1690	IVQKSG|SGPQFP	Papain-like protease, PFAM: PF08715
Nsp4	S2581 – Q3058	478	SSLQ|AGLR	Membrane spanning domain, PFAM: PF16348
Nsp5	A3059 - Q3360	302	VTLQ|GGRK	3C-like protease, PFAM: PF05409
Nsp6	G3361 – Q36439	279	SSVQ|SKLT	Membrane spanning protein, PFAM: PF19213
Nsp7	S3640 – Q3722	83	AMLQ|SIAS	RNA replicate protein complex, PFAM: PF08716
Nsp8	S3723 – Q3917	195	VKLQ|NNEV	Transferase activity, PFAM: PF08717
Nsp9	N3918 – Q4026	109	IRLQ|AGKQ	Single strain RNA binding protein, PFAM: PF08710
Nsp10	A4027 – Q4161	135	ANVQ|SFDQ	Nucleic-binding protein, PFAM: PF09401
Nsp11	A4162 - D4178	17	-	The short peptide in C-terminate of ORF1a
Nsp12	A4162 - Q5062	901	TVLQ|ASGM	RNA-depend RNA polymerase, PFAM: PF06478
Nsp13	A5063 – Q5659	597	TDLQ|ATEG	Helicase, Interpro: IRP027351
Nsp14	A5660 – Q6178	519	TKIQ|GLEN	Exoribonuclease and Guanine-N7 methyltransferase, Interpro: IPR009466
Nsp15	G6179 - Q6526	347	PQLQ|SAEW	EndoU-like endoribonuclease, PFAM: PF19215
Nsp16	S6526 – K6825	300	-	O-methyltransferase, PFAM: PF06460

[1] Number indicated the position of amino acid in the nonstructural protein 1a or 1ab.

1.3.2. Genetic characterization of torque teno viruses

In this study, pigs showing signs of respiratory problems (n = 470) collected on the detection rates of TTSuVs in 2017 and 2018, the positive rate of TTSuV1 were 17% (47/280), 15% (28/190) in 2017 and 2018, and in TTSuV2, it was 34 % (95/280), 39% (73/190) in 2017 and 2018 respectively. In total, positive 16% (75/470) and 36% (168/470) were detected in TTSuV1 and TTSuV2. Also, coinfection of both group (TTSuV1 and TTSuV2) was 8% (38/470). Among of positive samples, 3 strains (M117, N86, and N116) registered in GenBank accession numbers: MK452763- MK452765. The genetic relationship within the complete genome references in TTSuVs, two strains of M117 and N86 belong to 1b and 1c of TTSuV1, the other N116 strain located in subtype 2b (Figure 15). From the collected samples (*n*=470), it is further investigated the most widely spread TTV3 genogroup to confirm cross-species infection. Interestingly, the results detected only 2 field strains (M265_Korea_2017; MK452766 and N119_Korea_2018; MK452767) of which PCR amplicon band site is 350 bps. In the sequencing blast results, the strains of M265 and N199 were shown 96% and 94% homology with TUPB (GeneBank accession no. AF247137) strain. For genetic characterization, the 2 strains (M265_Korea_2017 and N119_Korea_2018) were completely sequenced by using a primer walking method (P. Biagini et al., 2000).

As focusing on the TTV 3 strains, it was found that M265 and N119 each

strains have 3,817 full-length genome, and the M265 have 3 ORFs (ORF1, ORF2, and ORF3) and N119 has 4 ORFs (ORF1, ORF2, ORF 2-2, and ORF 3) (Figure 16a, b). The strains showed of full-length G+C contents 50.79% and 50.87%, which were ORF1, ORF2, and ORF3 sequences encoded 760, 156, and 98 aa. One more found of the N119 strain in ORF2-2 was 163 aa.

The complete genome sequences of each strain have 98.4% homology. In the ORF1, every 2 strains showed 98.2% similarity in nucleotide and 95.4% in amino acid, and ORF 2 showed 95.9% and 92.3%, and ORF3 showed 98.9 % and 98%, respectively. As inferred based on the ORF1 aligned with previous phylogenetic tree study within TTVs, the M265 and N119 strains belonging to genogroup 3 of subgroup 3c, which close to the TUPB (GeneBank accession no. AF247137) strain (Figure 16c).

Further analysis indicated that the putative ORF1 of both two TTV genogroup 3 strains contained (i) the Agrinine-rich region located at N-terminate and (ii) three conserved motifs of replicate-associated protein including motif 1 (FSL); motif 3 (YxxK) and motif 4 (GxGK: P-loop) (Figure 17a, b). Similarly, the conserved motif ($WX_7HX_3CXCX_5H$) of ORF2-TTV was observed in M265 strain while an aa change H→Q in the first histidine of the motif was found in N119 (Figure 17c). Of the putative ORF3, a serine-rich domain was found in the C-terminate of both strains (Figure 17d).

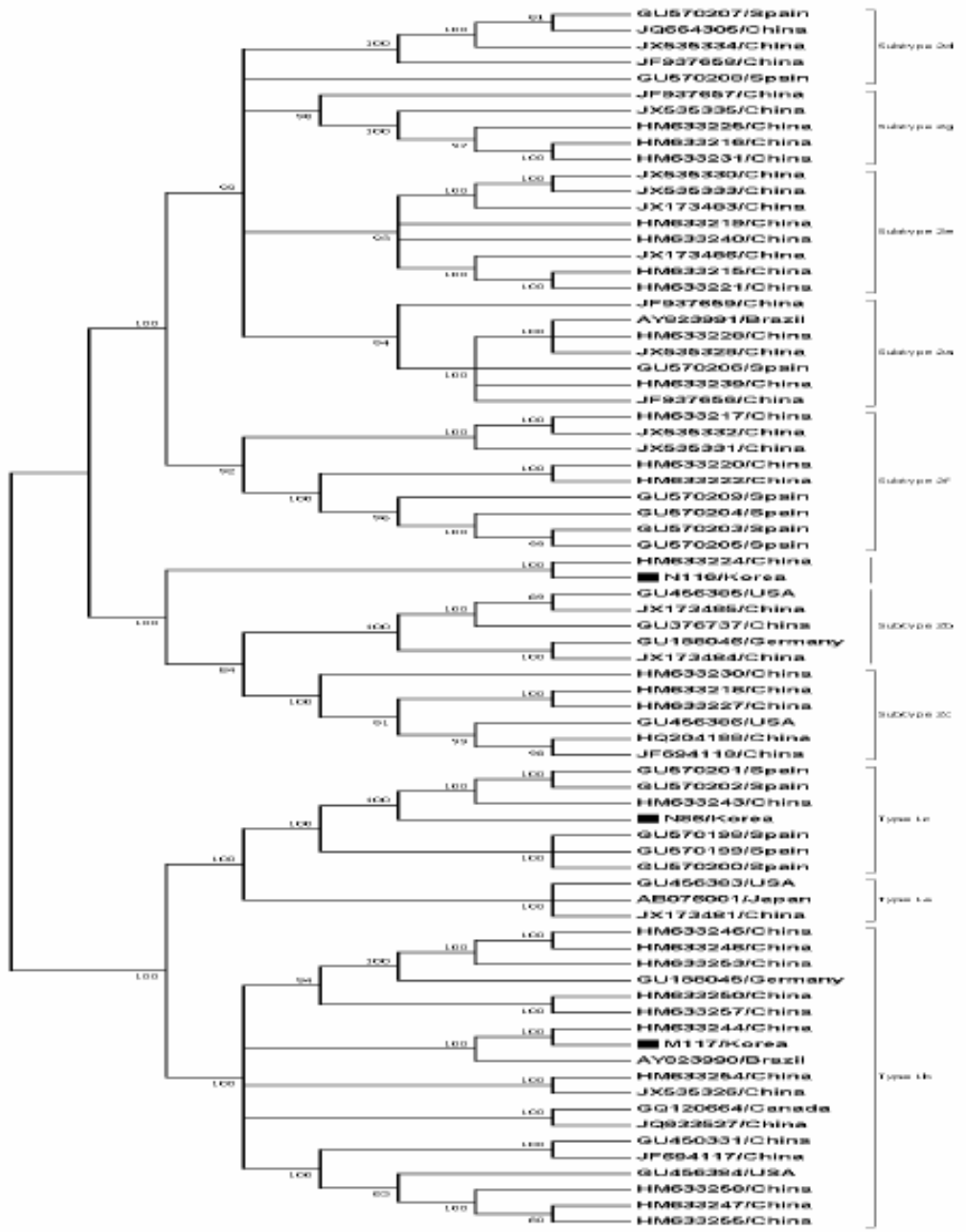

Figure 15. Phylogenetic tree of genotype TTSuVs. Samples N86, M117 and N116 were clustered to several known TTSuV1 and TTSuV2 sequences. (Highlighted in square box ■)

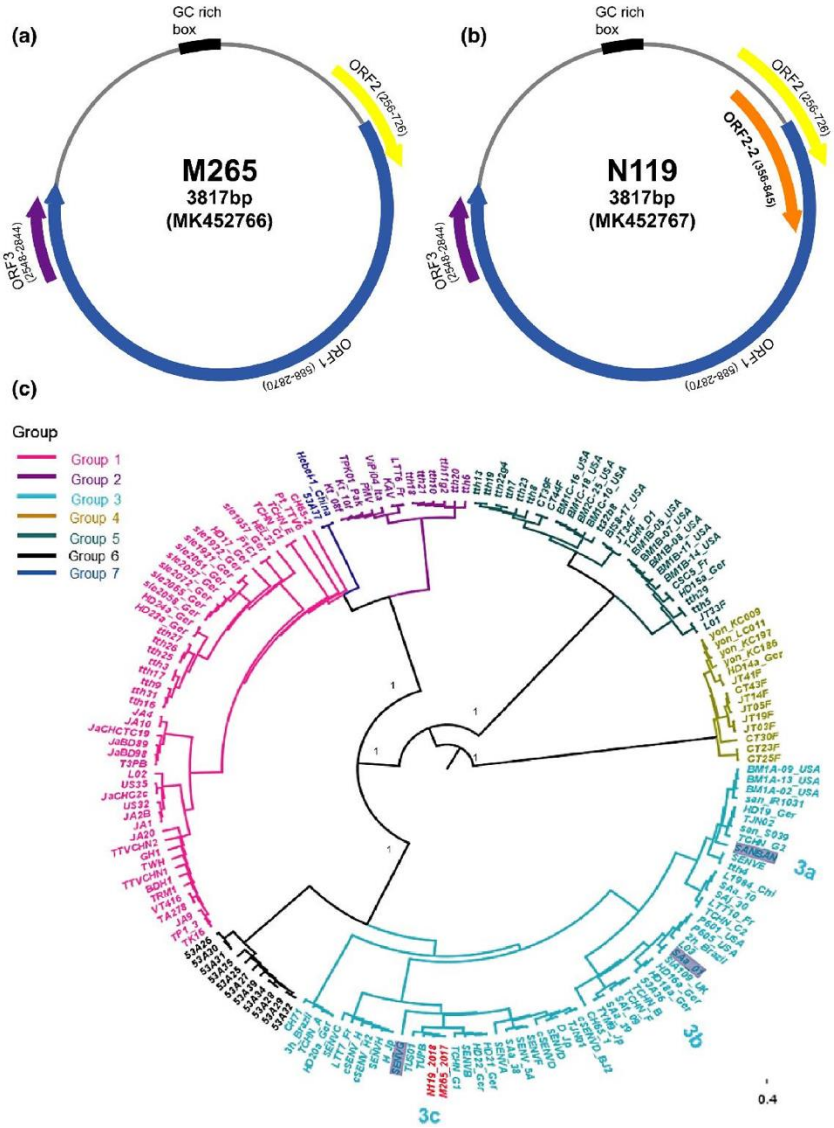

Figure 16. Predicted genome map of Torque teno viruses (TTVs) of M265 (a) and N119 (b) strains. Each strain including ORF frame site with arrow sign. The phylogenetic tree (c) is constructed using the maximum likelihood trees of TTVs ORF1 genomes with bootstrap 1,000, automatically best fitting model selected by IQ-TREE. The M265 and N199 (in this study) strains were highlighted with red color, and the posterior supported values were represented in the node bar. The SANBAN, SAa-01 and SENVG grey colors are representative for showing subgroup 3a, 3b and 3c, respectively.

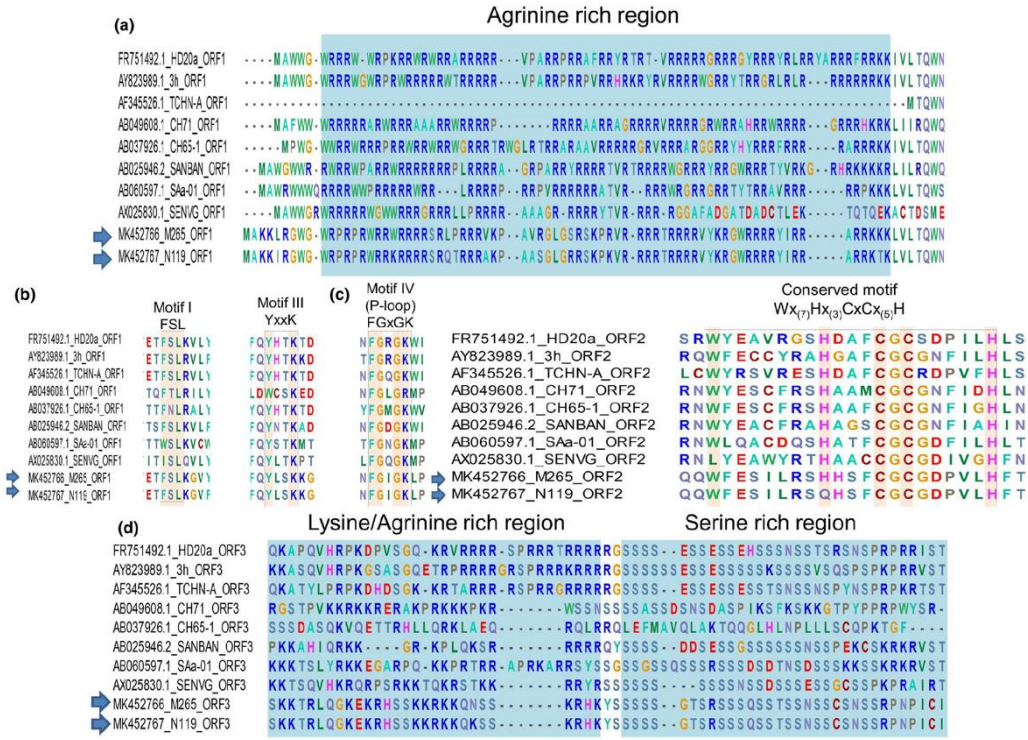

Figure 17. Functional domains of the putative ORF1 (a,b), ORF2 (c), and ORF3 (d). Torque teno viruses (TTVs) strains M265 and N119 (arrows) were predicted to contain several conserved regions (highlighted as light blue) and motifs (indicated as dash boxes). The well-conserved amino acid in each motif are highlighted; 'x' was any amino acid

1.4. Discussion

In this study, several bat species belonging to genera Eptesicus, Myotis, and Pipistrellus have been investigated for the presence of coronavirus. These species share their habitat niches with other wild and/or livestock animals, thereby increasing the risk of cross-contamination to humans involving any of the viruses they carry. Of these samples, a distantly genetically related viral isolate belonging to alphacoronavirus was detected in E. serotinus. This result further contributed to the genetic diversity of bat coronavirus in general and alphacoronavirus in particular.

Whole genome comparison indicated that the HCQD-2020 strain was distantly related to other known species of alphacoronavirus (Figure 9). Genome-based and functional-genes-based phylogeny constructions also indicated that this strain formed a separate branch in phylogenetic trees (Figures 11, 13). Recent metagenomic studies of bat virome revealed several potential novel species within alphacoronavirus detected in bats around the world (Bergner, Orton, & Streicker, 2020; Lazov, Belsham, Botner, & Rasmussen, 2021; Prada, Boyd, Baker, O'Dea, & Jackson, 2019; H. Zhou et al., 2021). This result, along with other up-to-date studies, once again supported the genetic heterogeneity of this genus.

All members of this genus share a similar genomic organization containing

ORF1ab – S – ORF3 – E – M – N. Furthermore, additional ORFs located downstream of nucleocapsid–encoding gene were also observed in many species of this genus like Transmissible gastroenteritis virus (TGEV,) BatCoV-HKU2, BatCoV-512, and Shrew coronavirus (W. Wang et al., 2017). Besides the common ORFs found in other alphacoronavirus's members, a putative ORF7 was found at the 3' terminator of HCQD-2020's genome (Figure 8). Its sequence at the amino acid level was not homologous with any of the known protein sequences. It should also be noted that this putative ORF was likely the most distinct ORF of the currently known alphacoronavirus (W. Wang et al., 2017).

Evidence of host jumping of coronavirus from bat to other species belonging to even-toed ungulate animals were characterized in the case of PEAV which shares high nucleotide identity (approximately 95% sequence similarity) with bat-HKU2 strains (Gong et al., 2017). In this study, *in silico* analysis indicated that HCQD-2020, a distantly related species belonging to alphacoronavirus, can infect another host, especially those in the order Artiodactyla, which include some species like camels and pigs. Recently, a novel alphacoronavirus belonging to the species alphacoronavirus *I* that is usually found in pigs, dogs, and cats was detected in children with pneumonia in Malaysia (Vlasova et al., 2021). In our study, HCQD-2020 was successfully isolated in Vero cells. However, several cell lines should be applied to investigate the possibility of

transmission of this strain into other hosts.

It was reported that TTSuVs infections existed in many countries around the world (N. McKeown, M. Fenaux, P. G. Halbur, & X. J. V. m. Meng, 2004). In this study, the prevalence of TTSuVs in Korea during 2017-2018 were 44% (the positive rate of TTSuV1 and TTSuV2 were 16% and 36%, respectively and the co-infection of both type of TTSuVs were approximate 8%). The prevalence of TTSuVs in Korea in this study was equivalent to the positive rate of that in Thailand (McKeown et al., 2004). However, the detection rate of TTSuV1 and/or TTSuV2 in this study was lower compared to other reports in other countries (Blois et al., 2014b; K. Li et al., 2013b; Sibila et al., 2009) and even in comparison to the report in Korea before 2004 (McKeown et al., 2004).

The focus of study is investigating the potential appearance of TTVs genogroup 3, the *Alphatorquevirus* that is highly prevalent in humans and in sick pigs. Based on the results, two out of 470 samples were TTV genogroup 3 positive. Sequence comparison and phylogeny analysis indicated that the two strains share 98.4% sequence homology and belong to the subgroup 3c.

The TTVs genogroup 3 detected in pigs were predicted to contain the three common ORFs observed in other TTVs. Within the ORF1, the N-terminated region was an arginine-rich region (Figure 17a) which was similar to the capsid protein of circoviruses (Mou, Wang, Pan, & Chen, 2019). Furthermore, three replication-associated motifs were observed (Figure 17b). The presence of these

motifs in ORF1 of TTVs was previously reported elsewhere (Tanaka et al., 2001). Of the remaining ORFs, putative ORF2 of M265 contained the well observed motifs of $Wx_{(7)}Hx_{(3)}CxCx_{(5)}H$ in TTVs while a cluster leucine rich regions followed by Serine rich regions in the C-terminus were observed in present strains. These features are highly conserved in other *Anelloviruses* (Vibin, Chamings, Klaassen, & Alexandersen, 2020). To our knowledge, this is the first time the strains belonging to *Alphatorquevirus* were detected and studied.

In colletively, this study described the nearly complete genome of an alphacoronavirus species originating from bats and the information of TTSuV's prevalence in Korean swine farms. Based on the low sequence identity in coronavirus studies, the presence of a putative ORF7 with no homology to any known genes in Genbank, and distant relation with other representative species of alphacoronavirus, the HCQD-2020 strain, was proposed as a novel strain of this genus. *In vitro* and *in silico* analyses both supported that this newly identified strain of coronavirus can infect other hosts, not limited to bats.

The phylogenetic analysis of these isolates suggested evidence for a zoonotic potential of alphacoronavirus and torque teno virus. Further studies should focus on understanding the diversity of coronavirus and the probability of host jumping. As the zoonotic potential of TTV is analyzed, further the transmissibility of TTV is important for surveillance.

Chapter II. Evaluation of antiviral activities by chitosan and nano-graphene oxide against coronaviruses

Abstract

The coronavirus disease (COVID-19) caused by SARS-CoV-2, a novel betacoronavirus originating from bats, has been causing a global pandemic situation and severely threatening public health and global economy (P. Zhou et al., 2020). Although to a lesser degree than the COVID-19, several species belonging to alphacoronavirus and betacoronavirus, like PEDV or BCoV, have also been causing serious economic losses in livestock production (Luo et al., 2020). Thus, novel antiviral substances to control virus infections broadly and effectively are being largely demanded.

Chitosan has numerous biological activities, for instance, antimicrobial, antitumor, and antioxidant (Muxika, Etxabide, Uranga, Guerrero, & De La Caba, 2017). proprieties. Due to its unique biological activities, chitosan has gained considerable attention in recent decades. Nano-graphene oxide (nanoGO) has also been considered to be a promising viral inhibitor. It was demonstrated that nanoGO has antiviral properties due to it's extraordinary nanosheet structure and negative charge (Ye et al., 2015).

In this study, the antiviral effect and mammalian-cell toxicity of chitosan and nanoGO were evaluated. As a result, a 0.01% chitosan solution was determined to be an effective disinfectant against PEDV without cytotoxicity. Evaluation of antiviral activity of nanoGO against porcine epidemic diarrhea virus (PEDV),

bovine coronavirus (BCoV), and SARS-CoV-2 also revealed the potent broad-spectrum antiviral activity of nanoGO with no evidence of cytotoxicity even in the presence of high level of serum solution. Collectively, these results suggested that chitosan and nanoGO could be used as major ingredients for nontoxic disinfectants to prevent transmission of various coronaviruses.

Keywords: : Chitosan; Nano-graphene oxide; Antiviral activity; Porcine epidemic diarrhea virus; Bovine coronavirus; SARS-CoV-2

1

2.1. Introduction

During the last two decades, coronaviruses (CoVs) have been the cause of local and global epidemics, including Severe acute respiratory syndrome (SARS), Middle East Respiratory Syndrome (MERS), and Porcine epidemic diarrhea virus (PEDV) with the mortality rate around 10%, 35% and 95% respectively, threatening human health and economic well-being. For instance, the latter caused ten percent reduction of pig population in the USA in 2013 (Stevenson et al., 2013). Of interest, a number of betacoronaviruses (e.g., bovine coronavirus (BCoV), canine coronavirus (CRCoV), and dromedary camel coronaviruses) are closely related to this human pathogen; it was suggested that these species recombine and new subspecies emerge (Decaro & Buonavoglia, 2008; Nathalie et al., 2016). Currently, the pandemic outbreak of the febrile respiratory disease, so called COVID-19 has created a global transmission network, leading to an international crisis related to the catastrophic losses of human lives and financial meltdowns. Vaccines are available for coronavirus, but these diseases are still frequently noted in the livestock industry, partly because of emergence of new variant strains (Ye et al., 2015). Thus, the exploration of effective antiviral agents that can be effective on coronavirus is of great importance.

Up to date, there are several kinds of agents that are known to have antiviral

activities (L. Chen & J. Liang, 2020).

The interest in chitosan, a biodegradable, non-antigenic, non-toxic, and biocompatible natural polymer derived from chitin, is because of chitosan's several health- beneficial effects including highly antioxidant and antimicrobial activities (Muxika et al., 2017). Chitosan has a strong antimicrobial activity against Gram-positive, Gram-negative bacteria in addition to fungi (Qin & Li, 2020). Chitosan is widely used in several biomedical and biological applications, including drug carriers, water treatment, and as a scaffold for tissue engineering (Islam, Shahruzzaman, Biswas, Sakib, & Rashid, 2020). The antimicrobial properties of chitosan are dependent on essential factors, including pathogen type, pH of the media, structural properties, source, and concentration of chitosan (Rabea, Badawy, Stevens, Smagghe, & Steurbaut, 2003). The pH of the media is a crucial element to the antimicrobial activity of chitosan. The chitosan was evaluated for disinfectant effect and safety using a porcine epidemic diarrhea virus (PEDV) and Vero cells to identify its potential as a disinfectant for coronavirus.

Graphene oxide is a two-dimensional crystal structure characterized by a single atomic thick sheet formed by carbon atoms arranged in a hexagonal lattice (Geim & Novoselov, 2007). The oxygen-containing functional groups and the unique physicochemical properties facilitate their applications in bioengineering (Ye et al., 2015). The nanoGO has also been regarded as an

excellent candidate for anti-inflammatory and microbial therapy (B. C. Lee et al., 2020). The biological characterizations of nanoGO vary based on its own physical properties like size, oxidative level, as well as those of its additional groups. However, the biological properties of nanoGO might be affected in the presence of serum (S. Song et al., 2020) and the cytotoxic effects of GO is size-depend (Zhao et al., 2016), thus its application in therapy has been limited so far. Faced with the serious pandemic of COVID-19, nanoGO and its deliveries were considered as a great virucidal material to be applied in antiviral surfaces and coatings (Palmieri & Papi, 2020; Seifi & Reza Kamali, 2021; Srivastava et al., 2020). Based on the great potential antiviral activity of this substance mentioned above, this study was carried out to evaluate the antiviral properties of nanoGO against coronaviruses.

2.2. Materials and methods

2.2.1. Antiviral activities of chitosan to porcine epidemic diarrhea virus.

For evaluation of disinfectant effect of chitosan, a 1% chitosan solution was prepared by dissolving chitosan (deacetylate level: 95%, MW: 30 kDa) (M.-H. Nguyen, Hwang, & Park, 2013) in 1% acetic acid solution from NoAH Biotech (Korea). The PEDV strain DR-13 was cultivated in Vero cells using the method

described by Song et al., 2003 (D. Song, Yang, Oh, Han, & Park, 2003). The DR-13 is an attenuated PEDV strain through serial passages resulting in 51 nucleotides deletion in ORF3 gene (Park et al., 2008) and it is being used for PED oral vaccine (DR13 10^5 $TCID_{50}$/mL) commercialized in 2003 by Green Cross Vet. Prod. (Korea). Virus titration was carried out using a 96-well microplate with Vero cells. Virus cultures were 10-fold serially diluted with the virus replication medium containing trypsin. Confluent Vero cells of the microplate were washed three times with PBS and inoculated at 0.1 mL per well into five wells. Following adsorption for 1 h at 37 ℃, the inocula were removed, and the cells were washed three times with PBS. Subsequently, 0.1 mL of fresh virus replication medium containing trypsin was transferred into each well, and the cells were further incubated for 5 days at 37 ◦C. Fifty percent tissue culture infective doses (TCID50) were expressed as the reciprocal of the highest virus dilution showing cytopathic effect (CPE) (Kusanagi et al., 1992). Finally, viral inocula were adjusted to $10^{6.9}$ $TCID_{50}$/mL with PBS.

The disinfectant test was performed separately with two conditions: hard water (0.305 g $CaCl_2$ and 0.139 g $MgCl_2 \cdot 6H_2O$ per 1 L distilled water) and organic water (5% fetal bovine serum in hard water). The original solution (1% chitosan) was diluted 100- to 800-fold in both hard and organic water. Each diluent (1 mL) was mixed with 1 mL of virus solution ($10^{6.9}$ $TCID_{50}$/mL) or with 1 mL of non-viral culture medium for the toxicity control. Hard or organic

water (1 mL) was mixed with 1 mL of the virus solution as the negative control. The mixtures and negative controls (Hard or organic water) were incubated at room temperature for 30 min. Subsequently, viral titrations of each mixture and the negative controls were performed using the method described above. Each sample was tested in three replicates. A maximum dilution factor, in which the virus titer was reduced by at least 4 log10, was determined to be an effective dilution factor (de Oliveira et al., 2011; Jimenez & Chiang, 2006). Additionally, Indirect Immunofluorescence Assay (IFA) assays were performed to more precisely detect the presence of the virus. Before mixture inoculation, all procedures were performed in the same manner as described above. IFA assay was carried out using the PEDV IFA kit (MEDIAN Diagnostics inc.) 24 h after inoculation.

For the safety test, the 1% chitosan solution was diluted 100- to 800-fold in hard water. Hard water without chitosan was used for the negative controls. A 0.5 mL aliquot of each diluent and the negative control was inoculated into 1.2 x 10^4 cells/well seeded in a 24-well in which Vero cells were grown in a monolayer. Each sample was tested in three replicates. Cell morphology was observed after 24 h.

To investigate an effect of chitosan on cell activity, cell culture medium containing chitosan (1% chitosan, 1% acetic acid, 5% FBS, penicillin 100 units/mL, streptomycin 100 μg /mL, and amphotericin B 0.25 g/mL in DMEM)

was prepared. The medium was diluted 2- to 800-fold with the same solution without chitosan, which was also used for the negative control. Cell counting was followed Countess™ Cell Counting kits with protocol (Thermo Fisher Scientific inc., USA) at 24, 48, 72, and 96 h after inoculation. Each sample was tested in duplicate. The cell counting data were analyzed with Tukey's test using SPSS statistics 20 (IBM Corp., USA).

2.2.2. Antiviral activities of nano-graphene oxides to porcine epidemic diarrhea virus, bovine coronavirus, and severe acute respiratory syndrome coronavirus 2.

In this study, nanoGO was evaluated for antiviral activity in a solution partially mimicking biological fluid with the use of serum. The active ingredient, 1% nanoGO solution (3mg/ mL), was prepared according to the previous publication (B. C. Lee et al., 2020). The morphology of nanoGO was observed by FE-SEM: XL30 (Philips Corp., Netherlands), HR-TEM: JEM-ARM200F Cold FEG (JEOL Ltd., Japan) and AFM: SPM-9700HT (Shimadzu Corp., Japan). The size of particles was analyzed by CPS DC24000 particle analyzer (CPS instrument Corp., USA). Other characteristics of nanoGO were identify by Raman Spectroscopy NRS-3300 (Jasco Inc., Japan), FT-IR (TENSOR27, Bruker Corp., Germany), XRD SmartLab (Rigaku Corp., Japan), and XPS AXIS SUPRA (Kratos Corp., UK)

Steps in testing the antiviral activity of nanoGO are summarized as follows. The original solution of nanoGO was diluted in DMEM supplemented with 5% FBS. Each dilution was mixed with an equal volume of virus solution with known titer or with suitable cell culture medium for control of nanoGO toxicity. The mixtures of virus- nanoGO and nanoGO control were incubated at a defined temperature for 60 min. Subsequently, viral titrations of each mixture were performed on a susceptible cell line.

More specifically, for antiviral activity against PEDV and BCoV, nanoGO was diluted 50- to 800-fold in DMEM supplemented with 5% FBS.Each dilution was mixed with equal volume of either PEDV (DR13 strain) or BCoV (BC94 strain) having a titer of 10^7 $TCID_{50}$/mL. The incubation time at room temperature was 60 min. PEDV and BCoV after treatment with nanoGO were titrated on Vero cells using the methods described previously (Hansa et al., 2013; D. Song et al., 2003). A maximum dilution factor, in which the virus titer was reduced by at least 4 log10, was determined to be an effective dilution factor (Agriculture- Forestry and Livestock Quarantine Headquarters, 2018). Antiviral effect of nanoGO was expressed by % inhibition, which was calculated as follows: [$\log_{10}$ ($TCID_{50}$/mL of virus) – $\log_{10}$ ($TCID_{50}$/mL of treatment)]/ ($\log_{10}$ ($TCID_{50}$/mL of virus) x 100% (Y.-N. Chen, Hsueh, Hsieh, Tzou, & Chang, 2016). Additionally, immunofluorescence assays (IFA) were performed to detect the replication of living virus post-treatment more precisely.

An IFA was performed 24 h post-inoculation using the PEDV IFA kit (MEDIAN Diagnostics, South Korea) and BCoV 1st antibody (provided by MEDIAN Diagnositic). Statistical analysis was performed using GraphPad Prism version 8.0.2. For antiviral activities against SARS-CoV-2, the neutralizing test was conducted using the previous method (Manenti et al., 2020) with modifications. The nanoGO solution was serially diluted two-fold in DMEM supplemented with 5% FBS. Subsequently, the SARS-CoV-2 (BetaCoV/Korea/KCDC03/2020) of 25 $TCID_{50}$/mL was mixed with equal volume of the diluted nanoGO. The mixtures were incubated for 60 min at 37°C. After incubation, 0.1 mL of each nanoGO mixture was infected to a monolayer of Vero E6 cells. The presence/absence of cytopathic effect (CPE) was monitored daily for 5 days. The neutralizing titers were expressed as the reciprocal of the highest dilution, which resulted in the inhibition of CPE. All experiments related to severe acute respiratory syndrome coronavirus 2 (SARS-CoV-2) were performed in BL3 facility.

2.3. Results

2.3.1. Antiviral activities of chitosan to porcine epidemic diarrhea virus.

In the disinfectant effect test, some dilutions of chitosan were highly efficacious at reducing the viral titer. The effective dilutions in the hard and organic waters conditions were 150-fold (0.0067% chitosan) and 100-fold (0.01% chitosan), respectively (Table 8).

The disinfectant effect of chitosan may be affected by organics, such as insoluble acid polysaccharides, in the medium due to the binding of chitosan to these substances (Chirkov, 2002), which possibly led to the differences between the two conditions in this study. Previous studies have found that chitosan has antiviral activity on some phages and plant and animal viruses (Chirkov, 2002; Davis, Zivanovic, D'Souza, & Davidson, 2012; Zheng et al., 2016). This activity is known to result from several mechanisms, including neutralization of virus infectivity by changing its membrane structure or integrity (Kochkina, Surgucheva, & Chirkov, 2000), blocking viral replication (Kochkina & Chirkov, 2000) and enhancing host immunity (Zheng et al., 2016). In this study, the cells were exposed to chitosan for only 1 hour during virus adsorption, thus there was less possibility of chitosan affecting viral replication. It was also difficult to assess chitosan’s immunological effect because the test was performed on Vero

cells, which are not immune cells in vitro. Therefore, it is believed that the antiviral activity of chitosan in this study was derived from its virus-neutralizing effect.

The disinfectant effect of chitosan was strongly supported by the results of the IFA assays (Figure 18). In the hard water conditions, there was no fluorescence seen for the 1-fold (1% chitosan) and 50-fold (0.02% chitosan) diluents. In the organic water conditions, no fluorescence was found for the 1-fold diluent. Therefore, this new disinfectant completely eliminated the virus at these dilution stages. Overall, the undiluted solution (1% chitosan) was the most effective. Nevertheless, considering both effective and economical aspects, a 0.01% chitosan solution is a reasonable concentration for commercial products.

In the safety test, there were no abnormal cell features observed. It is noteworthy that all the chitosan dilutions enhanced cell proliferation (Figures 19 and 20), and the 50-fold dilution (0.02% chitosan) resulted in the greatest effect (Figure 19).

2.3.2. Antiviral activities of nano-graphene oxides to porcine epidemic diarrhea virus, bovine coronavirus, and severe acute respiratory syndrome coronavirus 2.

In this study, using improved Hummer’s method described before, the

nanoGO material sharing similar size with that of the study conducted by B.-C. Lee et al. (2020) was obtained. In brief, FE-SEM results indicated that the lateral size of nanoGO particles was less than 50 nm with irregular shapes. Particle analysis results indicated that most of the material were less than 30 nm in size with the average size of 20 nm. HR-TEM had previously been applied to observe the layer structure of nano particles (Çelik, Flahaut, & Suvacı, 2017; Gonçalves et al., 2014; C. Yang et al., 2014). Therefore, this method is applied in combination with image analysis to determine the diameter of particles. The results revealed that most of nanoGO particles contained 1 to 3 layers. AFM results also indicated that the heigh of nanoGO particles were around 1 - 2 nm, supporting the HR-TEM result. Raman spectra analysis exhibited the D peak of approximately 1350 cm^{-1} and a G band at 1600 cm^{-1}, which are known peaks specific to GO. Functional groups and oxidative state of nanoGO were measured by the Fourier-transform infrared spectroscopy (FT-IR), X-ray photoelectron spectroscopy (XPS), and X-ray diffraction (XRD). GQD's FT-IR spectrum analysis revealed the major peaks of O-H (around 3420 cm^{-1}), C-H (2928 and 2850 cm^{-1}), COOH (1730 cm^{-1}), C=O (1630 cm^{-1}), CH_2 (1465 cm^{-1}), and C-O (1044 cm^{-1})). XRD analysis clearly showed a peak at a low diffraction angle (2 theta = 10.32^{o} with an interlayer spacing about 8.57 A^{o}) which represents a high oxidative level of this material. In XPS analysis, the binding energy of C–C (284.50 eV), C–O (286.68 eV), and C=O (288.36 eV) were

measured.

The toxicological effect is the highest criteria for consideration before applying nanomaterial in reality. In this study, cytotoxicity of nanoGO, which was represented as the presence of CPE, was not observed in vero cell at the lowest dilution of 1/50 (Table 9). Additionally, CPE was not observed at the dilution factor of ½ when neutralization test was performed against SARS-CoV-2 (Figure 23). Therefore, it is reasonable to conclude that there was no cytotoxicity of nanoGO at the investigated concentration.

The antiviral activity of nanoGO was initially demonstrated for coronaviruses (PEDV, BCoV) inducing diseases of animals. It was observed that increasing the dilution of nanoGO (1/50 to 1/800) increased the titers of PEDV/ BCoV from 0.0 to 6.3/ 6.4 $\log_{10}$ $TCID_{50}$, gradually approaching the titers in the mock-treated groups (both were 6.6 $\log_{10}$ $TCID_{50}$). The results implied that nanoGO exerted *in vitro* antivirus activity against PEDV/ BCoV in a dose- dependent manner. In detail, the highest antiviral activities of nanoGO against PEDV and BCoV were achieved at 72.1% and 61.9%, respectively. However, there was little to no antiviral effect of nanoGO obtained for PEDV and BCoV when the nanoGO solution was dissolved to the concentrations of 0.00125% and 0.2% ($p>0.05$) (Figure 21). Furthermore, at up to 1/300 dilution, nanoGO revealed the more effective antiviral agent against PEDV than against BCoV ($p<0.01$) (Figure 21). At 100 times diluted, nanoGO blocked more efficiently the

replication of viruses (Table 10). The virucidal activity of nanoGO was also confirmed by IFA staining (Figure 22). The infected cells (green fluorescence) were not observed at low dilution (1/50) of nanoGO (Figure 22 a and f). However, the active agent at a dilution of 1/100 or higher (Figures 22 b, c, g and h) was unable to completely inactivate the viruses. The antiviral activity of nanoGO was also detected for another coronavirus, SARS-CoV-2 which is the causative agent of the COVID-19 pandemic (P. Zhou et al., 2020). As shown in Figure 23, nanoGO in the range of 1/2 - 1/8 dilution inhibited the replication of SARS-CoV-2 (no cytopathic effects were observed). From the 1/16 dilution, nanoGO failed to inactivate the replication of the virus. However, the level of SARS-CoV-2 inhibition was not determined in this study. Combining the results presented in Table 10 and Figures 21 - 23, it was inferred that nanoGO was a broad-spectrum antiviral agent against different coronaviruses causing diseases in animals and humans.

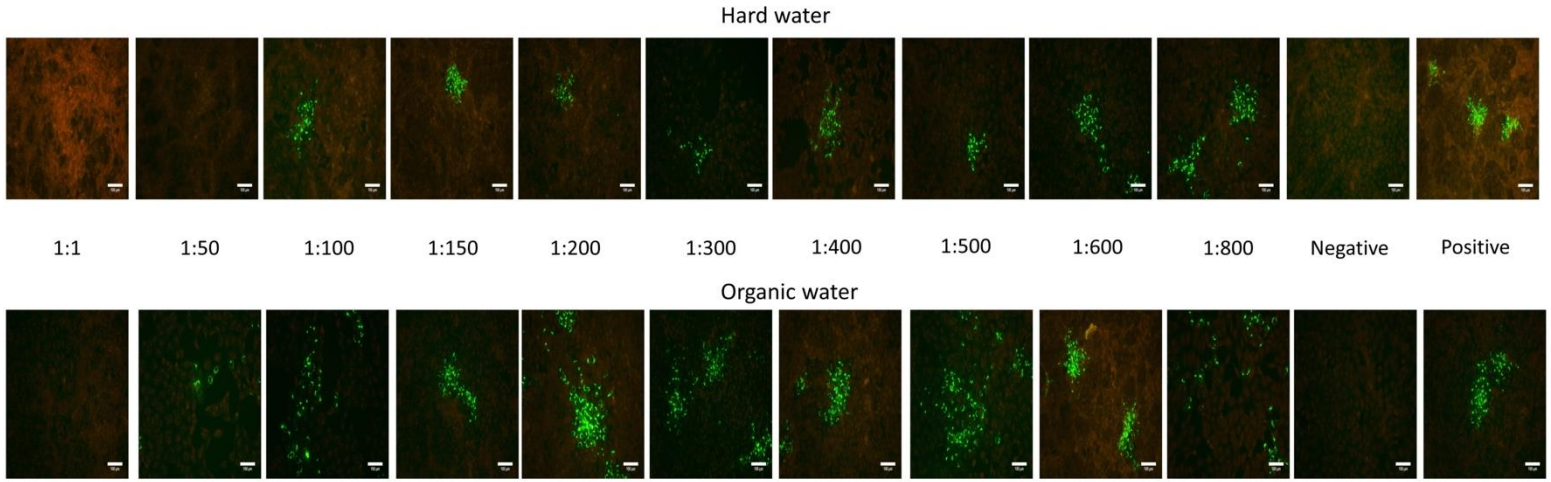

Figure 18. Indirect immunofluorescence assay (IFA) of chitosan.

Under hard water condition, no fluorescence was observed for the 1-fold (1% chitosan) and 50-fold (0.02% chitosan) dilutions. Under organic water conditions, there was no evidence of fluorescence in the 1-fold dilutions.

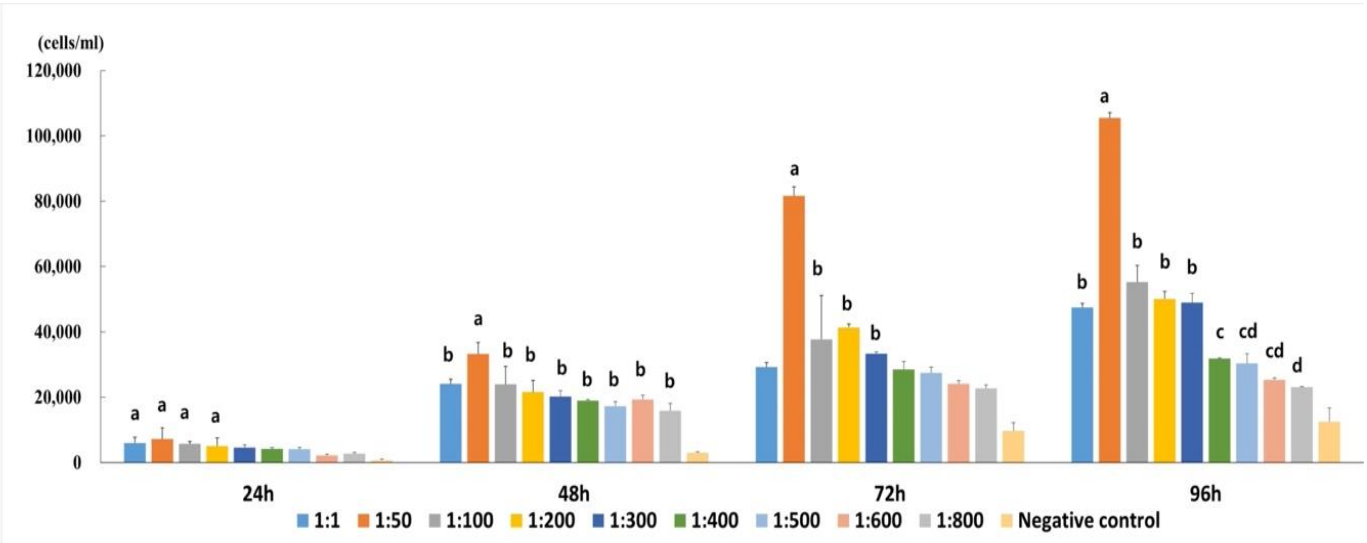

Figure 19. Effect of chitosan on the proliferation of Vero cells.

Overall, chitosan promoted cell proliferation at all dilutions tested in this study, and the 50-fold dilution (0.02% chitosan) showed the greatest effect. Letters a, b, c and d indicated chitosan dilution factors showing significant differences ($P < 0.05$) compared to negative control (culture medium without chitosan). Different letters mean that there was a significant difference ($P < 0.05$) between two groups.

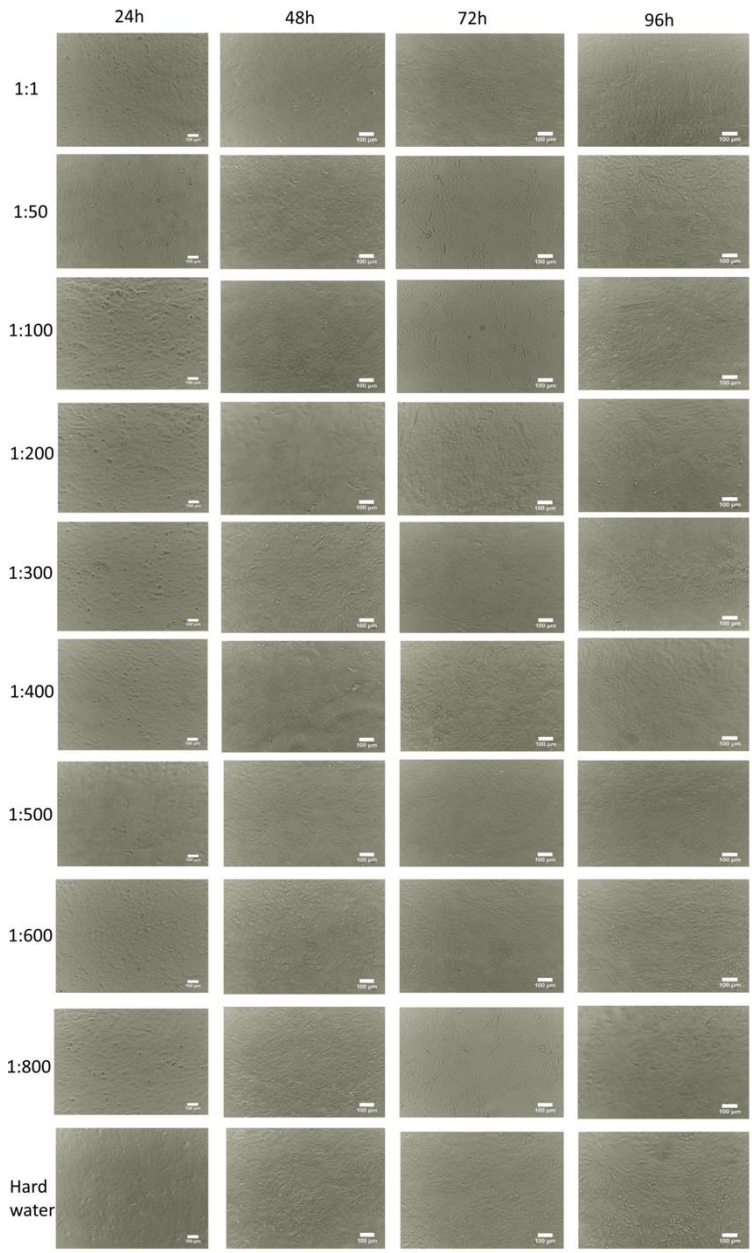

Figure 20. Image of the proliferation of Vero cells in culture.

No abnormal-appearing cells were observed for any of the chitosan dilutions during the experiment.

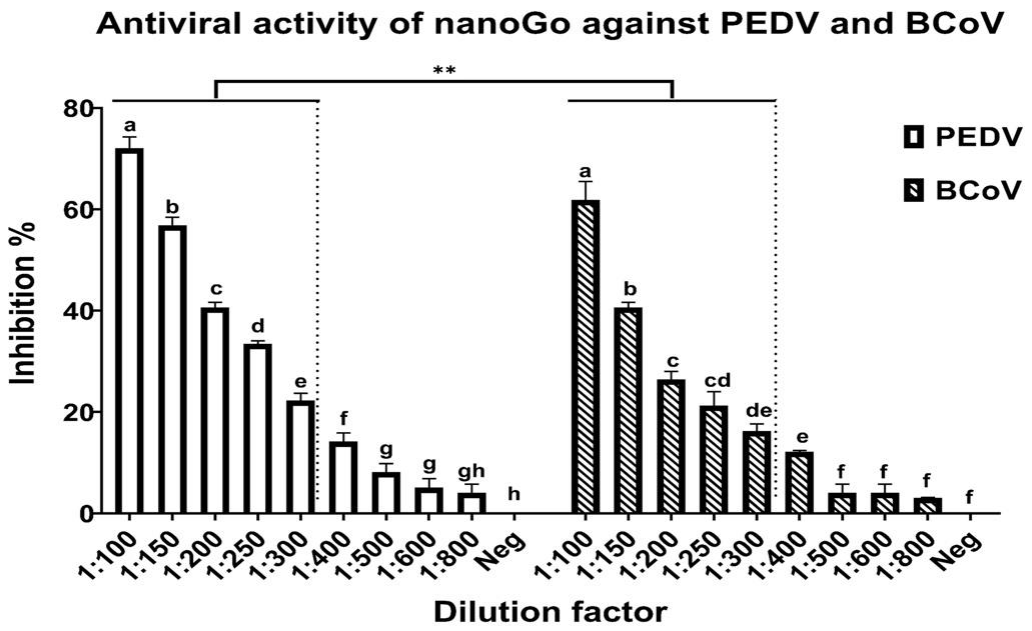

Figure 21. Antiviral activity of nanoGO against PEDV and BCoV in different dilution factors. The denoted letters indicate the statistically significant differences among dilution factors in each group ($p<0.05$). The asterisk demonstrated the significant differences among groups (*: $p<0.05$;**: $p<0.01$).

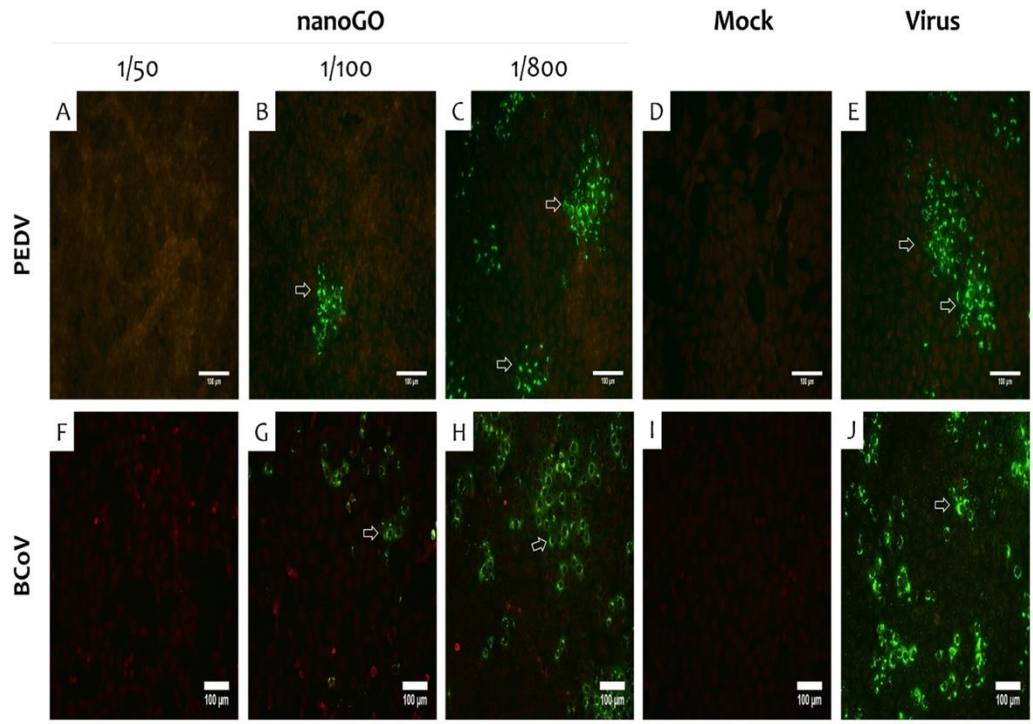

Figure 22. IFA assay demonstrating the replication of PEDV and BCoV post nanoGO incubation. Cells with fluorescent signals (arrows) were virally infected. The higher number of fluorescent cells, the higher the amount of viral replication.

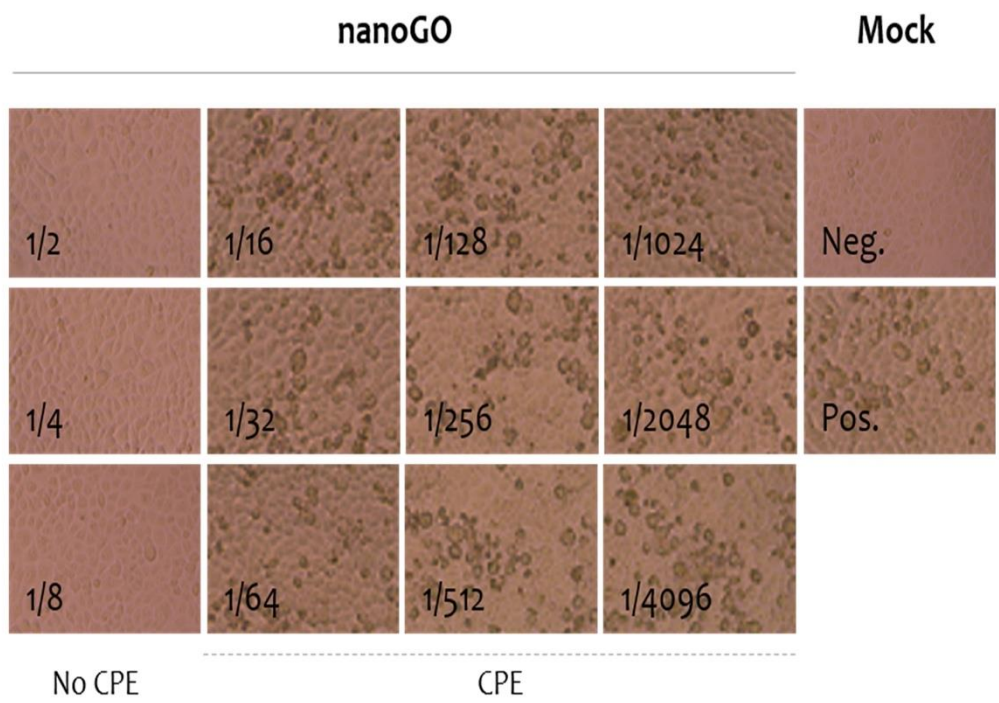

Figure 23. The cytopathic effects (CPE) induced by SARS-CoV-2 under different concentrations of nanoGO. It was observed that nanoGO at a dilution higher than 1/8 failed to completely inhibit the replication of the virus (CPE positive).

Table 8. Antiviral activity of chitosan on porcine epidemic diarrhea virus.

Treatment condition	Experiment (log $TCID_{50}$/mL)					Effective dilution factor
	Dilution	First	Second	Third	Median	
Hard water	1:100	0.9	0.9	1.1	0.9	1:150
	1:150	1.5	1.5	1.5	1.5	
	1:200	2.9	3.1	3.1	3.1	
	1:250	3.3	3.3	3.5	3.3	
	1:300	3.7	3.9	3.9	3.9	
	1:400	4.3	4.3	4.3	4.5	
	1:500	5.5	5.5	5.5	5.5	
	1:600	5.7	5.9	5.7	5.7	
	1:800	6.1	6.1	6.1	6.1	
Organic water	1:100	2.3	2.1	2.1	2.1	1:100
	1:150	2.9	3.1	3.1	3.1	
	1:200	3.9	3.9	3.9	3.9	
	1:250	4.3	4.5	4.5	4.5	
	1:300	4.9	5.1	5.1	5.1	
	1:400	5.9	5.9	5.9	5.9	
	1:500	6.1	6.1	6.1	6.1	
	1:600	6.3	6.3	6.3	6.3	
	1:800	6.5	6.5	6.5	6.5	
Negative control	-	6.7	6.7	6.9	6.7	-
Toxicity control	1:100	NC*	NC	NC	-	-
	1:150	NC	NC	NC	-	
	1:200	NC	NC	NC	-	
	1:250	NC	NC	NC	-	
	1:300	NC	NC	NC	-	
	1:400	NC	NC	NC	-	
	1:500	NC	NC	NC	-	
	1:600	NC	NC	NC	-	
	1:800	NC	NC	NC	-	

*NC; No cytopathic effect (NC < 0.5)

Table 9. Cytotoxic analysis of nanoGO on Vero cell.

	NanoGO dilution	CPE test
		Mean titer (log10 $TCID_{50}$)
NanoGO Toxicity control	1/50	NC*
	1/100	NC
	1/150	NC
	1/200	NC
	1/250	NC
	1/300	NC
	1/400	NC
	1/500	NC
	1/600	NC
	1/800	NC

* NC; No cytopathic effect (NC < 0.5).

Table 10. Antiviral activity of nanoGO against PEDV and BcoV.

Treatment condition	NanoGO dilution	PEDV	BcoV
		Mean titer (log10 $TCID_{50}$)	***Mean titer (log10 $TCID_{50}$)***
Virus + nanoGO	1/50	0.0	0.0
	1/100	1.8	2.5
	1/150	2.8	3.9
	1/200	3.9	4.8
	1/250	4.4	5.2
	1/300	5.1	5.5
	1/400	5.6	5.8
	1/500	6.0	6.3
	1/600	6.2	6.3
	1/800	6.3	6.4
Virus	NA*	6.6	6.6

*Not applicable (NA); ** % inhibition = [$\log_{10}$ (TCID50/mL of virus) – $\log_{10}$ ($TCID_{50}$/mL of treatment)]/ ($\log_{10}$ ($TCID_{50}$/mL of virus) x 100%. Underlines denote a maximum dilution factor, in which the virus titer of the treatment group (1.8 for PEDV and 2.5 for BcoV) was reduced by at least 4 log10 in comparing to that of the mock- treated group (6.6 for both PEDV and BcoV).

2.4. Discussion

The antiviral activity of chitosan to PEDV and nanoGO to PEDV, BcoV, and SARS-CoV-2 was demonstrated in this study. In the evaluation of antiviral activity, some dilutions of chitosan were highly efficacious at reducing the viral titer. The antiviral effect of chitosan may be affected by the presence of organic compounds, such as insoluble acid polysaccharides, in the medium, as chitosan binds to these substances (Chirkov, 2002), which possibly led to the differences observed between the two conditions in this study. Antiviral activity of nanoGO against alphacoronavirus and betacoronavirus was demonstrated in this study with an expansion to the emerging SARS-CoV-2 (Figures 21–23). These results were highly supported by a recent study that confirmed the trapping effect of nanoGO against SARS-CoV-2 (De Maio et al., 2021). However, this study also demonstrated other virucidal aspects of GO by finding that its viral inhibition remained to a certain extent in the presence of high organic material (5% FBS). This fact should be further investigated due to a significant difference in dose-response of nanoGO against PEDV/ BCoV (Figures 21 and 22) and SARS-CoV-2 (Figure 23).

The antiviral effect of chitosan and nanoGO on coronaviruses was strongly supported by the results of the IFA assays (Figures 18 and 22). Under hard water conditions, no fluorescence was seen for the 1-fold (1% chitosan) and 50-

fold (0.02% chitosan) dilutions. Under organic water conditions, no fluorescence was found for the 1-fold dilution of chitosan and 50-fold dilution of nanoGO. These results indicate that these materials completely eliminated the virus at these degrees of dilution.

It was reported that chitosan and nanoGO has antiviral activity on other viruses. Previous studies have found that chitosan has antiviral activity on some phages as well as plant and animal viruses (Chirkov, 2002; Davis et al., 2012). NanoGO is known for its inhibition property against a wide range of viruses, both non-enveloped and enveloped (Y. N. Chen et al., 2016), DNA and RNA viruses (Ye et al., 2015).

This antiviral activity of chitosan and nanoGO is known to result from several mechanisms. The antiviral mechanism of chitosan was reported that the neutralization of virus infectivity by changing its membrane structure or integrity (Kochkina et al., 2000), blocking viral replication (Kochkina & Chirkov, 2000) and enhancing host immunity (Zheng et al., 2016). In this study, the cells were exposed to chitosan for only 1 hour during virus adsorption, thus there was less possibility of chitosan affecting viral replication. It was also difficult to assess the immunological effect of chitosan because the test was performed on Vero cells, which are not immune cells *in vitro*. Therefore, it is thought that the antiviral effect of chitosan in this study was derived from its virus-neutralizing effect. The antiviral mechanism of nanoGO against

coronaviruses was discussed to be based on the interaction between negatively charged surfaces of GO with sharp edges, and positively charged viruses (Seifi & Kamali, 2021). NanoGO could trigger the cytokine response that might inhibit the viral replication process in the host cell (Lategan et al., 2018). The anti-microbial effects of nanoGO highly depend on several factors like exposed time, concentration, and lateral size.

In the safety test, no abnormal cell features were observed in chitosan and nanoGO. It is noteworthy that all the chitosan dilutions enhanced cell proliferation (Figures 19 and 20), and the 50-fold dilution (0.02% chitosan) resulted in the greatest effect (Figure 19). chitosan is expected to provide significant benefits to researchers using this cell line. However, chitosan is known to affect cell proliferation positively or negatively, depending on its concentration and molecular and biochemical features. According to previous study, chitosan enhanced the proliferation of human dermal fibroblasts but inhibited that of immortalized human keratinocytes. Thus, further studies on other cell lines are required. Although it is often thought that disinfectants have broad-spectrum efficacy, certain substances can be effective or ineffective against specific pathogens, thus a specific evaluation is necessary (McDonnell & Russell, 1999).

In literature, graphene oxide (GO) is known to be a biocompatible substance with no indication for causing any harmful effects in experimental animals (B.

C. Lee et al., 2020) and with low cytotoxicity to cell lines (Kuo et al., 2017). Previous studies indicated that the bactericidal and cytotoxic activities of nanoGO depended on its size (Liu et al., 2012; Zhao et al., 2016). In brief, nanoGO with lateral dimensions larger than 50 nm significantly reduced the viability of *Escherichia coli* and macrophage cells. In this study, the nanoGO was used with the average size of 20 nm, which caused no harmful effects on Vero cells. Additionally, this type of nanoGO was also demonstrated as safe in *in vivo* models (B. C. Lee et al., 2020). Therefore, chitosan and nanoGO appears to be a promising non-toxic and economical ingredient for disinfectants to be used for preventing coronavirus transmission.

This study focused on the effectiveness of chitosan under liquid conditions. However, in many situations disinfectants are also used on hard surfaces, thus further studies are required to validate the efficacy of chitosan and nanoGO in such situations.

General discussions

Bats and pigs are presumed reservoirs of several viral pathogens transmissible to humans and livestock. The first evidence of rabies virus transmission from bats was reported in 1921. After that, an increasing number of human and animal viral diseases such as the Hendra virus, Nipah virus, and Pteropine orthoreovirus were detected in bats. Zoonoses such as Cysticercosis, Swine Influenza virus, Nipah virus, Menangle virus, porcine Hepatitis E, *Staphylococcus aureus* and *Streptococcus suis* have been reported in pigs and there is clear potential for domestic swine to act as a reservoir for many emerging and re-emerging infectious diseases (Banks et al., 2004; Myers, Olsen, & Gray, 2007; T. C. Smith et al., 2011). Since the development of sequencing technology, as well as the emergence of the deadly pathogen SARS-CoV, studies related to the diversity of bat virome, including members with risks of zoonotic infection belonging to *Coronaviridae*, *Paramyxoviridae*, *Reoviridae*, *Rhabdoviridae*, and *Filoviridae*, have been done. Metagenomic analysis revealed that the presence of some viruses for example Torque teno viruses (TTVs) that have previously been found to occur regularly in pigs (Masembe et al., 2012). Climate change and human activities result in close contact between wild animals and humans, consequentially increasing the risk of host transmission of viruses. Serological evidence revealed the multi-infection of

SARS-related coronavirus from bats to humans (H. Li et al., 2019). In this study, several species belonging to genera *Eptesicus*, *Myotis*, and *Pipistrellus* have been investigated for the presence of coronavirus. These species share their habitat niches with other wild and/or livestock animals, thereby increasing the risk of cross contamination to humans involving any of the viruses they carry. Of these samples, a distantly genetically related viral isolate belonging to alphacoronavirus was detected in *E. serotinus*. This result further contributed to the genetic diversity of bat coronavirus in general and alphacoronavirus. It is generally accepted that the alphacoronavirus genus is extremely diverse. To date, 19 different species belonging to 14 sub-genera of alphacoronavirus have been officially accepted by ICTV. In this study, a whole-genome comparison revealed that the HCQD-2020 strain was distantly related to other known species of alphacoronavirus. Genome based and functional gene-based phylogeny constructions also indicated that this strain formed a separate branch in phylogenetic trees. Recent metagenomic studies of bat virome revealed several potential novel species within alphacoronavirus detected in bats around the world. This result, along with other up-to-date studies, once again supported the genetic heterogeneity of this genus. All members of this genus have similar genomic organization, containing ORF1ab–S–ORF3–E–M–N. Furthermore, additional ORFs located downstream of the nucleocapsid– encoding gene were also observed in many species of this genus such as TGEV, BatCoV-HKU2,

BatCoV-512, and Shrew coronavirus. In addition to the common ORFs found in other alphacoronavirus's members, a putative ORF7 was found at the 3' terminator of HCQD-2020's genome. Its sequence at the amino acid level was not homologous with any of the known protein sequences. It should also be noted that this putative ORF was likely the most distinct ORF of the currently known alphacoronavirus. Alphacoronavirus contains several harmful viruses such as TGEV, Porcine epidemic diarrhea virus (PEDV), and Porcine enteric alphacoronavirus (PEAV) that cause serious economic losses in pig production. The last two species were considered to originate from bats. Evidence of the host jumping of coronavirus from bat to other species belonging to even-toed ungulate animals was characterized in the case of PEAV, which shares high nucleotide identity (approximately 95% sequence similarity) with bat-HKU2 strains. In this study, an *in silico* analysis indicated that HCQD-2020, a distantly related species belonging to alphacoronavirus, can infect another host, especially those in the order Artiodactyla, which include some species such as camels and pigs. Camels were previously determined as the intermediate hosts of the MERS virus. Focusing on the genus alphacoronavirus, strains that were closely related to the human alphacoronavirus E229 were detected in domestic camels. Recently, a novel alphacoronavirus belonging to the species alphacoronavirus I that is usually found in pigs, dogs, and cats was detected in children with pneumonia in Malaysia. Therefore, it is important to investigate

potential hosts besides bats for newly detected coronaviruses. It was reported that TTSuV infections existed in many countries around the world (N. McKeown, M. Fenaux, P. G. Halbur, & X. Meng, 2004). In this study, the prevalence rate of TTSuVs in Korea during 2017–2018 was 44%. The positive rates of TTSuV1 and TTSuV2 were 16% and 36%, respectively, and the coinfection of both type of TTSuVs was approximately 8%. The prevalence of TTSuVs in Korea in this study was equivalent to the positive rate of one in Thailand (McKeown et al., 2004). However, the detection rate of TTSuV1 and TTSuV2 in this study was lower compared with reports in other countries (Blois et al., 2014a; K. Li et al., 2013) and even that of Korea before 2004 (McKeown et al., 2004). In this study, investigation of sick pigs in the potential appearance of TTVs genogroup 3 was performed. As a result, two out of 470 samples were TTV genogroup 3 positive. Sequence comparison and phylogeny analysis indicated that the two strains share 98.4% sequence homology and belonged to the subgroup 3c. Interestingly, genome organization prediction of N119 strain revealed an additional ORF2-2 besides the common ORFs 1-3 found in *Anelloviridae* family (P. B. Biagini, Mauro ; Hino, Shigeo ; Kakkola, Laura ; Mankertz, Annette ; Niel, C ; Okamoto, H ; Raidal, S ; Teo, CG ; Todd, Daniel, 2011). In this study, the TTVs genogroup 3 detected in pigs were predicted to contain the three common ORFs observed in other TTVs. Of the ORF1, the N-terminated region was featured by the Arginine-rich region

(Figure 17a) which is similar to capsid proteins of circoviruses (Mou et al., 2019). Furthermore, three replication-associated motifs were also observed (Figure 17b). The presented motifs in ORF1 in TTVs were previously reported elsewhere (Tanaka et al., 2001). Previous study suggested that ORF1 might encode a bifunctional structural protein: the N-terminus played a role as capsid while the function of the C-terminus might be a co-response to the replication (Kakkola et al., 2008). Of the remaining ORFs, putative ORF2 of M265 contained the well-observed motifs of $WX_7HX_3CXCX_5H$ in TTVs while a cluster of Leucine rich regions followed by Serine rich regions in C-terminus were observed in the present strains. These features are highly conserved in other *Anelloviruses* (Vibin, Chamings, Klaassen, & Alexandersen, 2020). This is the first time the strains belonging to *alphaternovirus* were detected and studied. In conclusion, the present study provided information of TTSuVs prevalent in swine farms in Korea. Our results also highlight the presence of TTV genogroup 3 strains in pig.

In the test of disinfectant effect, some dilutions of chitosan were highly efficacious at reducing the viral titre. The disinfectant effect of chitosan may be affected by the presence of organic compounds, such as insoluble acid polysaccharides, in the medium, as chitosan binds to these substances (Chirkov, 2002), which possibly led to the differences observed between the two conditions in this study. The enormous release of adulterated and uncontrolled

infection-preventing household products such as the antibacterial active liquid soap and ABHS in the global markets have several potential adverse health effects on human such as dehydrated skin, irritation, poisoning, and cancer among others. Thus, the careful adoption of hand washing with selected safe liquid soap should be encouraged by all. Improvement in hand hygiene is akin to the containment of the spread of germs, including the ravaging viral infection, COVID-19. However, when the use of hand sanitizer is inevitable, consumers should be cautious of the chemical constituents as well as the concentration of each constituent. These measures are important to the prevention of avoidable implications such as unintentional or deliberate ingestion or chemical absorption through the skin which could lead to incidences such as irreversible blindness, depression, intoxication, liver cirrhosis, acidosis, headache, central nervous system depression, seizure, hypoglycemia, coma, and death. While preventing infections such as the COVID-19 and other microbial-induced infections, slow and systematic death should be meticulously avoided. Otherwise, the prevention mode could lead to higher fatality than the infection being avoided.

Previous studies have found that chitosan has antiviral activity on some phages as well as plant and animal viruses (Chirkov, 2002; Davis et al., 2012; Zheng et al., 2016). This activity is known to result from several mechanisms, including the neutralization of virus infectivity by changing its membrane

structure or integrity (Kochkina et al., 2000), blocking viral replication (Kochkina & Chirkov, 2000) and enhancing host immunity (Zheng et al., 2016). In this study, the cells were exposed to chitosan for only 1 hour during virus adsorption, thus there was less possibility of chitosan affecting viral replication. It was also difficult to assess the immunological effect of chitosan because the test was performed on Vero cells, which are not immune cells *in vitro*. Therefore, it is thought that the disinfectant effect of chitosan in this study was derived from its virus-neutralizing effect. The disinfectant effect of chitosan was strongly supported by the results of the IFA assays. Under hard water conditions, no fluorescence was seen for the 1-fold (1% chitosan) and 50-fold (0.02% chitosan) dilutions. Under organic water conditions, no fluorescence was found for the 1-fold dilution. Chitosan completely eliminated the virus at these degrees of dilution. Overall, the undiluted solution (1% chitosan) was the most effective. Nevertheless, considering both efficacy and economic aspects, a 0.01% chitosan solution is a reasonable concentration for commercial products. In the safety test, no abnormal cell features were observed. It is noteworthy that all the chitosan dilutions enhanced cell proliferation, and the 50-fold dilution (0.02% chitosan) resulted in the greatest effect. As a result, chitosan is expected to provide significant benefits to researchers using this cell line. However, chitosan is known to affect cell proliferation positively or negatively, depending on its concentration and molecular and biochemical features. According to

literature, chitosan enhanced the proliferation of human dermal fibroblasts but inhibited that of immortalized human keratinocytes. Thus, further studies on other cell lines are required. Although it is often thought that disinfectants have broad-spectrum efficacy, certain substances can be effective or ineffective against specific pathogens, thus a specific evaluation is necessary (McDonnell & Russell, 1999). This study is the first to confirm the disinfectant effect of chitosan on PEDV. Coronaviruses infect a wide range of host species, including reptiles, birds, and mammals, and can cause respiratory or intestinal disease in most hosts. Moreover, the recently emerged coronaviruses causing SARS and MERS, which originated from bats, pose a serious threat to human health. Generally, it has been known that various types of coronaviruses resemble each other in morphology and chemical structure (Tyrrell & Myint, 1996). Thus, it is also expected that chitosan is highly likely to exert a disinfectant effect on other coronavirus types including human coronaviruses when considering its virus neutralization mechanism. However, further investigations on other coronaviruses are required to confirm the hypothesis.

In literature, graphene oxide (GO) is known to be a biocompatible substance with no indication for causing any harmful effects in experimental animals (B.-C. Lee et al., 2020) and with low cytotoxicity to cell lines (Kuo et al., 2017; Ye et al., 2015). Previous studies indicated that the bactericidal and cytotoxic activities of nanoGO depended on its size. In brief, nanoGO with lateral

dimensions larger than 50 nm significantly reduced the viability of *Escherichia coli* and macrophage cells. In this study, the nanoGO was used with the average size of 20 nm, which caused no harmful effects on Vero cells. Additionally, this type of nanoGO was also demonstrated as safe in *in vivo* models (B. C. Lee et al., 2020). NanoGO is known for its inhibition property against a wide range of viruses, both non-enveloped and enveloped (Y.-N. Chen et al., 2016), DNA and RNA viruses (Ye et al., 2015). NanoGO could trigger the cytokine response that might inhibit the viral replication process in the host cell (Lategan et al., 2018). The anti-microbial effects of nanoGO highly depend on several factors like exposed time, concentration, and lateral size. Furthermore, virucidal activities of nanoGO are also varied against different viruses. NanoGO and its deliveries significantly inactivated PRV and PEDV at the concentration of 6 μg/mL after 1 hour by destroying viral morphology (Ye et al., 2015). In literature, graphene oxide alone or in combination with nano-silver applied to inhibit different types of viruses. The results indicated that only GO – Ag showed the effective antiviral activities against low titer of FeCoV and IBDV at 0.125 mg/mL while GO only inhibited the infection of FeCoV after a 1-hour treatment. However, the authors using another method for preparing GO resulted in a difference of oxidized carbon material (Marcano et al., 2010). Antiviral activity of GO against alphacoronavirus and betacoronavirus was demonstrated in this study with an expansion to the emerging SARS-CoV-2. Our results were highly

supported by a recent study that confirmed the trapping effect of nanoGO against SARS-CoV-2 (De Maio et al., 2021). However, our study also demonstrated other virucidal aspects of GO by finding that its viral inhibition remained to a certain extent in the presence of high organic material (5% FBS). This fact should be further investigated due to a significant difference in dose-response of nanoGO against PEDV/ BCoV and SARS-CoV-2.

Collectively, the results of this study demonstrated the prevalence and genetic features of the potential zoonotic pathogens in animal reservoir, alphacoronaviruses in wild bats and TTSuV in domestic pigs. In addition, strong antiviral activities of chitosan and nanoGO against various coronaviruses in a various biological conditions suggest that these nontoxic agents can further be used to eliminate viral contaminants and to stop the spread of zoonotic diseases.

General conclusions

Phylogenetic analysis of potential zoonotic viruses isolated from wild bats and domestic pigs revealed their close genetic relatedness to those isolated from humans. Since various animals are considered to be important reservoir for many zoonotic viral pathogens, studies of more fully characterized viral genomes from diverse host species will improve understanding of viral evolution and cross-species transmissions. In addition, development of effective disinfectants against these zoonotic viral pathogens are essential requirement for an immediate response to an outbreak situation.

1. Phylogenetic characterization of zoonotic potential viruses isolated from animals in Korea

A whole-genome comparison indicated that the HCQD-2020 strain was distantly related to other known species of alphacoronavirus. Genome-based and functional gene-based phylogeny constructions also indicated that this strain formed a separate branch in phylogenetic trees. Based on the low sequence identity, the presence of a putative ORF7 with no homology to any known genes in Genbank, and distant relation to other representative species of alphacoronavirus, the HCQD-2020 strain was proposed as a novel strain of this

genus. In this study, an *in silico* analysis indicated that HCQD-2020, a distantly related species belonging to alphacoronavirus, can infect another host, especially those in the order Artiodactyla, which include some species such as camels and pigs.

The prevalence rate of TTSuVs in Korea during 2017–2018 was 44% . The positive rates of TTSuV1 and TTSuV2 were 16% and 36%, respectively, and the co-infection of both type of TTSuVs was approximately 8%. Focusing on the TTV 3 strains, it was found that each M265 and N119 strain has a 3,817 full-length genome and the M265 has three ORFs (ORF1, ORF2 and ORF3) while the N119 strain has four ORFs (ORF1, ORF2, ORF 2-2 and ORF 3). Two out of 470 samples were TTV genogroup 3 positive. Sequence comparison and phylogeny analysis indicated that the two strains share 98.4% sequence homology and belonged to the subgroup 3c. Interestingly, genome organization prediction of N119 strain revealed an additional ORF2-2 besides the common ORFs 1-3 found in *Anelloviridae* family. In this study, the TTVs genogroup 3 detected in pigs were predicted to contain the three common ORFs observed in other TTVs.

2. Application of chitosan and nano-graphene oxide as nontoxic disinfectant against coronaviruses

The antiviral activity of chitosan and nanoGO was evaluated against coronaviruses using Vero cells. in this study. 0.01% and 0.0067% chitosan solutions were determined to be effective disinfectant for PEDV in hard and organic water conditions respectively. The highest antiviral activities of nanoGO against PEDV and BCoV were achieved at 72.1% and 61.9% respectively. The nanoGO in range of 1/2-1/8 dilution inhibited the replication of SARS-CoV-2. In addition, no evidence of toxicity was observed during the cell toxicity test of chitosan and nanoGO. It is noteworthy that all the chitosan dilutions enhanced cell proliferation. The results indicated that the antimicrobial effects of chitosan and nanoGO depend on concentration. In the test of disinfectant effect, some dilutions of chitosan were efficacious at reducing the viral titer. The concentration dependent fashion of viral inhibition of nanoGO was observed for all enveloped viruses of PEDV, BCoV, and SARS-CoV-2.

It has been demonstrated that chitosan and nanoGO exhibit antiviral activity to PEDV, BCoV, and SARS-CoV-2 at non-cytotoxic concentrations. Especially nanoGO exhibits significant antiviral properties against SARS-CoV-2. Chitosan appears to be a promising non-toxic and economical ingredient for disinfectants used to prevent coronavirus transmission. The antiviral activities of chitosan and nanoGO may shed some light on novel virucide development.

In collectively, continuous monitoring programs of potential zoonotic viral

pathogens in various animal species are required to prevent possible outbreak situation in the future. Besides the surveillance program, development of novel anti-viral strategies using nontoxic agents, such as chitosan and nanoGO, should be in place for immediate action against the zoonotic diseases.

References

Abe, K., Inami, T., Ishikawa, K., Nakamura, S., & Goto, S. (2000). TT virus infection in nonhuman primates and characterization of the viral genome: identification of simian TT virus isolates. *Journal of Virology,* 74(3), 1549-1553.

AbuOdeh, R., Al-Mawlawi, N., Al-Qahtani, A. A., Bohol, M. F. F., Al-Ahdal, M. N., Hasan, H. A., . . . & Nasrallah, G. K. (2015). Detection and genotyping of torque teno virus (TTV) in healthy blood donors and patients infected with HBV or HCV in Qatar. *Journal of Medical Virology,* 87(7), 1184-1191.

Agriculture Forestry and Livestock Quarantine Headquarters. (2018). Guidelines for validation of virus disinfectants. *Agriculture, Forestry and Livestock Quarantine Headquarters Notice No. 2018-16.*, 5.

Aliyev, E., Filiz, V., Khan, M. M., Lee, Y. J., Abetz, C., & Abetz, V. (2019). Structural characterization of graphene oxide: Surface functional groups and fractionated oxidative debris. *Nanomaterials,* 9(8), 1180.

Amor, G., Sabbah, M., Caputo, L., Idbella, M., De Feo, V., Porta, R., . . . & Mauriello, G. (2021). Basil essential oil: Composition, antimicrobial properties, and microencapsulation to produce active chitosan films for food packaging. *Foods,* 10(1), 121.

Aramouni, M., Segalés, J., Cortey, M., & Kekarainen, T. (2010). Age-related tissue distribution of swine Torque teno sus virus 1 and 2. *Veterinary Microbiology,* 146(3-4), 350-353.

Artan, M., Karadeniz, F., Karagozlu, M. Z., Kim, M. M., & Kim, S. K. (2010). Anti-HIV-1 activity of low molecular weight sulfated chitooligosaccharides. *Carbohydrate Research,* 345(5), 656-662.

Babayan, S. A., Orton, R. J., & Streicker, D. G. (2018). Predicting reservoir hosts and arthropod vectors from evolutionary signatures in RNA virus genomes. *Science,* 362(6414), 577-580.

Bankevich, A., Nurk, S., Antipov, D., Gurevich, A. A., Dvorkin, M., Kulikov, A. S., . . . & Pevzner, P. A. (2012). SPAdes: a new genome assembly algorithm and its applications to single-cell sequencing. *Journal of Computational Biology,* 19(5), 455-477.

Banks, M., Bendall, R., Grierson, S., Heath, G., Mitchell, J., & Dalton, H. (2004). Human and porcine hepatitis E virus strains, United Kingdom. *Emerging Infectious Diseases,* 10(5), 953.

Bergner, L. M., Orton, R. J., & Streicker, D. G. (2020). Complete Genome Sequence of an Alphacoronavirus from Common Vampire Bats in Peru. *Microbiology Resource Announcements,* 9(34), e00742-00720.

Bernardin, F., Operskalski, E., Busch, M., & Delwart, E. (2010). Transfusion transmission of highly prevalent commensal human viruses. *Transfusion*, 50(11), 2474-2483.

Biagini, P., Attoui, H., Gallian, P., Touinssi, M., Cantaloube, J. F., de Micco, P., & de Lamballerie, X. (2000). Complete sequences of two highly divergent European isolates of TT virus. *Biochemical and Biophysical Research Communications*, 271(3), 837-841.

Biagini, P. (2011). Genus alphatorquevirus. In King, A. M., Lefkowitz, E., Adams, M. J., & Carstens, E. B. (Eds.), *Virus Taxonomy : Ninth Report of the International Committee on Taxonomy of Viruses*. (pp. 333-334). Elsevier Scientific Publishing. Amsterdam, Netherlands.

Bigarré, L., Beven, V., De Boisséson, C., Grasland, B., Rose, N., Biagini, P., & Jestin, A. (2005). Pig anelloviruses are highly prevalent in swine herds in France. *Journal of General Virology*, 86(3), 631-635.

Blois, S., Mallus, F., Liciardi, M., Pilo, C., Camboni, T., Macera, L., . . . & Manzin, A. (2014). High prevalence of co-infection with multiple Torque teno sus virus species in Italian pig herds. *PLoS One*, 9(11), e113720.

Boni, M. F., Lemey, P., Jiang, X., Lam, T. T. Y., Perry, B. W., Castoe, T. A., . . . & Robertson, D. L. (2020). Evolutionary origins of the SARS-CoV-2 sarbecovirus lineage responsible for the COVID-19 pandemic. *Nature Microbiology*, 5(11), 1408-1417.

Brassard, J., Gagné, M. J., Lamoureux, L., Inglis, G., Leblanc, D., & Houde, A. (2008). Molecular detection of bovine and porcine Torque teno virus in plasma and feces. *Veterinary Microbiology*, 126(1-3), 271-276.

Calisher, C. H., Childs, J. E., Field, H. E., Holmes, K. V., & Schountz, T. (2006). Bats: important reservoir hosts of emerging viruses. *Clinical Microbiology Reviews*, 19(3), 531-545.

Çelik, Y., Flahaut, E., & Suvacı, E. (2017). A comparative study on few-layer graphene production by exfoliation of different starting materials in a low boiling point solvent. *FlatChem*, 1, 74-88.

Chen, L. L., Ou, H. Y., Zhang, R., & Zhang, C. T. (2003). ZCURVE_CoV: a new system to recognize protein coding genes in coronavirus genomes, and its applications in analyzing SARS-CoV genomes. *Biochemical and Biophysical Research Communications*, 307(2), 382-388.

Chen, L., & Liang, J. (2020). An overview of functional nanoparticles as novel emerging antiviral therapeutic agents. *Materials Science and Engineering: C*, 112, 110924.

Chen, Y. N., Hsueh, Y. H., Hsieh, C. T., Tzou, D. Y., & Chang, P. L. (2016). Antiviral activity of graphene–silver nanocomposites against non-

enveloped and enveloped viruses. *International Journal of Environmental Research and Public Health,* 13(4), 430.

Chirkov, S. (2002). The antiviral activity of chitosan. *Applied Biochemistry and Microbiology,* 38(1), 1-8.

Cortey, M., Olvera, A., Grau-Roma, L., & Segalés, J. (2011). Further comments on porcine circovirus type 2 (PCV2) genotype definition and nomenclature. *Veterinary Microbiology,* 149(3-4), 522-523.

Costantini, M., Barbetta, A., Swieszkowski, W., Seliktar, D., Gargioli, C., & Rainer, A. (2021). Photocurable Biopolymers for Coaxial Bioprinting. In A. Rainer & L. Moroni (Eds.), *Computer-Aided Tissue Engineering* (pp. 45-54), Humana, New York, NY.

Davis, R., Zivanovic, S., D'Souza, D. H., & Davidson, P. M. (2012). Effectiveness of chitosan on the inactivation of enteric viral surrogates. *Food Microbiology,* 32(1), 57-62.

Davydova, V., Nagorskaya, V., Gorbach, V., Kalitnik, A., Reunov, A., Solov'Eva, T., & Ermak, I. (2011). Chitosan antiviral activity: dependence on structure and depolymerization method. *Applied Biochemistry and Microbiology,* 47(1), 103-108.

De Maio, F., Palmieri, V., Babini, G., Augello, A., Palucci, I., Perini, G., . . . & Papi, M. (2021). Graphene nanoplatelet and Graphene oxide functionalization of face mask materials inhibits infectivity of trapped SARS-CoV-2. *iScience,* 24(7), 102788.

De Oliveira, T. M., Rehfeld, I. S., Guedes, M. I., Ferreira, J. M., Kroon, E. G., & Lobato, Z. I. (2011). Susceptibility of Vaccinia virus to chemical disinfectants. *The American Journal of Tropical Medicine and Hygiene,* 85(1), 152-157.

De Villiers, E. M., & Hausen, H. Z. (2009). TT Viruses: The Still Elusive Human Pathogens. In E. M. Villiers, & H. Hausen (Eds.), *Current Topics in Microbiology and Immunology*, 311(v-vi). Springer-Verlag, Amsterdam, Netherlands.

Decaro, N., & Buonavoglia, C. (2008). An update on canine coronaviruses: viral evolution and pathobiology. *Veterinary Microbiology,* 132(3-4), 221-234.

Dencs, A., Hettmann, A., Szomor, K. N., Kis, Z., & Takács, M. (2009). Prevalence and genotyping of group 3 torque teno viruses detected in health care workers in Hungary. *Virus Genes,* 39(1), 39-45.

Divya, K., Vijayan, S., George, T. K., & Jisha, M. S. (2017). Antimicrobial properties of chitosan nanoparticles: Mode of action and factors affecting activity. *Fibers and Polymers,* 18(2), 221-230.

Dobson, A. P., & Carper, E. R. (1996). Infectious diseases and human population history. *Bioscience,* 46(2), 115-126.

Ege, D., Kamali, A. R., & Boccaccini, A. R. (2017). Graphene oxide/polymer-based biomaterials. *Advanced Engineering Materials*, 19(12), 1700627.

Ellis, J. A., Allan, G., & Krakowka, S. (2008). Effect of coinfection with genogroup 1 porcine torque teno virus on porcine circovirus type 2–associated postweaning multisystemic wasting syndrome in gnotobiotic pigs. *American Journal of Veterinary Research*, 69(12), 1608-1614.

Fan, Y., Zhao, K., Shi, Z. L., & Zhou, P. (2019). Bat coronaviruses in china. *Viruses*, 11(3), 210.

Gallei, A., Pesch, S., Esking, W. S., Keller, C., & Ohlinger, V. F. (2010). Porcine Torque teno virus: determination of viral genomic loads by genogroup-specific multiplex rt-PCR, detection of frequent multiple infections with genogroups 1 or 2, and establishment of viral full-length sequences. *Veterinary Microbiology*, 143(2-4), 202-212.

Gao, Y., Liu, W., Wang, W., Zhang, X., & Zhao, X. (2018). The inhibitory effects and mechanisms of 3, 6-O-sulfated chitosan against human papillomavirus infection. *Carbohydrate Polymers*, 198, 329-338.

Ge, X. Y., Li, J. L., Yang, X. L., Chmura, A. A., Zhu, G., Epstein, J. H., . . . & Peng, C. (2013). Isolation and characterization of a bat SARS-like coronavirus that uses the ACE2 receptor. *Nature*, 503(7477), 535-538.

Geim, A. K., & Novoselov, K. S. (2007). The rise of graphene. *Nature materials*, 6(3), 91-183.

Gonçalves, G., Vila, M., Bdikin, I., de Andrés, A., Emami, N., Ferreira, R. A., . . . & Marques, P. A. (2014). Breakdown into nanoscale of graphene oxide: confined hot spot atomic reduction and fragmentation. *Scientific Reports*, 4(1), 1-8.

Gong, L., Li, J., Zhou, Q., Xu, Z., Chen, L., Zhang, Y., . . . & Cao, Y. (2017). A new bat-HKU2–like coronavirus in swine, China, 2017. *Emerging Infectious Diseases*, 23(9), 1607.

Graham, R. L., & Baric, R. S. (2010). Recombination, Reservoirs, and the Modular Spike: Mechanisms of Coronavirus Cross-Species Transmission. *Journal of Virology*, 84(7), 3134-3146.

Guan, Y., Zheng, B. J., He, Y. Q., Liu, X. L., Zhuang, Z. X., Cheung, C. L., . . . & Poon, L. L. (2003). Isolation and characterization of viruses related to the SARS coronavirus from animals in southern China. *Science*, 302(5643), 276-278.

Guo, J., Wang, W., Yu, D., & Wu, Y. (2011). Spinoculation triggers dynamic actin and cofilin activity that facilitates HIV-1 infection of transformed and resting CD4 T cells. *Journal of Virology*, 85(19), 9824-9833.

Hallett, R., Clewley, J., Bobet, F., McKiernan, P., & Teo, C. (2000). Characterization of a highly divergent TT virus genome. *Journal of General Virology,* 81(9), 2273-2279.

Hansa, A., Rai, R. B., Dhama, K., Wani, M. Y., Saminathan, M., & Ranganath, G. J. (2013). Isolation of bovine coronavirus (bcoV) in vero cell line and its confirmation by direct FAT and RT-PCR. *Pakistan Journal of Biological Sciences: PJBS,* 16(21), 1342-1347.

Hijikata, M., Takahashi, K., & Mishiro, S. (1999). Complete circular DNA genome of a TT virus variant (isolate name SANBAN) and 44 partial ORF2 sequences implicating a great degree of diversity beyond genotypes. *Virology,* 260(1), 17-22.

Hoang, D. T., Chernomor, O., Von Haeseler, A., Minh, B. Q., & Vinh, L. S. (2018). UFBoot2: improving the ultrafast bootstrap approximation. *Molecular Biology and Evolution,* 35(2), 518-522.

Hsiao, K. L., Wang, L. Y., Lin, C. L., & Liu, H. F. (2016). New phylogenetic groups of torque teno virus identified in eastern Taiwan indigenes. *PLoS One,* 11(2), e0149901.

Hu, X., Mu, L., Wen, J., & Zhou, Q. (2012). Covalently synthesized graphene oxide-aptamer nanosheets for efficient visible-light photocatalysis of nucleic acids and proteins of viruses. *Carbon,* 50(8), 2772-2781.

Huang, Y., Dryman, B., Harrall, K., Vaughn, E., Roof, M., & Meng, X. (2010). Development of SYBR green-based real-time PCR and duplex nested PCR assays for quantitation and differential detection of species-or type-specific porcine Torque teno viruses. *Journal of Virological Methods,* 170(1-2), 140-146.

Huang, Y., & Meng, X. (2010). Novel strategies and approaches to develop the next generation of vaccines against porcine reproductive and respiratory syndrome virus (PRRSV). *Virus Research,* 154(1-2), 141-149.

Hussain, S., Pan, J. a., Chen, Y., Yang, Y., Xu, J., Peng, Y., . . . & Tien, P. (2005). Identification of novel subgenomic RNAs and noncanonical transcription initiation signals of severe acute respiratory syndrome coronavirus. *Journal of Virology,* 79(9), 5288-5295.

Inami, T., Obara, T., Moriyama, M., Arakawa, Y., & Abe, K. (2000). Full-length nucleotide sequence of a simian TT virus isolate obtained from a chimpanzee: evidence for a new TT virus-like species. *Virology,* 277(2), 330-335.

Islam, M. M., Shahruzzaman, M., Biswas, S., Sakib, M. N., & Rashid, T. U. (2020). Chitosan based bioactive materials in tissue engineering applications-A review. *Bioactive Materials,* 5(1), 164-183.

Jiménez-Melsió, A., Parés, S., Segalés, J., & Kekarainen, T. (2013). Detection of porcine anelloviruses in pork meat and human faeces. *Virus Research*, 178(2), 522-524.

Jimenez, L., & Chiang, M. (2006). Virucidal activity of a quaternary ammonium compound disinfectant against feline calicivirus: a surrogate for norovirus. *American Journal of Infection Control*, 34(5), 269-273.

Johnson, M., Zaretskaya, I., Raytselis, Y., Merezhuk, Y., McGinnis, S., & Madden, T. L. (2008). NCBI BLAST: a better web interface. *Nucleic Acids Research*, 36, W5-W9.

Jones, J. E., Le Sage, V., & Lakdawala, S. S. (2021). Viral and host heterogeneity and their effects on the viral life cycle. *Nature Reviews Microbiology*, 19(4), 272-282.

Jones, K. E., Patel, N. G., Levy, M. A., Storeygard, A., Balk, D., Gittleman, J. L., & Daszak, P. (2008). Global trends in emerging infectious diseases. *Nature*, 451(7181), 990-993.

Kakkola, L., Bondén, H., Hedman, L., Kivi, N., Moisala, S., Julin, J., . . . & Hedman, K. (2008). Expression of all six human Torque teno virus (TTV) proteins in bacteria and in insect cells, and analysis of their IgG responses. *Virology*, 382(2), 182-189.

Kalvari, I., Nawrocki, E. P., Ontiveros-Palacios, N., Argasinska, J., Lamkiewicz, K., Marz, M., . . . & Petrov, A. I. (2021). Rfam 14: expanded coverage of metagenomic, viral and microRNA families. *Nucleic Acids Research*, 49(D1), D192-D200.

Kalyaanamoorthy, S., Minh, B. Q., Wong, T. K. F., Von Haeseler, A., & Jermiin, L. S. (2017). ModelFinder: fast model selection for accurate phylogenetic estimates. *Nature Methods*, 14(6), 587-589.

Kamahora, T., Hino, S., & Miyata, H. (2000). Three spliced mRNAs of TT virus transcribed from a plasmid containing the entire genome in COS1 cells. *Journal of Virology*, 74(21), 9980-9986.

Katoh, K., & Standley, D. M. (2013). MAFFT Multiple Sequence Alignment Software Version 7: Improvements in Performance and Usability. *Molecular Biology and Evolution*, 30(4), 772-780.

Kekarainen, T., & Segalés, J. (2009). Torque teno virus infection in the pig and its potential role as a model of human infection. *The Veterinary Journal*, 180(2), 163-168.

Kekarainen, T., Sibila, M., & Segalés, J. (2006). Prevalence of swine Torque teno virus in post-weaning multisystemic wasting syndrome (PMWS)-affected and non-PMWS-affected pigs in Spain. *Journal of General Virology*, 87(4), 833-837.

Khor, E., & Lim, L. Y. (2003). Implantable applications of chitin and chitosan. *Biomaterials*, 24(13), 2339-2349.

Kim, A. R., Chung, H. C., Kim, H. K., Kim, E. O., Choi, M. G., Yang, H. J., . . . & Park, B. K. (2014). Characterization of a complete genome of a circular single-stranded DNA virus from porcine stools in Korea. *Virus Genes*, 48(1), 81-88.

Kochkina, Z., & Chirkov, S. (2000). Effect of chitosan derivatives on the reproduction of coliphages T2 and T7. *Microbiology*, 69(2), 208-211.

Kochkina, Z., Surgucheva, N., & Chirkov, S. (2000). Inactivation of coliphages by chitosan derivatives. *Microbiology*, 69(2), 212-216.

Krakowka, S., & Ellis, J. A. (2008). Evaluation of the effects of porcine genogroup 1 torque teno virus in gnotobiotic swine. *American Journal of Veterinary Research*, 69(12), 1623-1629.

Krakowka, S., Hartunian, C., Hamberg, A., Shoup, D., Rings, M., Zhang, Y., . . . & Ellis, J. A. (2008). Evaluation of induction of porcine dermatitis and nephropathy syndrome in gnotobiotic pigs with negative results for porcine circovirus type 2. *American Journal of Veterinary Reserach*, 69(12), 1615-1622.

Krishnamoorthy, K., Mohan, R., & Kim, S. J. (2011). Graphene oxide as a photocatalytic material. *Applied Physics Letters*, 98(24), 244101.

Kuo, W. S., Chen, H. H., Chen, S.Y., Chang, C. Y., Chen, P. C., Hou, Y. I., . . . & Wang, J. Y. (2017). Graphene quantum dots with nitrogen-doped content dependence for highly efficient dual-modality photodynamic antimicrobial therapy and bioimaging. *Biomaterials*, 120, 185-194.

Kusanagi, K. I., Kuwahara, H., Katoh, T., Nunoya, T., Ishikawa, Y., Samejima, T., & Tajima, M. (1992). Isolation and serial propagation of porcine epidemic diarrhea virus in cell cultures and partial characterization of the isolate. *Journal of Veterinary Medical Science*, 54(2), 313-318.

Lacroix, A., Duong, V., Hul, V., San, S., Davun, H., Omaliss, K., . . . & Buchy, P. (2017). Genetic diversity of coronaviruses in bats in Lao PDR and Cambodia. *Infection, Genetics and Evolution*, 48, 10-18.

Lategan, K., Alghadi, H., Bayati, M., Cortalezzi, D., Fidalgo, M., & Pool, E. (2018). Effects of graphene oxide nanoparticles on the immune system biomarkers produced by RAW 264.7 and human whole blood cell cultures. *Nanomaterials*, 8(2), 125.

Lazov, C. M., Belsham, G. J., Botner, A., & Rasmussen, T. B. (2021). Full-genome sequences of alphacoronaviruses and astroviruses from myotis and pipistrelle bats in Denmark. *Viruses*, 13(6), 1073.

Leary, T. P., Erker, J. C., Chalmers, M. L., Desai, S. M., & Mushahwar, I. K. (1999). Improved detection systems for TT virus reveal high prevalence in humans, non-human primates and farm animals. *Journal of General Virology*, 80(8), 2115-2120.

Lee, B. C., Lee, J. Y., Kim, J., Yoo, J. M., Kang, I., Kim, J. J., . . . & Kang, K. S. (2020). Graphene quantum dots as anti-inflammatory therapy for colitis. *Science Advances*, 6(18), eaaz2630.

Lee, S.S., Sunyoung, S., Jung, H., Shin, J., & Lyoo, Y. S. (2010). Quantitative detection of porcine Torque teno virus in Porcine circovirus-2–negative and Porcine circovirus–associated disease-affected pigs. *Journal of Veterinary Diagnostic Investigation*, 22(2), 261-264.

Leopardi, S., Holmes, E. C., Gastaldelli, M., Tassoni, L., Priori, P., Scaravelli, D., . . . & De Benedictis, P. (2018). Interplay between co-divergence and cross-species transmission in the evolutionary history of bat coronaviruses. *Infection, Genetics and Evolution*, 58, 279-289.

Letko, M., Seifert, S. N., Olival, K. J., Plowright, R. K., & Munster, V. J. (2020). Bat-borne virus diversity, spillover and emergence. *Nature Reviews Microbiology*, 18(8), 461-471.

Li, H., Mendelsohn, E., Zong, C., Zhang, W., Hagan, E., Wang, N., . . . & Daszak, P. (2019). Human-animal interactions and bat coronavirus spillover potential among rural residents in Southern China. *Biosafety and Health*, 1(02), 84-90.

Li, K., Wang, L. Q., Wu, Y. Y., Chao, A. J., Lu, Q. W., Wei, Z. Y., . . . & Chen, H. Y. (2013). Molecular detection and genomic characterization of Torque teno sus virus 1 and 2 from domestic pigs in central China. *Virus Genes*, 46(3), 479-486.

Li, L. Q., Huang, T., Wang, Y. Y., Wang, Z. P., Liang, Y., Huang, T. B., . . . & Wang, Y. (2020). COVID-19 patients' clinical characteristics, discharge rate, and fatality rate of meta-analysis. *Journal of Medical Virology*, 92(6), 577-583.

Lin, X. D., Wang, W., Hao, Z. Y., Wang, Z. X., Guo, W. P., Guan, X. Q., . . . & Zhang, Y. Z. (2017). Extensive diversity of coronaviruses in bats from China. *Virology*, *507*, 1-10.

Lisitsyn, N., Lisitsyn, N., & Wigler, M. (1993). Cloning the differences between two complex genomes. *Science*, 259(5097), 946-951.

Liu, S., Hu, M., Zeng, T. H., Wu, R., Jiang, R., Wei, J., . . . & Chen, Y. (2012). Lateral dimension-dependent antibacterial activity of graphene oxide sheets. *Langmuir*, 28(33), 12364-12372.

Loh, E. H., Zambrana-Torrelio, C., Olival, K. J., Bogich, T. L., Johnson, C. K., Mazet, J. A., . . . & Daszak, P. (2015). Targeting transmission pathways for emerging zoonotic disease surveillance and control. *Vector-Borne and Zoonotic Diseases*, 15(7), 432-437.

Luo, X., Zhou, G. Z., Zhang, Y., Peng, L. H., Zou, L. P., & Yang, Y. S. (2020). Coronaviruses and gastrointestinal diseases. *Military Medical Research*, 7(1), 49.

Maggi, F., & Bendinelli, M. (2009). Immunobiology of the Torque teno viruses and other anelloviruses. In E. M. De Villiers & H. Zur Hausen (Eds.), *Current Top Microbiology Immunology*. (pp. 65-90). Springer Science & Business Media, Berlin, Germany.

Manenti, A., Maggetti, M., Casa, E., Martinuzzi, D., Torelli, A., Trombetta, C. M., . . . & Montomoli, E. (2020). Evaluation of SARS-CoV-2 neutralizing antibodies using a CPE-based colorimetric live virus micro-neutralization assay in human serum samples. *Journal of Medical Virology,* 92(10), 2096-2104.

Mansouri, S., Lavigne, P., Corsi, K., Benderdour, M., Beaumont, E., & Fernandes, J. C. (2004). Chitosan-DNA nanoparticles as non-viral vectors in gene therapy: strategies to improve transfection efficacy. *European Journal of Pharmaceutics and Biopharmaceutics,* 57(1), 1-8.

Marcano, D. C., Kosynkin, D. V., Berlin, J. M., Sinitskii, A., Sun, Z., Slesarev, A., . . . & Tour, J. M. (2010). Improved synthesis of graphene oxide. *ACS Nano,* 4(8), 4806-4814.

Masembe, C., Michuki, G., Onyango, M., Rumberia, C., Norling, M., Bishop, R. P., . . . & Fischer, A. (2012). Viral metagenomics demonstrates that domestic pigs are a potential reservoir for Ndumu virus. *Virology Journal,* 9(1), 1-7.

McDonnell, G., & Russell, A. D. (1999). Antiseptics and disinfectants: activity, action, and resistance. *Clinical Microbiology Reviews,* 12(1), 147-179.

McKeown, N., Fenaux, M., Halbur, P. G., & Meng, X. (2004). Molecular characterization of porcine TT virus, an orphan virus, in pigs from six different countries. *Veterinary Microbiology,* 104(1-2), 113-117.

Meng, X. J. (2012). Emerging and re-emerging swine viruses. *Transboundary and Emerging Diseases,* 59, 85-102.

Mi, Z., Yuan, X., Pei, G., Wang, W., An, X., Zhang, Z., . . . & Tong, Y. (2014). High-throughput sequencing exclusively identified a novel Torque teno virus genotype in serum of a patient with fatal fever. *Virologica Sinica,* 29(2), 112-118.

Minh, B. Q., Schmidt, H. A., Chernomor, O., Schrempf, D., Woodhams, M. D., Von Haeseler, A., & Lanfear, R. (2020). IQ-TREE 2: New models and efficient methods for phylogenetic inference in the genomic era. *Molecular Biology and Evolution,* 37(5), 1530-1534.

Mitchell, A. L., Attwood, T. K., Babbitt, P. C., Blum, M., Bork, P., Bridge, A., . . . & Fraser, M. I. (2019). InterPro in 2019: improving coverage, classification and access to protein sequence annotations. *Nucleic Acids Research,* 47(D1), D351-D360.

Miyata, H., Tsunoda, H., Kazi, A., Yamada, A., Khan, M. A., Murakami, J., . . . & Hino, S. (1999). Identification of a novel GC-rich 113-nucleotide

region to complete the circular, single-stranded DNA genome of TT virus, the first human circovirus. *Journal of Virology*, 73(5), 3582-3586.
Morse, S. S., Mazet, J. A., Woolhouse, M., Parrish, C. R., Carroll, D., Karesh, W. B., . . . & Daszak, P. (2012). Prediction and prevention of the next pandemic zoonosis. *The Lancet*, 380(9857), 1956-1965.
Mou, C., Wang, M., Pan, S., & Chen, Z. (2019). Identification of nuclear localization signals in the ORF2 protein of porcine circovirus type 3. *Viruses*, 11(12), 1086.
Mushahwar, I. K., Erker, J. C., Muerhoff, A. S., Leary, T. P., Simons, J. N., Birkenmeyer, L. G., . . . & Dexai, S. M. (1999). Molecular and biophysical characterization of TT virus: evidence for a new virus family infecting humans. *Proceedings of the National Academy of Sciences of the United States of America*, 96(6), 3177-3182.
Muxika, A., Etxabide, A., Uranga, J., Guerrero, P., & De La Caba, K. (2017). Chitosan as a bioactive polymer: Processing, properties and applications. *International Journal of Biological Macromolecules*, 105, 1358-1368.
Myers, K. P., Olsen, C. W., & Gray, G. C. (2007). Cases of swine influenza in humans: a review of the literature. *Clinical Infectious Diseases*, 44(8), 1084-1088.
Nathalie, K., Miszczak, F., Diancourt, L., Caro, V., Moutou, F., Vabret, A., & Gouilh, M. A. (2016). Comparative molecular epidemiology of two closely related coronaviruses, bovine coronavirus (BCoV) and human coronavirus OC43 (HCoV-OC43), reveals a different evolutionary pattern. *Infection, Genetics and Evolution*, 40, 186-191.
Nguyen, L. T., Schmidt, H. A., von Haeseler, A., & Minh, B. Q. (2014). IQ-TREE: a fast and effective stochastic algorithm for estimating maximum-likelihood phylogenies. *Molecular Biology and Evolution*, 32(1), 268-274.
Nguyen, M. H., Hwang, I. C., & Park, H. J. (2013). Enhanced photoprotection for photo-labile compounds using double-layer coated corn oil-nanoemulsions with chitosan and lignosulfonate. *Journal of Photochemistry and Photobiology B: Biology*, 125, 194-201.
Niel, C., Diniz-Mendes, L., & Devalle, S. (2005). Rolling-circle amplification of Torque teno virus (TTV) complete genomes from human and swine sera and identification of a novel swine TTV genogroup. *Journal of General Virology*, 86(5), 1343-1347.
Nieto, D., Aramouni, M., Grau-Roma, L., Segales, J., & Kekarainen, T. (2011). Dynamics of Torque teno sus virus 1 (TTSuV1) and 2 (TTSuV2) DNA loads in serum of healthy and postweaning multisystemic wasting syndrome (PMWS) affected pigs. *Veterinary Microbiology*, 152(3-4), 284-290.

Ninomiya, M., Takahashi, M., Nishizawa, T., Shimosegawa, T., & Okamoto, H. (2008). Development of PCR assays with nested primers specific for differential detection of three human anelloviruses and early acquisition of dual or triple infection during infancy. *Journal of Clinical Microbiology*, 46(2), 507-514.

Nishizawa, T., Okamoto, H., Konishi, K., Yoshizawa, H., Miyakawa, Y., & Mayumi, M. (1997). A novel DNA virus (TTV) associated with elevated transaminase levels in posttransfusion hepatitis of unknown etiology. *Biochemical and Biophysical Research Communications*, 241(1), 92-97.

Ogando, N. S., Ferron, F., Decroly, E., Canard, B., Posthuma, C. C., & Snijder, E. J. (2019). The curious case of the nidovirus exoribonuclease: its role in RNA synthesis and replication fidelity. *Frontiers in Microbiology*, 10, 1813.

Okamoto, H., Takahashi, M., Nishizawa, T., Tawara, A., Fukai, K., Muramatsu, U., . . . & Yoshikawa, A. (2002). Genomic characterization of TT viruses (TTVs) in pigs, cats and dogs and their relatedness with species-specific TTVs in primates and tupaias. *Journal of General Virology*, 83(6), 1291-1297.

Olival, K. J., Hosseini, P. R., Zambrana-Torrelio, C., Ross, N., Bogich, T. L., & Daszak, P. (2017). Host and viral traits predict zoonotic spillover from mammals. *Nature*, 546(7660), 646-650.

Palmieri, V., & Papi, M. (2020). Can graphene take part in the fight against COVID-19?. *Nano Today*, 33, 100883.

Park, S. J., Moon, H. J., Luo, Y., Kim, H. K., Kim, E. M., Yang, J. S., . . . & Park, B. K. (2008). Cloning and further sequence analysis of the ORF3 gene of wild-and attenuated-type porcine epidemic diarrhea viruses. *Virus Genes*, 36(1), 95-104.

Peixoto, F. P., Braga, P. , & Mendes, P. (2018). A synthesis of ecological and evolutionary determinants of bat diversity across spatial scales. *BMC Ecology*, 18(1), 18.

Peng, Y., Nishizawa, T., Takahashi, M., Ishikawa, T., Yoshikawa, A., & Okamoto, H. (2002). Analysis of the entire genomes of thirteen TT virus variants classifiable into the fourth and fifth genetic groups, isolated from viremic infants. *Archives of Virology*, 147(1), 21-41.

Pinho-Nascimento, C. A., Leite, J. P. G., Niel, C., & Diniz-Mendes, L. (2011). Torque teno virus in fecal samples of patients with gastroenteritis: prevalence, genogroups distribution, and viral load. *Journal of Medical Virology*, 83(6), 1107-1111.

Poon, L. L., Chu, D. K., Chan, K. H., Wong, O. K., Ellis, T. M., Leung, Y. H. C., . . . & Peiris, J. S. M. (2005). Identification of a novel coronavirus in bats. *Journal of Virology*, 79(4), 2001-2009.

Pozzuto, T., Mueller, B., Meehan, B., Ringler, S. S., McIntosh, K. A., Ellis, J. A., . . . & Krakowka, S. (2009). In utero transmission of porcine torque teno viruses. *Veterinary Microbiology*, 137(3-4), 375-379.

Prada, D., Boyd, V., Baker, M. L., O'Dea, M., & Jackson, B. (2019). Viral Diversity of Microbats within the South West Botanical Province of Western Australia. *Viruses*, 11(12), 1157.

Qin, Y., & Li, P. (2020). Antimicrobial chitosan conjugates: Current synthetic strategies and potential applications. *International Journal of Molecular Sciences*, 21(2), 499.

Qinna, N. A., Akayleh, F. T., Al Remawi, M. M., Kamona, B. S., Taha, H., & Badwan, A. A. (2013). Evaluation of a functional food preparation based on chitosan as a meal replacement diet. *Journal of Functional Foods*, 5(3), 1125-1134.

Raafat, D., & Sahl, H. G. (2009). Chitosan and its antimicrobial potential–a critical literature survey. *Microbial Biotechnology*, 2(2), 186-201.

Rabea, E. I., Badawy, M. E. T., Stevens, C. V., Smagghe, G., & Steurbaut, W. (2003). Chitosan as antimicrobial agent: applications and mode of action. *Biomacromolecules*, 4(6), 1457-1465.

Ray, S. C., (2015). Application and uses of graphene oxide and reduced graphene oxide. In S.C. Ray (Ed.), *Applications of Graphene and Graphene-Oxide Based Nanomaterials.* (pp. 39-55). William Andrew Publishing: Oxford, Amsterdam, Netherlands.

Rhazouani, A., Gamrani, H., El Achaby, M., Aziz, K., Gebrati, L., Uddin, M. S., & AZIZ, F. (2021). Synthesis and toxicity of graphene oxide nanoparticles: a literature review of In vitro and In vivo studies. *BioMed Research International*, 2021, 5518999.

Romeo, R., Hegerich, P., Emerson, S. U., Colombo, M., Purcell, R. H., & Bukh, J. (2000). High prevalence of TT virus (TTV) in naive chimpanzees and in hepatitis C virus-infected humans: frequent mixed infections and identification of new TTV genotypes in chimpanzees. *Microbiology*, 81(4), 1001-1007.

Sanchez, V. C., Jachak, A., Hurt, R. H., & Kane, A. B. (2012). Biological interactions of graphene-family nanomaterials: an interdisciplinary review. *Chemical Research in Toxicology*, 25(1), 15-34.

Sarairah, H., Bdour, S., & Gharaibeh, W. (2020). The molecular epidemiology and phylogeny of torque teno virus (TTV) in Jordan. *Viruses*, 12(2), 165.

Sawicki, S. G., Sawicki, D. L., & Siddell, S. G. (2007). A contemporary view of coronavirus transcription. *Journal of Virology*, 81(1), 20-29.

Scobie, L., & Takeuchi, Y. (2009). Porcine endogenous retrovirus and other viruses in xenotransplantation. *Current Opinion in Organ Transplantation,* 14(2), 175-179.

Scotto–Lavino, E., Du, G., & Frohman, M. A. (2006). 5´ end cDNA amplification using classic RACE. *Nature Protocols,* 1(6), 2555.

Segalés, J., Urniza, A., Alegre, A., Bru, T., Crisci, E., Nofrarías, M., . . . & Xu, Z. (2009). A genetically engineered chimeric vaccine against porcine circovirus type 2 (PCV2) improves clinical, pathological and virological outcomes in postweaning multisystemic wasting syndrome affected farms. *Vaccine,* 27(52), 7313-7321.

Seifi, T., & Kamali, A. R. (2021). Anti-pathogenic activity of graphene nanomaterials: A review. *Colloids and Surfaces B: Biointerfaces,* 199, 111509.

Seifi, T., & Reza Kamali, A. (2021). Antiviral performance of graphene-based materials with emphasis on COVID-19: A review. *Medicine in Drug Discovery,* 11, 100099.

Sibila, M., Martínez-Guinó, L., Huerta, E., Llorens, A., Mora, M., Grau-Roma, L., . . . & Segales, J. (2009). Swine torque teno virus (TTV) infection and excretion dynamics in conventional pig farms. *Veterinary Microbiology,* 139(3-4), 213-218.

Simas, P. V. M., de Souza Barnabé, A. C., Durães-Carvalho, R., de Lima Neto, D. F., Caserta, L. C., Artacho, L., . . . & Ams, C. W. (2015). Bat coronavirus in Brazil related to appalachian ridge and porcine epidemic diarrhea viruses. *Emerging Infectious Diseases,* 21(4), 729.

Slingenbergh, J., Gilbert, M., Balogh, K. d., & Wint, W. (2004). Ecological sources of zoonotic diseases. *Revue Scientifique et Technique-Office International des Epizooties,* 23(2), 467-484.

Smith, C. S., de Jong, C. E., Meers, J., Henning, J., Wang, L. F., & Field, H. E. (2016). Coronavirus infection and diversity in bats in the Australasian region. *Ecohealth,* 13(1), 72-82.

Smith, T. C., Harper, A. L., Nair, R., Wardyn, S. E., Hanson, B. M., Ferguson, D. D., & Dressler, A. E. (2011). Emerging swine zoonoses. *Vector-Borne and Zoonotic Diseases,* 11(9), 1225-1234.

Snijder, E. J., Van Der Meer, Y., Zevenhoven-Dobbe, J., Onderwater, J. J., Van Der Meulen, J., Koerten, H. K., & Mommaas, A. M. (2006). Ultrastructure and origin of membrane vesicles associated with the severe acute respiratory syndrome coronavirus replication complex. *Journal of Virology,* 80(12), 5927-5940.

Song, D., Yang, J., Oh, J., Han, J., & Park, B. (2003). Differentiation of a Vero cell adapted porcine epidemic diarrhea virus from Korean field strains

by restriction fragment length polymorphism analysis of ORF 3. *Vaccine*, 21(17-18), 1833-1842.

Song, J., Wang, X., & Chang, C. T. (2014). Preparation and characterization of graphene oxide. *Journal of Nanomaterials*, 2014, 276143.

Song, S., Shen, H., Wang, Y., Chu, X., Xie, J., Zhou, N., & Shen, J. (2020). Biomedical application of graphene: From drug delivery, tumor therapy, to theranostics. *Colloids and Surfaces B: Biointerfaces*, 185, 110596.

Song, Z., Wang, X., Zhu, G., Nian, Q., Zhou, H., Yang, D., . . . & Tang, R. (2015). Virus capture and destruction by label-free graphene oxide for detection and disinfection applications. *Small*, 11(9-10), 1171-1176.

Sosa, M. A. G., Fazely, F., Koch, J. A., Vercellotti, S. V., & Ruprecht, R. M. (1991). N-Carboxymethylchitosan-N, O-sulfate as an anti-HIV-1 agent. *Biochemical and Biophysical Research Communications*, 174(2), 489-496.

Srivastava, A. K., Dwivedi, N., Dhand, C., Khan, R., Sathish, N., Gupta, M. K., . . . & Kumar, S. (2020). Potential of graphene-based materials to combat COVID-19: properties, perspectives, and prospects. *Materials Today Chemistry*, 18, 100385.

Ssemadaali, M. A., Effertz, K., Singh, P., Kolyvushko, O., & Ramamoorthy, S. (2016). Identification of heterologous Torque Teno Viruses in humans and swine. *Scientific Reports*, 6(1), 1-10.

Stevenson, G. W., Hoang, H., Schwartz, K. J., Burrough, E. R., Sun, D., Madson, D., . . . & Schmitt, B. J. (2013). Emergence of porcine epidemic diarrhea virus in the United States: clinical signs, lesions, and viral genomic sequences. *Journal of Veterinary Diagnostic Investigation*, 25(5), 649-654.

Su, S., Wong, G., Shi, W., Liu, J., Lai, A. C., Zhou, J., . . . & Gao, G. F. (2016). Epidemiology, genetic recombination, and pathogenesis of coronaviruses. *Trends in Microbiology*, 24(6), 490-502.

Su, S., Wong, G., Shi, W., Liu, J., Lai, A. C. K., Zhou, J., . . .& Gao, G. F. (2016). Epidemiology, genetic recombination, and pathogenesis of coronaviruses. *Trends in Microbiology*, 24(6), 490-502.

Sui, Z., Chen, Q., Wu, R., Zhang, H., Zheng, M., Wang, H., & Chen, Z. (2010). Cross-protection against influenza virus infection by intranasal administration of M2-based vaccine with chitosan as an adjuvant. *Archives of Virology*, 155(4), 535-544.

Tanaka, Y., Primi, D., Wang, R. Y., Umemura, T., Yeo, A. E., Mizokami, M., . . . & Shih, J. W. (2001). Genomic and molecular evolutionary analysis of a newly identified infectious agent (SEN virus) and its relationship to the TT virus family. *The Journal of Infectious Diseases*, 183(3), 359-367.

Tang, B., Bragazzi, N. L., Li, Q., Tang, S., Xiao, Y., & Wu, J. (2020). An updated estimation of the risk of transmission of the novel coronavirus (2019-nCov). *Infectious Disease Modelling*, 5, 248-255.

Teeling, E. C., Springer, M. S., Madsen, O., Bates, P., O'brien, S. J., & Murphy, W. J. (2005). A molecular phylogeny for bats illuminates biogeography and the fossil record. *Science*, 307(5709), 580-584.

Tomihata, K., & Ikada, Y. (1997). In vitro and in vivo degradation of films of chitin and its deacetylated derivatives. *Biomaterials*, 18(7), 567-575.

Tyrrell, D. A., & Myint, S. H. (1996). Coronaviruses. In S. Baron (Ed.), *Medical Microbiology. 4th edition*. Chapter 60. Galveston, Texas, USA.

Ukita, M., Okamoto, H., Nishizawa, T., Tawara, A., Takahashi, M., Iizuka, H., . . . & Mayumi, M. (2000). The entire nucleotide sequences of two distinct TT virus (TTV) isolates (TJN01 and TJN02) remotely related to the original TTV isolates. *Archives of Virology*, 145(8), 1543-1559.

Vibin, J., Chamings, A., Klaassen, M., & Alexandersen, S. (2020). Metagenomic characterisation of additional and novel avian viruses from Australian wild ducks. *Scientific Reports*, 10(1), 1-14.

Vlasova, A. N., Diaz, A., Damtie, D., Xiu, L., Toh, T. H., Lee, J. S. Y., . . . & Gray, G. C. (2021). Novel canine coronavirus isolated from a hospitalized pneumonia patient, East Malaysia. *Clinical Infectious Diseases*, ciab456.

Wang, L. F., & Cowled, C. (2015). Bat and reverse transcribing RNA and DNA viruses. In L. F. Wang & C. Cowled (Eds.), *Bats and viruses: a New Frontier of Emerging Infectious Diseases*, John Wiley & Sons, Hoboken, New Jersey, USA.

Wang, L. F., Walker, P. J., & Poon, L. L. (2011). Mass extinctions, biodiversity and mitochondrial function: are bats 'special'as reservoirs for emerging viruses?. *Current Opinion in Virology*, 1(6), 649-657.

Wang, W., Lin, X. D., Guo, W. P., Zhou, R. H., Wang, M. R., Wang, C. Q., . . . & Zhang, Y. Z. (2015). Discovery, diversity and evolution of novel coronaviruses sampled from rodents in China. *Virology*, 474, 19-27.

Wang, W., Lin, X. D., Liao, Y., Guan, X. Q., Guo, W. P., Xing, J. G., . . . & Zhang, Y. Z. (2017). Discovery of a highly divergent coronavirus in the Asian house shrew from China illuminates the origin of the alphacoronaviruses. *Journal of Virology*, 91(17), e00764-00717.

Webster, J. P., Borlase, A., & Rudge, J. W. (2017). Who acquires infection from whom and how? Disentangling multi-host and multi-mode transmission dynamics in the 'elimination'era. *Philosophical Transactions of the Royal Society B: Biological Sciences*, 372(1719), 20160091.

White, R. J., & Razgour, O. (2020). Emerging zoonotic diseases originating in mammals: a systematic review of effects of anthropogenic land-use change. *Mammal Review*, 50(4), 336-352.

Woo, P. C., Lau, S. K., Lam, C. S., Lau, C. C., Tsang, A. K., Lau, J. H., . . . & Wang, M. (2012). Discovery of seven novel Mammalian and avian coronaviruses in the genus deltacoronavirus supports bat coronaviruses as the gene source of alphacoronavirus and betacoronavirus and avian coronaviruses as the gene source of gammacoronavirus and deltacoronavirus. *Journal of Virology*, 86(7), 3995-4008.

Woo, P. C., Lau, S. K., & Yuen, K. Y. (2006). Infectious diseases emerging from Chinese wet-markets: zoonotic origins of severe respiratory viral infections. *Current Opinion in Infectious Diseases*, 19(5), 401-407.

Woo, P. C. Y., Lau, S. K., Huang, Y., & Yuen, K. Y. (2009). Coronavirus diversity, phylogeny and interspecies jumping. *Experimental Biology and Medicine*, 234(10), 1117-1127.

Woo, P. C., Lau, S. K., Lam, C. S., Lau, C. C., Tsang, A. K., Lau, J. H., . . . & Yuen, K. Y. (2012). Discovery of seven novel Mammalian and avian coronaviruses in the genus deltacoronavirus supports bat coronaviruses as the Gene Source of alphacoronavirus and betacoronavirus and avian coronaviruses as the gene source of gammacoronavirus and deltacoronavirus. *Journal of Virology*, 86(7), 3995-4008.

Woolhouse, M., Scott, F., Hudson, Z., Howey, R., & Chase-Topping, M. (2012). Human viruses: discovery and emergence. *Philosophical Transactions of the Royal Society B: Biological Sciences*, 367(1604), 2864-2871.

Wu, Z., Yang, L., Ren, X., He, G., Zhang, J., Yang, J., . . . & Zhu, Y. (2016). Deciphering the bat virome catalog to better understand the ecological diversity of bat viruses and the bat origin of emerging infectious diseases. *The ISME Journal*, 10(3), 609-620.

Yang, C., Xu, Y., Zhang, C., Sun, Z., Chen, C., Li, X., . . . & Man, B. (2014). Facile synthesis 3D flexible core-shell graphene/glass fiber via chemical vapor deposition. *Nanoscale Research Letters*, 9(1), 1-6.

Yang, X. L., Tan, C. W., Anderson, D. E., Jiang, R. D., Li, B., Zhang, W., . . . & Liu, X. L. (2019). Characterization of a filovirus (Měnglà virus) from Rousettus bats in China. *Nature Microbiology*, 4(3), 390-395.

Ye, S., Shao, K., Li, Z., Guo, N., Zuo, Y., Li, Q., . . . & Han, H. (2015). Antiviral activity of graphene oxide: how sharp edged structure and charge matter. *ACS Applied Materials & Interfaces*, 7(38), 21571-21579.

Zhang, Y. Z., & Holmes, E. C. (2020). A genomic perspective on the origin and emergence of SARS-CoV-2. *Cell*, 181(2), 223-227.

Zhao, L., Duan, G., Yang, Z., Weber, J. K., Liu, X., Lu, S., . . . & Xu, J. (2016). Particle size-dependent antibacterial activity and murine cell

cytotoxicity induced by graphene oxide nanomaterials. *Journal of Nanomaterials*, 2016, 6709764.

Zheng, M., Qu, D., Wang, H., Sun, Z., Liu, X., Chen, J., . . . & Chen, Z. (2016). Intranasal administration of chitosan against influenza A (H7N9) virus infection in a mouse model. *Scientific Reports*, 6(1), 1-11.

Zhou, H., Ji, J., Chen, X., Bi, Y., Li, J., Wang, Q., . . . & Shi, W. (2021). Identification of novel bat coronaviruses sheds light on the evolutionary origins of SARS-CoV-2 and related viruses. *Cell*, 184(17), 4380-4391.

Zhou, P., Fan, H., Lan, T., Yang, X. L., Shi, W. F., Zhang, W., . . . & Mani, S. (2018). Fatal swine acute diarrhoea syndrome caused by an HKU2-related coronavirus of bat origin. *Nature*, 556(7700), 255-258.

Zhou, P., Yang, X. L., Wang, X. G., Hu, B., Zhang, L., Zhang, W., . . . & Shi, Z. L. (2020). A pneumonia outbreak associated with a new coronavirus of probable bat origin. *Nature*, 579(7798), 270-273.

Ziebuhr, J., Snijder, E. J., & Gorbalenya, A. E. (2000). Virus-encoded proteinases and proteolytic processing in the Nidovirales. *Microbiology*, 81(4), 853-879.

국문 초록

동물에서 잠재적 인수공통성 바이러스 검출 및 코로나바이러스에 대한 키토산과 나노그래핀 옥사이드의 항바이러스 효능 연구

김 청 웅

(지도 교수: 양 수 진)

서울대학교 대학원 수의학과

수의병인생물학 및 예방수의학 전공

최근 신종 및 변종 인수공통 바이러스(zoonotic virus)의 출현으로 전 세계의 공중보건학 위험의 증가와 함께 막대한 경제적 손실을 초래하고 있다. 이들 대부분 바이러스는 동물에서 유래하였으며, 향후 사람에게 질병을 유발할 수 있는 잠재적인 인수공통 바이러스들이 여전히 자연계에 존재하고 있다. 따라서 사람으로의 종간 전파를 초래할 수 있는 동물 바이러스들을 조사하고, 이들 바이러스의 인체 감염 가능성을 선제적으로 평가하는 것이 중요하다.

본 연구에서는 국내 서식 박쥐와 국내 사육 돼지에서 각각 신종 바이러스를 분리하고, 이들 바이러스가 인수공통 바이러스로서 인체에

잠재적인 위험이 있는지를 평가하기 위하여 유전체 분석 및 계통유전학적 분석을 하였다. 그리고, 이러한 인수공통 바이러스의 전파를 효과적으로 차단·제어할 수 있는 소독제 개발을 위하여 천연물질인 키토산 (chitosan)과 나노그래핀 옥사이드 (nano-graphene oxide, nanoGO)의 코로나바이러스에 대한 소독 효과를 평가하였다

먼저, 2020년 7월부터 9월까지 강원과 경북지역에 서식하고 있는 박쥐 4종 6개체에서 신종 바이러스 분리를 시도하였다. 그 결과 경북 지역에서 서식하고 있는 문둥이박쥐 (*Eptesicus serotinus*)에서 코로나바이러스를 분리하였으며, 바이러스 분리주 HCQD-2020는 전자현미경 관찰에서 코로나바이러스의 특징적인 형태를 보였다. 또한 계통유전학적 분석 결과 이 바이러스는 알파코로나바이러스에 속하였으며, 그동안 밝혀지지 않은 새로운 종(species)으로 밝혀졌다. 전장유전체 시퀀싱 결과 HCQD-2020의 유전체의 길이는 28,000 bp 이며 총 7개의 Open reading frame (ORF)로 이루어져있었다. 알파코로나바이러스에서 보존된 부위로 알려진 아미노산 영역(region)은 총 7개로서 nonstructural proteins (Nsp) 3, Nsp5, 및 Nsp12~16이다. HCQD-2020과 다른 알파코로나바이러스를 비교 분석한 결과 7개 영역 모두에서 유사도가 International Committee on Taxonomy of

Viruses (ICTV)에서 지정하는 intraspecsies cutoff 기준인 90% 이하였다. 또한 전장유전체를 이용한 계통유전학적 분석 결과 HCQD-2020는 알파코로나바이러스에 속하였다. ORF1a, ORF1b 및 4개의 주요 단백질 코딩 유전자 대상으로 topology 분석을 하였으며 ORF1a, ORF1b를 제외한 다른 유전자에서는 다른 종과 유사도가 낮았다. 다른 숙주 감염 가능성을 평가하기 위해 *In silico* 분석한 결과 우제목 (*Artiodactyla*)와 양박쥐아목 (*Vespertilioniformes*) 모두 감염될 수 있으며 이는 HCQD-2020가 종간 전염을 일으킬 수 있는 것으로 예측되었다.

다음으로, 돼지 유래 토크티노바이러스 (Torque teno sus virus, TTSuV)로 인한 국내 사육 돼지에서의 유병률을 조사하고, 돼지에서 유행하고 있는 바이러스와 사람 바이러스 간의 유전적 관련성을 계통유전학적으로 분석하였다. 전국 9개 지방에서 2017~2018년에 걸쳐 총 470 샘플을 수집하였으며 TTSuV1 양성검출률은 16%(38/470)였으며 TTSuV2의 경우 36%(168/470) 였다. TTSuV1 과 TTSuV2 동시 감염 양성검출률은 8%(38/470) 였다. 양성샘플 중 3 종(M117, N86, N116)에 대하여 전장유전체분석을 진행하였고 M117과 N86은 각각 TTSuV1 subtype 1b와 1c에 속하며

N116은 TTSuV2 subtype 2b에 속하였다. 추가적으로 돼지샘플에서 사람에게서 발견되는 TTV genogroup 3을 검출하였다. 총 2개의 종(M265, N119)이 검출되었으며 모두 전장유전체는 3,817 bp 이며 M265는 3개의 ORF(ORF1, ORF2, ORF3)로 N119는 4개의 ORF(ORF1, ORF2-1, ORF2-2, ORF3)으로 구성되어 있었다. 이 종들은 98.4%의 일치율을 보였으며, ORF1 기준으로 다른 TTVs 와 계통유전학적 분석 결과 genogroup3의 subgroup 3c에 속하였다. ORF1, ORF2, ORF3 아미노산 비교분석 결과 분리된 두 스트레인은 다른 TTVs 와 아르기닌 풍부 지역 또는 motif 같은 공통적인 서열이 확인되었다. 이는 돼지에서 발견된 스트레인이 사람에게서 발견된 TTV와 관련성이 있음을 의미한다.

사람과 동물에서 공중보건학적 및 경제적 피해를 초래하는 코로나바이러스들에 대한 소독제 연구가 활발히 이루어지고 있다. 본 연구에서는 천연물질인 키토산과 나노그래핀 옥사이드가 코로나바이러스에 대한 항바이러스 효능이 있는지를 *in vitro* cell culture 시스템을 이용하여 경수 희석액 과 유기물 희석액 조건에서 평가하였다. 키토산의 경우 porcine epidemic diarrhea virus (PEDV)를, nanoGO의 경우 PEDV, bovine corona virus (BCoV), 및 SARS-CoV-2를 사용하여

항바이러스 효능을 평가하였다. 키토산은 1% 수용액으로 100~800배수 희석농도로 30분간 처리하였을 때 경수 희석액 조건에서 150배 희석배수까지, 유기물 희석액 조건에서는 100배 희석배수까지 PEDV 감염 역가 (infectious titer)가 control 바이러스에 비해 10^4 이상이 감소하였다. 나노그래핀 옥사이드는 1% 수용액으로 50~800배수 희석농도로 30분간 처리하였을 때 유기물 희석액 조건에서는 100배 희석 배수까지 PEDV와 BCoV 감염 역가가 대조군보다 10^4 이상이 감소하였다. 키토산과 나노그래핀 옥사이드는 실험한 모든 희석농도에서 세포독성을 보이지 않았다. Immunofluorescence assay (IFA) 결과에서는 키토산이 경수 희석액 조건에서는 50배 희석배수, 유기물 희석액 조건에서는 1배 희석배수까지 PEDV의 감염 억제하였으며, 나노그래핀 옥사이드는 유기물 희석액 조건에서 50배 희석배수까지 PEDV 및 BCoV의 감염을 억제하였다. 또한 나노그래핀은 중화 실험에서 8배 희석배수까지 SARS-CoV-2를 억제하는 것을 확인하였다. 결론적으로 키토산과 나노그래핀 옥사이드는 코로나바이러스에 대하여 유의미한 제어 효과가 있으며 또한 세포독성을 나타내지 않았다.

이상의 결과를 종합할때, 야생동물 및 주요 산업동물에서

코로나바이러스 및 토크티노바이러스와 같은 인수공통전염병 유발 바이러스들이 존재하고 있어 이에 대한 지속적인 감시 및 연구가 필요하고, 이들 바이러스의 전파 및 감염병 발병을 최소화할 수 있는 신규제어물질에 대한 지속적인 연구 또한 필요하다고 판단된다.

주요어: 계통유전학적 분석; 박쥐 알파코로나바이러스; 토크티노바이러스; 키토산; 나노그래핀옥사이드; 소독제

학번: 2016-21763